# STRATIGRAPHY AND GEOCHEMISTRY
# OF
# THE MAKGANYENE FORMATION,
# TRANSVAAL SUPERGROUP, NORTHERN CAPE, SOUTH AFRICA.

by

**STEPHANE POLTEAU**

February 2000

This dissertation is Submitted in Partial Fulfilment of the Degree of MASTER OF SCIENCE (ECONOMIC GEOLOGY) of Rhodes University.

**DECLARATION**

All work in this thesis is the original work of the author, except where specific acknowledgement is made to the work of others.

**SIGNED**

S. POLTEAU

June 2000

# ACKNOWLEDGMENTS

I wish to thank Prof. J.Moore. He provided the subject of this thesis when I initially arrived in SA with very little knowledge of the stratigraphy of the Transvaal Supergroup. He also helped me with some of the problems I encountered during these past two years. Also, he made me discover what a conference is about, and I hope I am going to attend some more in the future.

Thank you Dr. Harilaos Tsikos for your help and fruitful discussions we had in Grahamstown or by e-mail when you left to Johannesburg. I have not forgotten that you did the stable isotopes analyses for me in UCT.

I wish to thank Boshoek and Sishen mines for providing the core samples I needed for this study. Meiring Burger, Marius, thank you for bringing me water in the Southern Kalahari when I was thirsty, and sending me to the restaurant "Inside Story" of Boshoek mine when I came back from the field. I have not forgotten the farmers who allowed me to map their land, even if permission was sometimes difficult to obtain.

A special thanks for the Lavoisey family who let me use their computer for a month at their home in Perpignan to correct the last chapter. This made me realise how important is to have your own computer. Also a special thanks to the Respaut family who accommodated me in their house in Cabestany, while I was doing these corrections in France.

I wish to thank all the geologists I met at Rhodes University, who opened my eyes to the real geology world that I did not know : the industry. But also for some social evenings where we learnt about each other. They include staff, students, and delegates.

Mum, dad, thank you for supporting me during these two years I spent far from the cheese and wine country which is mine. I missed your "blanquette de veau", mum. Dad, I wish I could have helped you more in the building of your house in Albertville.

Alison Blake, thank you so much for reading and correcting the last draft of this thesis.

Nomzi Kumalo, thank you so much for your patience when I was correcting this thesis. I was very happy when I would come back home for lunch and it was ready to eat. I will never kiss you enough for what you have done for me.

Finally, I do not thank the French army who affected my mental health. You are supposed to stop this military service for everybody, and you are waiting for me the 1st of April. 1st of April? This must be a joke...

ABSTRACT

The Makganyene Formation forms the base of the Postmasburg Group in the Transvaal Supergroup of the Northern Cape Province. The Makganyene Formation has diamictite as the main rock type, but siltstone, sandstone, shale, and iron-formations are also present. A glacial origin has been proposed in the past due to the presence of dropstones, faceted and striated pebbles. Typically, the Makganyene Formation contains banded iron-formations interbedded with clastic rocks (shale, siltstone, sandstone and diamictites) at the contact with the underlying iron-formations. This transitional zone is generally overlain by massive or layered diamictites which contain poorly sorted clasts (mainly chert) within a shaly matrix. Striated pebbles have been found during field work, and dropstones have been observed in diamictites and banded iron-formations during the study. The top of the Makganyene Formation contains graded cycles interbedded with diamictites and thin layers of andesitic lavas from the Ongeluk Formation.

The basal contact of the Makganyene Formation with the underlying Koegas Subgroup was described as unconformable by previous workers. However field work localised in the Rooinekke area shows a broadly conformable and interbedded contact with the underlying Koegas Subgroup. As described above, banded iron-formations are interbedded with the clastic rocks of the Makganyene Formation. Moreover, boreholes from the Sishen area display the same interbedding at the base of the Makganyene Formation. This suggests that no significant time gap is present in the whole succession between the Ghaap and Postmasburg Group. The Transvaal Supergroup in the Northern Cape displays the following succession : carbonates-BIFs-diamictites/lava-BIFs-carbonates. The Makganyene Formation is thus at the centre of a symmetrical lithologic succession.

Bulk rock compositions show that the diamictites have a similar composition to banded iron-formation with regard to their major element contents. Banded iron-formations acted as a source for the diamictites with carbonates and igneous rocks representing minor components. Differences in bulk composition between the Sishen and Matsap areas emphasize that the source of the diamictite was very localised. The Chemical Index of Alteration (CIA) has been calculated, but since the source dominant rock was iron-formation, this index cannot be usefully applied to the diamictites. ACN, A-CN-K, and A-CNK-FM diagrams confer a major importance in sorting processes due to the separation between the fine and coarse diamictites. The interbedded iron-formations display little clastic contamination indicating deposition in clear water conditions. However, dropstones are present in one borehole from the Matsap area, indicating that iron-

formation took place under ice cover, or at least under icebergs. Stable isotope studies show that the iron-formations, interbedded towards the base of the Makganyene Formation, have similar values to the iron-formations of the Koegas Subgroup.

As a result of the above observations, new correlations are proposed in this study, relating the different Transvaal Supergroup basins located on the Kaapvaal Craton. The Pretoria Group of the Transvaal Basin has no correlative in the Griqualand West Basin, and the Postmasburg Group of the Northern Cape Basin has no lateral equivalent in the Transvaal Basin. These changes have been made to overcome problems present in the current correlations between those two basins.

The Makganyene Formation correlates with the Huronian glaciations which occurred between 2.4 and 2.2 Ga ago in North America. Another Precambrian glaciation is the worldwide and well-studied Neoproterozoic glaciation (640 Ma). At each of these glaciations, major banded iron-formation deposition took place with associated deposition of sedimentary manganese in post-glacial positions. The central position of the Makganyene Formation within the Transvaal Supergroup in the Northern Cape emphasizes this glacial climatic dependence of Paleoproterozoic banded iron-formation and manganese deposition. However these two Precambrian glaciations are interpreted in paleomagnetic studies as having occurred near to the equator. The controversial theory of the Snowball Earth has been proposed which proposes that the Earth was entirely frozen from pole to pole. Results from field work, sedimentology, petrography and geochemistry were integrated in a proposed depositional model of the Makganyene Formation occurring at the symmetrical centre of the lithologic succession of the Transvaal Supergroup. At the beginning of the Makganyene glaciation, a regression occurred and glacial advance took place. The diamictites are mostly interpreted as being deposited from wet-based glaciers, probably tidewater glaciers, where significant slumping and debris flows occurred. Any transgression would cause a glacial retreat by rapid calving, re-establishing the chemical sedimentation of banded iron-formations. These sea-level variations are responsible for the interbedding of these different types of rocks (clastic and chemical). The end of the Makganyene glacial event is characterised by subaerial eruptions of andesitic lava of the Ongeluk Formation bringing ashes into the basin.

Banded iron-formation and associated manganese accumulations are climate-dependant. Glacial events are responsible for the build up of metallic ions such as iron and manganese in solution in deep waters. A warmer climate would induce a transgression and precipitation of these metallic ions when Eh conditions are favourable. In the Transvaal Supergroup, the climatic variations from warm to cold, and cold to warm are expressed by the lithologic succession. The warm climates are represented by carbonates. Cold climates are represented by banded iron-formations and the peak in cold climate represented by the diamictites of the Makganyene Formation. These changes in climate are gradual, which contradict the dramatic Snowball Earth event : a rapid spread of glaciated areas over low-latitudes freezing the Earth from pole-to-pole. Therefore, to explain low-latitude glaciations at sea-level, a high obliquity of the ecliptic is most likely to have occurred. This high obliquity of the ecliptic was acquired at 4.5 Ga when a giant impactor collided into the Earth to form the Moon. Above the critical value of 54° of the obliquity of the ecliptic, normal climatic zonation reverts, and glaciations will take place preferentially at low-latitudes only when favourable conditions are gathered (relative position of the continents and $p_{CO2}$ in the atmosphere).

TABLE OF CONTENTS

List of figures

List of tables

List of photographs

# I Introduction

## I.1. Aims of the project

The Makganyene diamictites could potentially play a role in the genesis of the banded iron formations and associated manganese concentrations in the Transvaal Supergroup. Many Fe-Mn formations are closely associated with glacial events and tillites/diamictites. The explanation of this association lies in the observation that cold stagnant oceanic water beneath ice-caps retain iron as $Fe^{2+}$ in solution under reducing conditions. Once warming and/or oxidation commences, the iron is rapidly precipitated as insoluble oxides. Cold, reducing conditions also suppress the precipitation of carbonates (including manganese).

In order to test the validity of such a theory, this thesis is a preliminary basic study of the Makganyene diamictite and its relationship with the adjacent banded iron formations and Ongeluk lava. The aims of this thesis are as follows :

1) to gain an understanding of the relationship with the underlying banded iron formations. The contact is described as an unconformity by previous workers.

2) to study the sedimentological and geochemical attributes of the diamictite and included minor units. This includes chemical studies using the index of alteration, which gives clues as to the climatic conditions of weathering during formation and examination of interbedded banded iron formation or ferruginous sediments in the diamictite.

3) to examine the larger clasts and comment on their potential source (local and/or distal).

4) to study the relationship with the overlying Ongeluk lavas (i.e. whether there is an obvious break between diamictite and volcanism or not).

From the study, a possible genetic model for the Makganyene diamictite and comments on its significance regarding banded iron formation (and Mn) generation will be presented.

## I.2. Generalities on Early Proterozoic Diamictites

Well-established Early Proterozoic tillites are present in North America (Young and McLennan, 1981; Houston et al., 1981; Kurtz, 1981; Young and Nesbitt, 1985; Miall, 1985 and Mustard and Donaldson, 1987), South Africa (Visser, 1971; De Villier and Visser, 1977), India (Marthur S.M., 1981) and Western Australia (Trendall, 1976, 1981).

The best known tillites occur in the Gowganda Formation, which forms part of the Huronian succession that is widespread in Ontario, Canada (Young and Nesbitt, 1985; Miall, 1985 and Mustard and Donaldson, 1987). According to Harland and Hambrey (1981), these are amongst the best-preserved Early Proterozoic tillites and are particularly noted for the good preservation of sedimentary structures indicative of glacial origin (i.e. striated stones and pavement, laminated argillite with dropstones). According to Miall (1985), there are three distinct major periods of glaciation represented by the Gowganda Formation itself, and two earlier distinctive formations : Ramsey Lake and Bruce Formations. However the timing of these events is not well precisely defined and according to Harland and Hambrey (1981), they occur within the interval 2.5-2.1 Ga, which is the time span for the whole Huronian succession.

Early Proterozoic diamictites of similar age to the Huronian succession occur in the Padlei Formation (Young and McLennan, 1981) of the Hudson Bay area of Northwest Territories (2.55-1.81 Ga) but a glacial origin is not yet well-established. In Southern Wyoming (Houston et al., 1981), three thick diamictite horizons strongly suggestive of both terrestrial and glaciomarine deposition, appear to be more than 2.1 Ga old, while in northern Michigan (Gair, 1981) a sequence apparently younger (2.1-2.0 Ga) than other North American Early Proterozoic glacigenic deposits is thought to reflect a local mountain glaciation. The metamorphosed diamictites in the Black Hills of South Dakota (Kurtz, 1981), falling in the very broad time interval of 2.56-1.62 Ga, may be of glaciomarine origin, but little evidence of the mode of deposition remains.

Overall, the picture that emerges for North America is an extensive global glaciation, with considerable glaciomarine deposition, in an interval of 300 to 400 Ma.

In Southern Africa some Early Proterozoic tillites occur within the interval 2.4-2.2 Ga. This thesis will show in the next chapters that at least 2 major glacial periods occurred in the Northern Cape Basin and in the Transvaal Basin. The oldest period occurs in both basins, represented by the Makganyene Formation in the Northern Cape Basin and the Duitsland Formation in the Transvaal Basin. The second event is only present in the Transvaal Basin, represented by the three formations forming the base of the Pretoria Group.

Early Proterozoic is represented in India by the Gangau Tillite of the Bijawar Group (Marthur, 1981) which shows evidence of glaciation (straited and faceted stones), but the age is not well

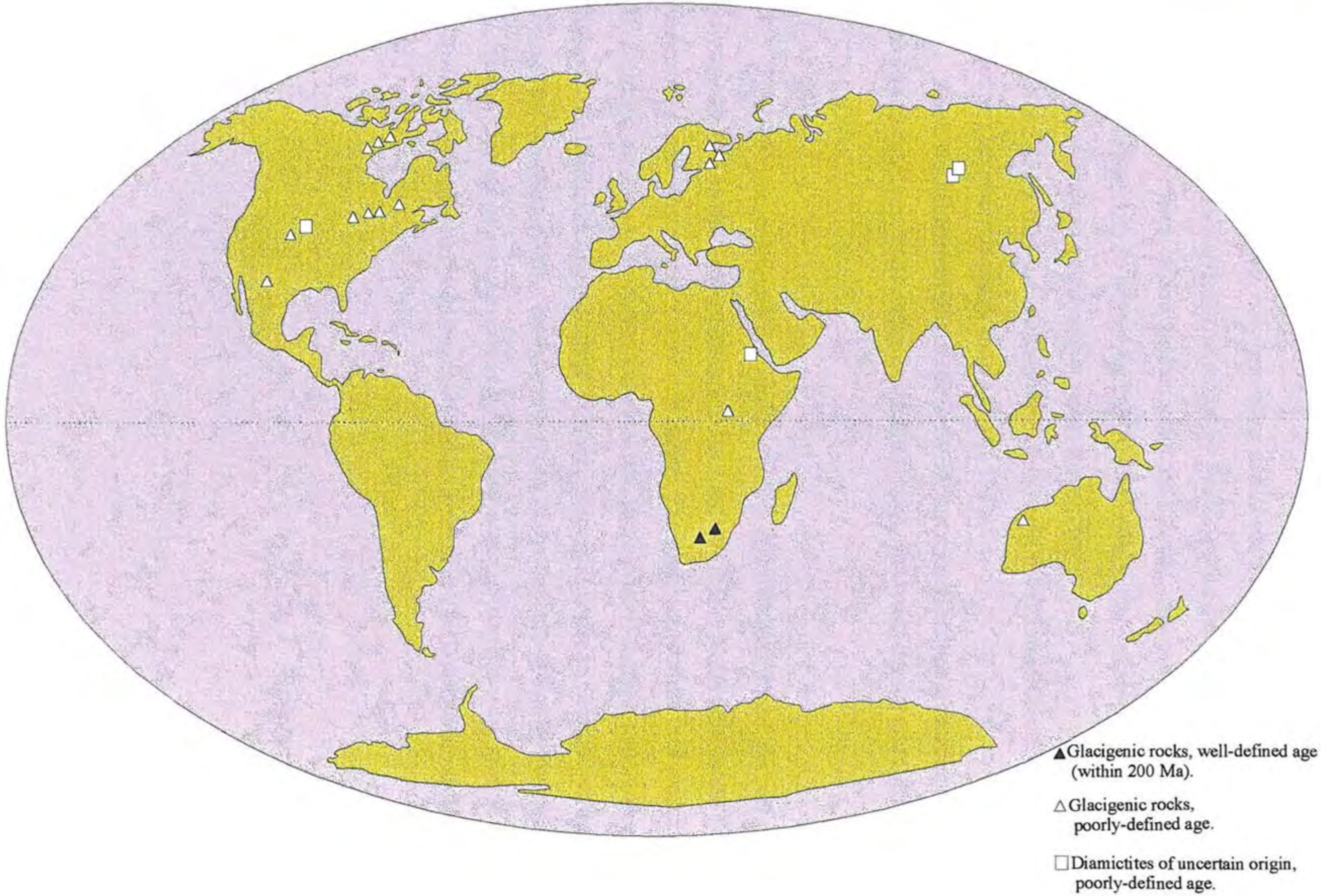


F. 1. World distribution map of diamictites for the Early Proterozoic (after Harland and Hambrey, 1981; Marko and Ojokangas, 1984; Strand and Laajoki, 1993) established and is thought to be 1.815 Ga.

In Western Australia, only one major glacial event occured in the time span of the Huronian Glaciation (2.5-2.0 Ga) and is represented by the Meteorite Bore Member of the Hamersley Basin (Trendall, 1976, 1981). Although the rocks are cleaved, and primary bedding (if ever present) obliterated, the boulders do not appear to have been affected by deformation and few retain striations that seem most likely to be glacigenic rather than tectonic.

Other diamictites are extensively distributed on the Baltic Shield, but none of these are regarded as glacigenic (Harland andHambrey, 1981).

These world distributions of the Early Proterozoicdiamicties is represented in figure 2 (after Harland and Hambrey, 1981; Marmo and Ojakangas, 1984; and Strand and Laajoki, 1993).

## I.3. Location

The Makganyene diamictite with the under- and overlying rocks are part of the Transvaal Supergroup, laid on the western margin of the Kaapvaal craton in the Griqualand West Basin in the Northern Cape Province in the southern Kalahari. The study area for the field work is focused on the Rooinekke mine area in the farms Valwater 84, Paauwvlei 190 and Koodooskloof 96 where the Makganyene diamictite does outcrop. This area is located between Griquatown and Postmasburg, south of the Maremane Dome, on the western part of the Ongeluk-Witwater Syncline, along the main sole thrust. One set of core samples is located just north of the field work area at Matsap Hills and a second set of core samples comes from Sishen iron mine. The locations are shown in figure I.3.(1) (after Grobbelaar et al., 1995)

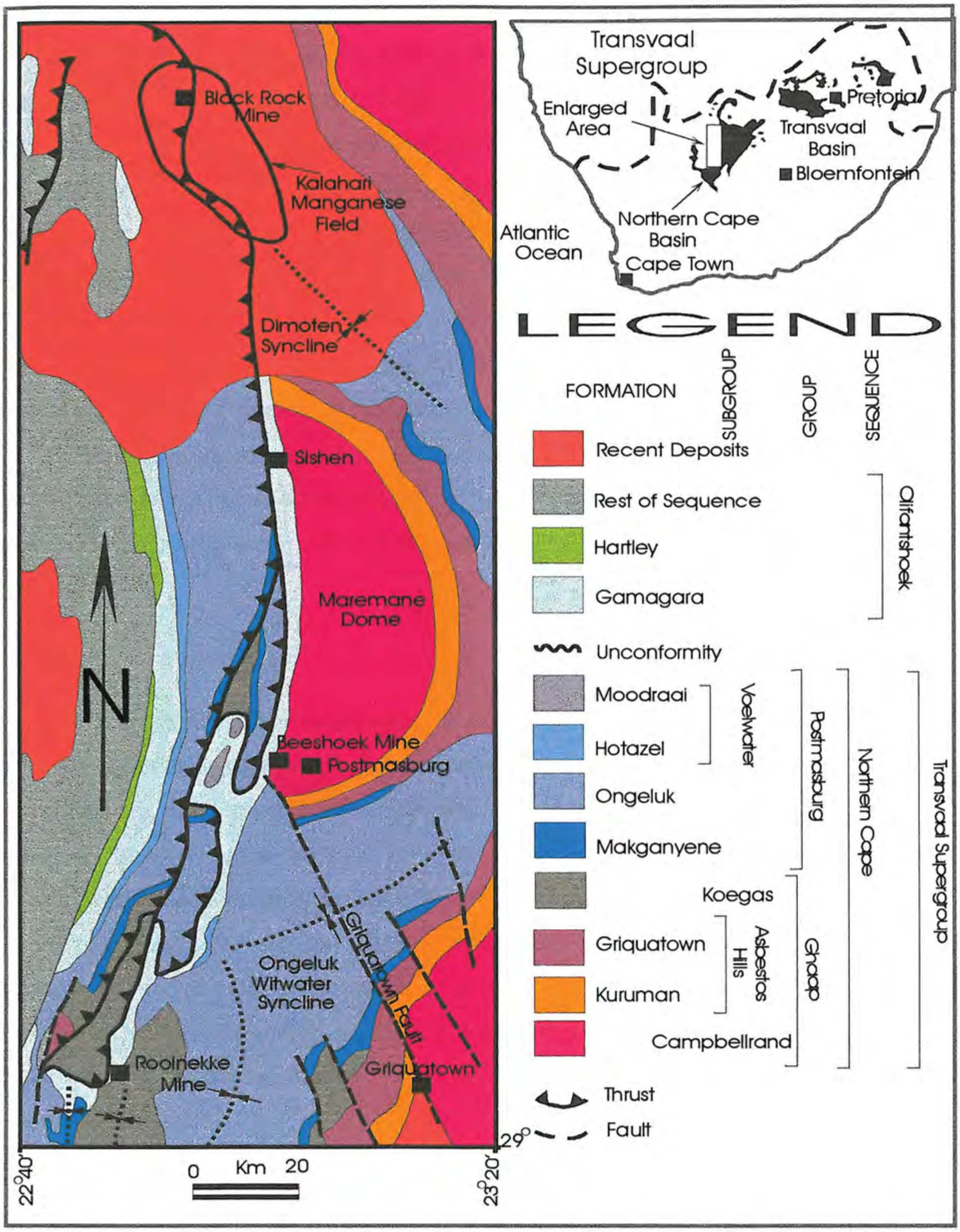


F. 2. Regional geological map with stratigraphic column used in this study and location (after Grobbelaar et al., 1995).

## I.4. Vegetation

A bushy type of vegetation, much of it thorn-bearing, is typical of this area. The bushes are concentrated from the foot of the relief to the top. The larger trees occur on deep sandy soils while low bushes and thorny scrubs grow on a shallower soils on the reliefs.

The larger tree members of the Acacia group are well represented, the Camelthorn (*Acacia giraffae*) being characteristic of the whole area (Truter et al., 1938). The Swart-haak (*Acacia detinens*) and the Haak-en-steek (*Acacia spirocarpoides*) flourish on the stony beds on the reliefs of the area.

Thornless scrubs are best represented by the Vaalbos (*Tarchonanthus camphoratus*) which favours areas occupied by sandy and calcareous soils like calcrete.

There are many varieties of perennial and annual grasses. The most characteristic species are the tall Bushman grass (*Aristida ciliata*) and the short Bushman grass (*Aristida obtusa*). The former is usually found on deep sandy soils and on dunes while the latter occurs on shallower soils (Truter et al., 1938).

## I.5. Fauna

The factor influencing the presence and distribution of animals in the Southern Kalahari is water. Surface drinking water is only available during summer rain-seasons and fairly irregularly. Thus the only species which can survive are those which can go for long periods of time without drinking water. A variety of ways are used to overcome the moisture shortage. Many species are physiologically adapted to make the most efficient use of the moisture taken with their diet, some to the extent of metabolic water and this is often sufficient. Numerous plant species have moisture storing bulbs which the animals can easily dig up from the soft sand. Nowadays, water points made available by the farmers to their live-stock in the farms attract wild-life. Overgrazing could be a problem for the wild life depending on the management of the farm on the rotation of the live-stock (sheep, goats and cattle).

# II GENERAL GEOLOGY

## II.1. Stratigraphy of the Transvaal Supergroup

The main rock types exposed in outcrops in the study area are from the Transvaal Supergroup. The latter in the west of the Northern Cape Basin, have been involved in folding, faulting and thrusting. The origin is dominantly sedimentary but andesitic lavas and dolerite dykes cutting through the Transvaal strata are also present. The regional distribution of the Transvaal Supergroup is shown in figure 3 (after Beukes, 1983).

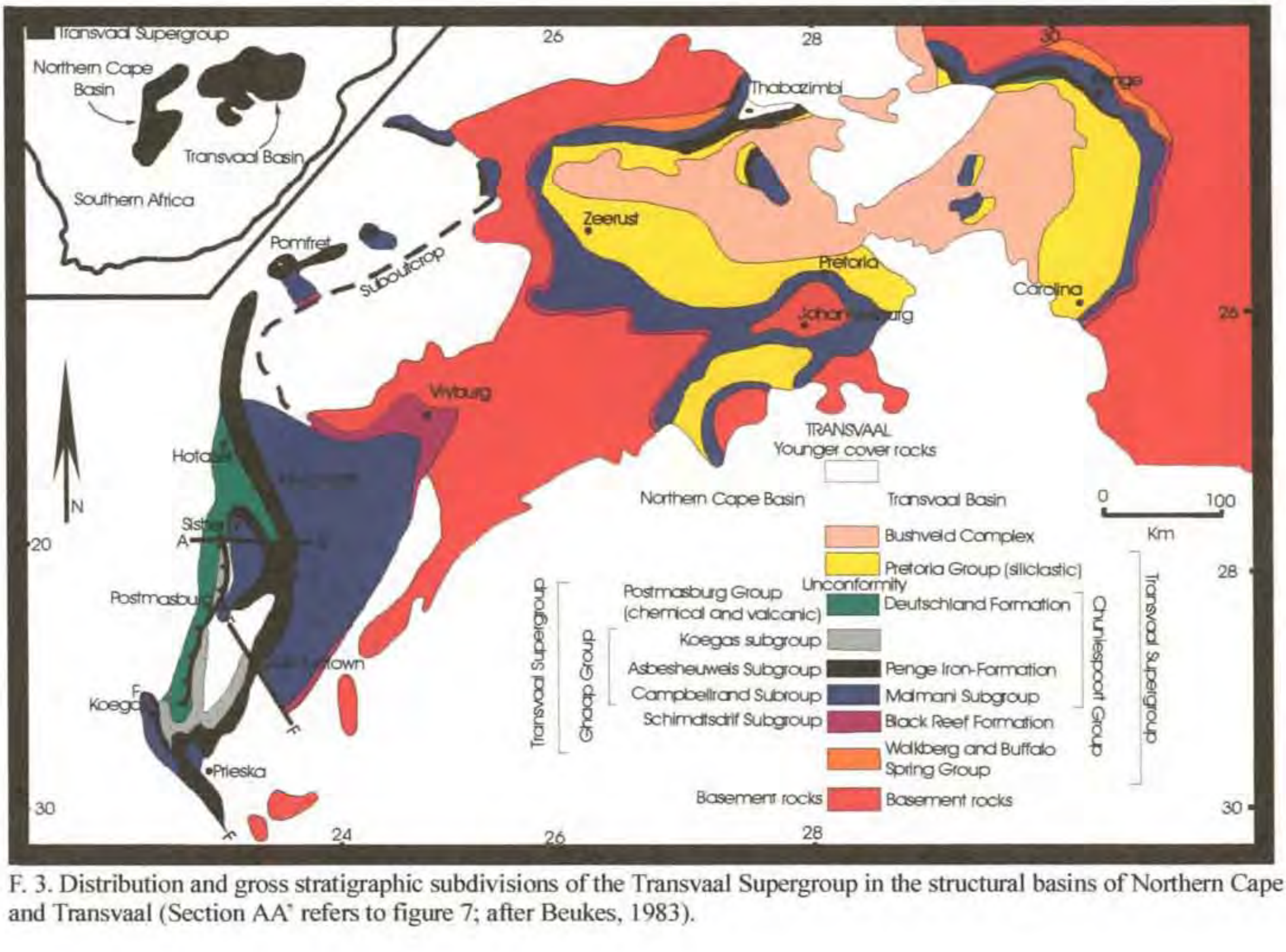


F. 3. Distribution and gross stratigraphic subdivisions of the Transvaal Supergroup in the structural basins of Northern Cape and Transvaal (Section AA' refers to figure 7; after Beukes, 1983).

The stratigraphy of the Transvaal Supergroup in Northern Cape consists of clastic and chemical sediments of the Ghaap Group (2.6 Ga; Cheney, 1996), followed by a volcanic-sedimentary sequence, the Postmasburg Group (2.2 Ga; Cheney, 1996). The Campbellrand Subgroup of the Ghaap Group consists predominantly of stromatolitic carbonates, which are covered by a transgressive Asbesheuwels Subgroup defined by ferhythmites of the Kuruman Iron-Formation and by clastic-textured Griquatown Iron-Formation (Beukes, 1983; Grobbelaar et al., 1995). These chemical sediments are followed by the Koegas Subgroup, which consists of alternating units of chloritic mudstone, siltstone, quartz wacke and iron-formations (Grobbelaar et al., 1995). On the Maremane Dome, an unconformity separates the Campbellrand Subgroup from the local variety of the Asbestos Hills Subgroup.

The Postmasburg Group was deposited with first the Makganyene Formation which overlies the Asbesheuwels Subgroup, topmost part of the Ghaap Group. The nature of the contact, i.e. conformable or unconformable, is not discussed here. The Makganyene Formation is followed conformably by the Ongeluk Lava (Nel, 1929; Truter et al., 1938; Visser, 1958, 1971, De Villier and Visser, 1977, Beukes, 1983; Evans et al., 1997) The Ongeluk Lava is characterised by pillow lavas and hyaloclastites. Conformably overlying the lava is the Hotazel Formation consisting of sedimentary jaspilites (Tsikos and Moore, 1997, 1998, 1999; Tsikos, 1999) with manganiferous layers (Beukes, 1983, Grobbelaar et al., 1995). In the Kalahari Manganese Field, dolomites of the Mooidraai Formation cover the Hotazel Formation. With the Hotazel Formation they form the Voëlwater Subgroup, at the top of the Postmasburg Group.

The Transvaal Supergroup is terminated by a period of erosion spreading from 2.2-2.1 to 1.9 Ga (Cheney, 1996) after which the Olifantshoek Supergroup deposition took place (1.9 Ga; Cheney, 1996) to unconformably overly the former. At the base is the Mapedi Formation with a basal conglomerate and interbedded lavas and shales. This is followed by the arenites of the Lucknow Formation. Locally, the Mapedi and Lucknow Formations are known as the Gamagara Formation with the basal Doornfontein Conglomerate Member followed by Sishen Shale Member, the Marthaspoort Quartzite Member and the Paling Shale Member (Grobbelaar et al., 1995). The succeeding Hartley Formation is an amygdaloidal andesitic lava with interbedded sedimentary rocks (SACS, 1980; Grobbelaar et al., 1995). The rest of the Olifantshoek

Supergroup consists mainly of arenitic red beds. The whole succession of the Transvaal Supergroup is summarised in figure 4 (after Beukes, 1983). According to Beukes (1983), the Transvaal Supergroup deposition began at around 2.46-2.5 Ga ago and ended prior to about 2.1 Ga ago.

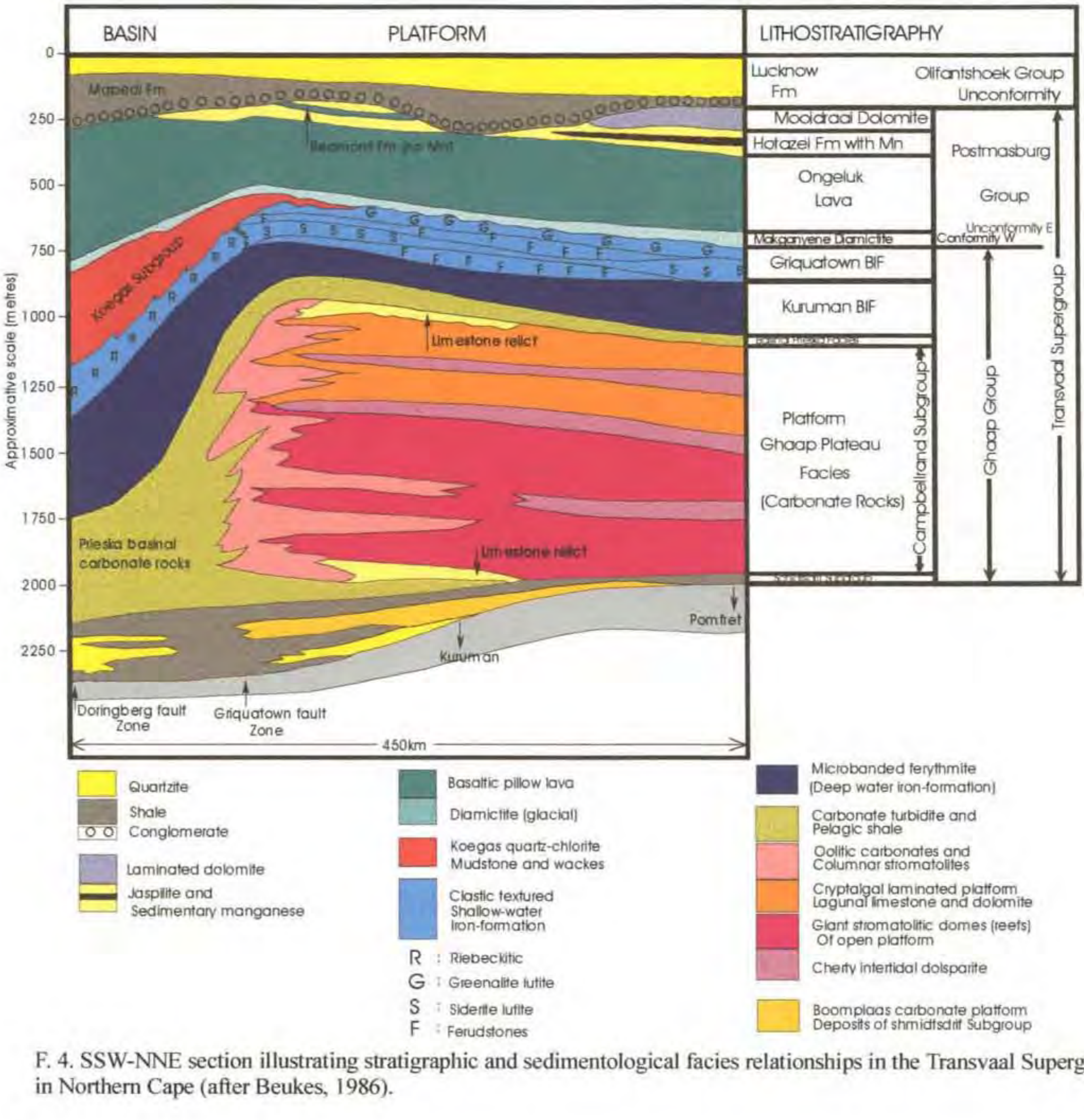


F. 4. SSW-NNE section illustrating stratigraphic and sedimentological facies relationships in the Transvaal Supergroup in Northern Cape (after Beukes, 1986).

II.1.1. The Transvaal Supergroup

II.1.1.1. The Ghaap Group

II.1.1.1.1. The Schmidtsrif Subgroup

The Schmidtsrif Subgroup consists of shales, dolomites, limestones, quartzites and lavas (Beukes, 1987). At the top of the sequence, banded siderite lutites of the Lokammona Formation overlie tuffaceous siltstone which was deposited in a lagoonal setting shoreward of platform-edge, carbonate-oolite-shoal and stromatolite-reef deposits. They are overlain by pyritic carbonaceous shale which possibly represents offshore marine muds (Beukes, 1983). Chert bands and nodules of the siderite lutites, representing devitrified volcanic ash bands and lapilli respectively, are also present in other units of the Schmidtsrif Group so that the setting of the Lokammona banded felutites in a lagoonal environment may be entirely coincidental.

II.1.1.1.2. The Campbellrand Subgroup

The Campbellrand Subgroup occurs mainly on the Ghaap plateau and comprises a large succession of limestones and dolomites, and associated with them are several bands, lenses, or nodular masses of chert and an occasional narrow shale bed (Nel, 1929). The Campbellrand Subgroup is present in the flat country to the south-west and south of the Gamagara ridge, and occupies most of the country between the ridge and the low hills to the east. It is frequently concealed by wide stretches of surface limestone, sand, or gravel so that the contact with the overlying banded iron-formations are scarce (Nel, 1929; Visser, 1944; Truter et al., 1938). The structure east of the Rooinekke and Postmasburg area approaches that of a broad low anticline, the Maremane Dome. The anticlinal structure is, however, not symmetrical, with subsequent movements complicating the structure. The general dip there is approximately 10° to the east.

Oolitic and pisolitic structures in the limestones are not unusual. Occasionally the oolitic limestone is silicified and altered into a rock which can hardly be distinguished from an ordinary quartzite (Nel, 1929). This is interpreted by Beukes (1983) as an intertidal to supratidal environment of deposition by Beukes (1983).

Chert becomes more abundant towards the top of the Campbell Rand Subgroup (Nel, 1929; Visser, 1944). Chert, partly of primary and secondary origin, is a common constituent of the Campbell Rand Subgroup. The primary chert is especially characteristic of the upper horizons where it occurs as inconsistent and somewhat sinuous seams which vary in thickness from 2.5 cm up to 60 cm or more. It is predominantly white, grey, greenish or black and may be either glassy, saccharoidal.

Beukes (1983) described carbonate rocks of this formation as clastic-textured, carbonaceous and ferruginous with associated ankerite-banded cherts, representing a deeper-water-carbonate turbidite facies which interfinger with a shallow stromatolitic-carbonate platform sequence onto the Kaapvaal craton. The latter unit is referred to as the Ghaap Plateau facies from a inter- to supra-tidal environment.

II.1.1.1.3. The Asbesheuwels Subgroup

Asbesheuwels Subgroup is conformable to the underlying dolomites of the Campbellrand Subgroup (Visser, 1944) as shown in figure 5 (after Beukes, 1983). This subgroup is characterised by the thinly bedded, fine-grained, ferruginous and siliceous nature of its sedimentary members, and the prominence of volcanic rocks. The banded iron-formations are thinly laminated and consist of alternating yellowish-brown, more siliceous, and red to dark brown even blue and green, more ferruginous bands, the colour depending on the concentration and state of oxidation or hydration of the iron whereas the blue and green colours are due to the presence of soda-amphibole. Each individual band has a thickness ranging from millimetre thick films up to more than 5 centimetres (Truter et al., 1938) which may split into slabs. Occasional almost black bands that are highly magnetic are present. This zone is exposed along the Dimoten and Ongeluk-Witwater synclines, where it dips westwards at 5-10°, and along part of the western flank, where, to the south-east and north-east of Postmasburg, it dips eastwards at 2-10°. According to Truter et al. (1938), the thickness of the Asbesheuwels Subgroup does not exceed 300 metres.

Beukes (1983) distinguished two different iron-formations within the Asbesheuwels Subgroup: the Kuruman Iron-Formation and the Griquatown Iron-Formation (see figure 5)

According to Beukes (1983), the Kuruman Iron-Formation may represent a third-order, upward-shallowing progradational sedimentary cycle. This cycle consists of carbonaceous shale at the base followed in turn by volcanogenic-biogenic macro-cycles deposited in different environments from a deep shelf to the toe of a slope below wave base to a shallow-water platform above the wave base.

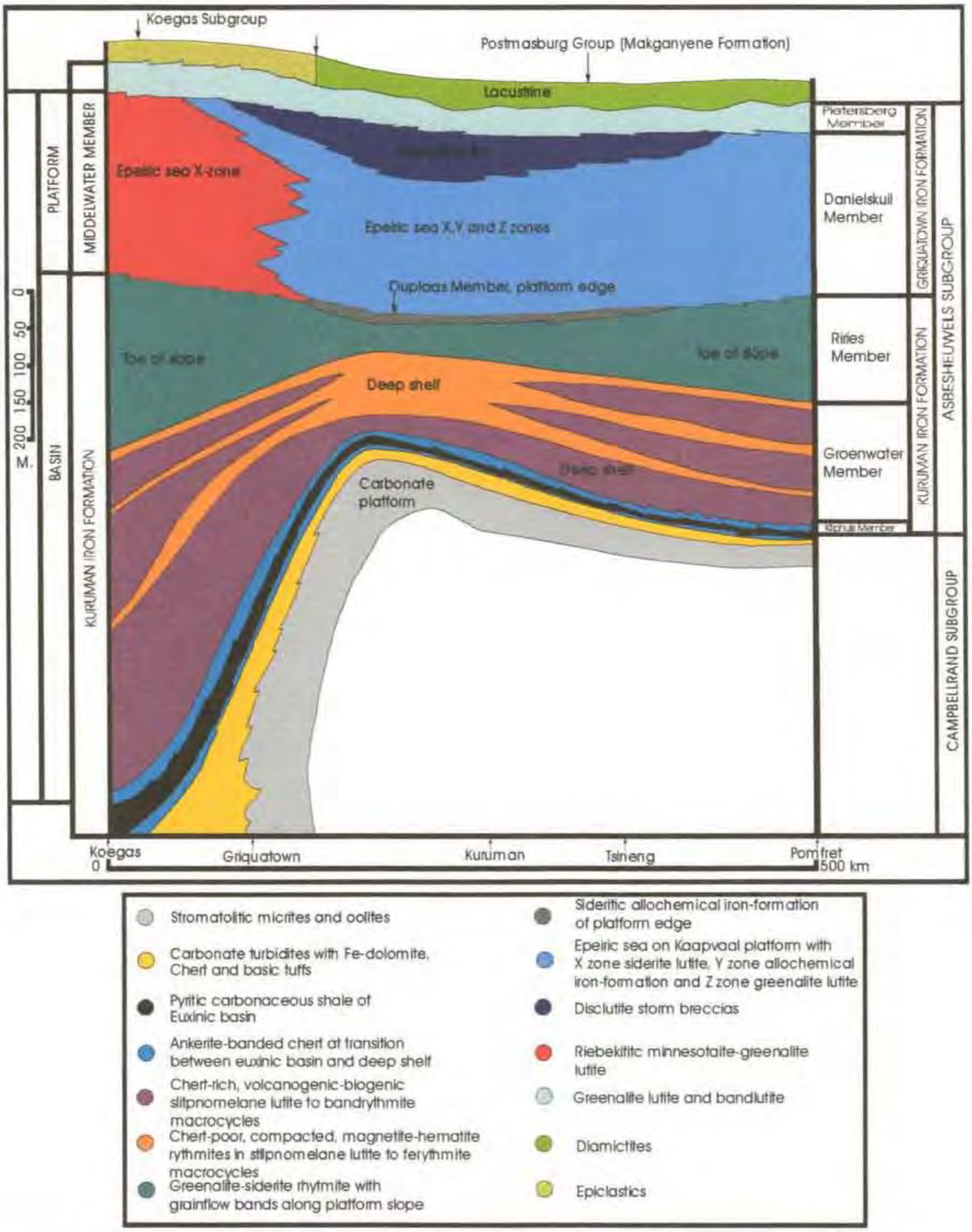


F. 5. SSW-NNE section illustrating stratigraphic relationships and inferred paleodepositional environments of the Asbesheuwels Subgroup in Northern Cape (after Beukes, 1983)

Beukes (1983) interpreted the four upward-coarsening second-order cycles of the Griquatown Iron-Formation as progradational sedimentary increments, consisting of low-energy subtidal siderite lutite, overlain by allochemical iron-formation of a high energy environment, and capped by a lagoonal greenalite lutite.

According to Beukes (1983), the transition between the Asbesheuwels Subgroup and the Koegas Subgroup is represented by an upward-coarsening sedimentary cycle which goes from a banded greenalite lutite (Pietersberg Formation) to a chloritic mudstone, siltstone, and quartz wacke of the Pannetjie Formation (basal part of the Koegas Subgroup). This cycle has been interpreted by Beukes (1983) as an infill of freshwater lake by deltaic sediments.

II.1.1.1.4. The Koegas Subgroup

The Doradale, Rooinekke and Nelani iron-formations each form the base of an upward-coarsening iron-formation to clastic sedimentary cycle (Beukes, 1983). Each of these cycles represent a progradational sedimentary increment consisting of distal iron-formations and proximal ferruginous green-coloured mudstone, siltstone and quartz wacke (Beukes, 1983) as shown in figure 6 (after Beukes, 1983).

The Doradale Iron Formation, just few metres thick, has the same characteristics as the Kuruman Iron-Formation, but northward towards the platform, it becomes brecciated. This is representative of a sediment gravity flow or shallow-water storm breccias (Beukes, 1983). The Doradale Iron Formation grades upwards into the Kwakwas Iron Formation which pinches out towards the north (towards the edges of the basin). The Kwakwas Iron Formation is overlain by the Naragas Formation which is an upward-coarsening siliclastic cycle which could either represent a progradational deltaic sequence, or the infill of the basin by offshore chloritic mudstones and near shore quartz wackes (Beukes, 1983).

The lower contact of the Naragas Formation is placed at the change-over from the iron-silicate lutite of the Kwakwas iron-formation, to quartz-chlorite mudstone (Thatcher et al., 1993). The generally accepted upper contact is placed at the first iron-formation (generally a hematite-bandlutite) for Thatcher (1993) or the first manganese-bearing quartz-chlorite-siltstone by Beukes (1983). However on Sandridge 191, the upper contact definition does not apply : the

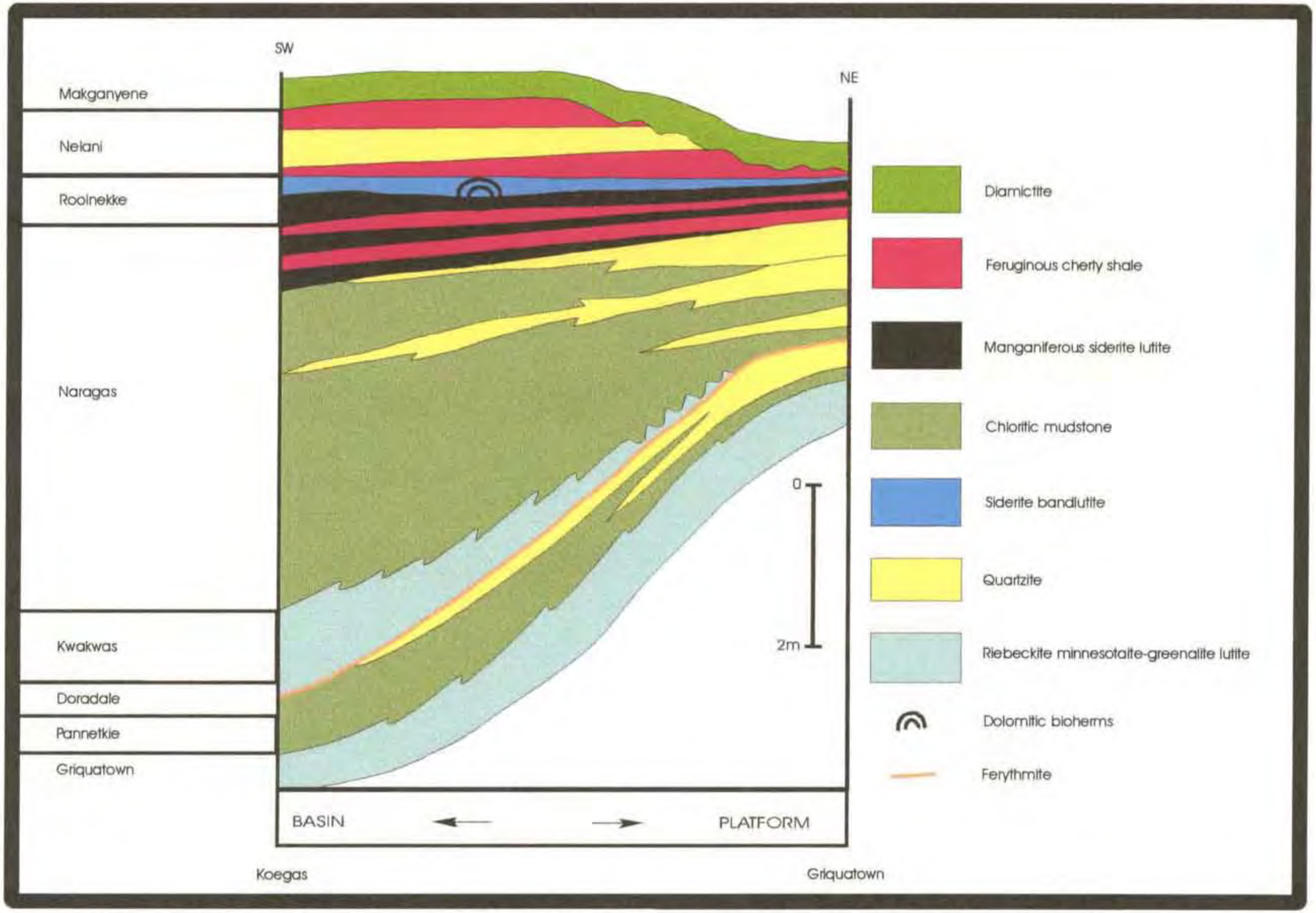


F. 6. Regional stratigraphic relationships within the Koegas Subgroup along a southwest-northeast section (modified from Beukes, 1983)

Rooinekke Formation is interpreted by Thatcher et al. (1993) to consist partly or almost entirely of dolomite bioherms with no iron-formation. Thus further investigations are required to define the upper contact between the two formations. The Naragas Formation consists essentially of a number of coarsening-upward cycles of quartz-chlorite mudstone to quartz-chlorite siltstone or wacke. The siltstones/wackes in the upper part of the sequence are manganiferous and often black in outcrop (Thatcher et al., 1993). Dolomite bioherms and clastic carbonates are found towards the top of the formation.

Overlying the Naragas Formation is the Rooinekke Formation, often referred to as Rooinekke Iron Formation due to its constitution. The Rooinekke Formation is well developed in the vicinity of the Rooinekke Mine on Paauwvlei 190, Koodooskloof 96, Cairntoul 189 and Waterkloof 95. Over most of the area, the formation consists of orthochemical iron-formations (haematite-band-, billow- and pillow-lutites) with relatively thin, interbedded shales, mudstones and siltstones. It is characterised by a relatively high manganese content which commonly results in the formation of a black coating to weathered outcrops. The formation usually stands out predominantly in the field as a black-stained escarpment consisting of broadly banded chert and haematite-lutite with chert billows and pillows being prominent on certain horizons. The iron-formations and chert are broken at irregular intervals by beds of mudstone, shale and siltstone which weather more deeply and often cause overhangs or steps in the escarpment.

According to Thatcher et al. (1993), a difference in the weathering colouration of the banded iron-formations is noted between the outcrops situated below or above the main thrust fault. Those situated above are usually more yellowish-brown in colour, whereas those below this thrust are usually black and white (or grey) with a pinkish or reddish tinge. This difference is often used as evidence whether or not an outcrop is situated above or below the main sole thrust in the field.

According to Beukes (1983), the Nelani Formation overlies conformably the Rooinekke Formation with a succession of ferruginous chloritic mudstones interbedded with chert from the Klipputs Member, at the base of the Nelani Formation. This facies is thought to represent nearshore lagoonal deposits of the Rooinekke sedimentary increment. Stromatolitic dolomite bioherms mark a transgression surface at the top of the Klipputs Member. The submergence of the siliclastic source provided clear water conditions where the bioherms could develop. The Nelani Formation is only present above ( to the west of ) the main thrust fault (Thatcher et al., 1993).

II.1.1.2. The Postmasburg Group

II.1.1.2.1. The Makganyene Formation

According to Nel (1929) and Visser (1958), northeast of Moosfontein farm, the Makganyene Formation lies immediately above the Nelani Formation (upper part of the Koegas Subgroup) on the northern part of the farm, but towards the south, quartzite bands (topmost part of the Nelani Formation) appear between the two. Moreover, Nel (1929) and Visser (1958) said that the Transvaal Supergroup is conformable throughout. Nel (1929) described another contact in a trench on the farm M.91 where limestones from the same stratigraphic level as the quartzite bands seem to grade into diamictites.

Visser (1944) observed the diamictite overlying conformably the Nelani Formation along the south-eastern flank of the nose of a southward-plunging dome south of Wolhaarkop. The sharp ridge extending from this point northwards to Lucasdam is also built of Nelani Formation conformably overlaid by the diamictites. Visser (1944) concluded that the Makganyene Formation is sandwiched conformably between the thick mass of Nelani Formation below and the massive Ongeluk Lava Formation above.

Truter et al. (1938) proposed a gradation from the underlying chemically precipitated sediments into the proper Makganyene Formation. The diamictites separate the upper part of the Nelani Formation from the Ongeluk lavas and so are a transitional zone. They also underlay local minor unconformities between the Makganyene Diamictites and the underlying Nelani Formation which, near their contact, commonly exhibit a brecciated appearance.

Visser (1971) stated that the Makganyene Diamictite and associated rock-types rest unconformably on the Campbellrand, Asbesheuwels, and Koegas Subgroups on an erosional surface. Thrusting onto the western edge of the Kaapvaal Craton duplicated the Transvaal Supergroup over itself (figure 7, after Beukes, 1983). The immediate result was to give to the Gamagara Formation an incorrect apparent stratigraphic position by interpreting thrusts as erosional surfaces (De Villiers, 1967; Visser, 1971; De Villiers and Visser, 1977; SACS, 1980). This confusion in the stratigraphic succession of the Transvaal Supergroup in the Northern Cape Basin placed systematically the Makganyene Formation on top of an unconformity and led De Villier and Visser (1977) to believe that the Gamagara Quartzite acted as source for the Makganyene Formation although they are younger than the latter.


F.7. Schematic profile of the thrust fault zone on the Maremane Dome (The section line AA' is shown on figure 3),(after Beukes, 1983).

Beukes (1983) shows that the unconformity below the Makganyene Formation cuts progressively down through the sequence from the Nelani Iron-Formation to the Griquatown Iron-Formation. In the Rooinekke area, the Makganyene Diamictite Formation unconformably overlies the Rooinekke Formation (Grobbelaar et al.,1995), but no evidence was given. The only evidence available is given by Beukes (1980) when he described in the Griquatown iron-formation the seventh megacycle of the Pietersberg Member. This cycle is not completely preserved in the type area because it is overlain by an erosional contact by the Makganyene Formation of the Postmasburg Group. Grobbelaar et al. (1996) and Beukes and Smit (1987) explained the origin of the presence of the unconformity at the base of the Makganyene Formation. According to them, the Transvaal strata were gently tilted to the west, involving a gentle warping of the lithosphere less than 1° in the Griqualand West region (Evans et al., 1997), and peneplaned prior the deposition of the Makganyene Formation giving a regional low-angle unconformity. For Altermann and Hälbich (1991), this contact is a high angle regional unconformity! These deformations which have induced the warping of the Transvaal strata are assumed to be older than the Kheis-Koranna orogeny and are thought to predate the deposition of the Makganyene Formation and the extrusion of the Ongeluk Formation, but postdate the deposition of the Koegas Subgroup (Altermann and Hälbich, 1991). This event is then, to date, the first orogenic event of post-Archaean but pre-Ongeluk age known in the region.

As explained in the next paragraph (II.3.1), field observations show that the Makganyene Formation is conformable to the underlying Koegas Subgroup in the Rooinekke area. Thus according to Clendenin et al. (1988) and Clendenin (1989), this unconformity is present in the Transvaal basin due to uplift after collision of the Zimbabwe craton with the Kaapvaal craton, providing rifting of the Transvaal basin and folding of the margins of the Kaapvaal craton. This unconformity seen by Clendenin et al. (1988) and Clendenin (1989) is a marginal unconformity which "passes laterally into conformable relationships". The uplift might have given rise to the Vryburg rise where the centre of glaciation was located.

Only two papers on the sedimentological and petrographical attributes of the Makganyene Formation have been published (Visser, 1971 and De Villier and Visser, 1977). These authors interpreted the diamictites as a glacial deposit, due to the evidence of striated clasts which are thought to have been deposited by floating ice some distance away from the source. According to Visser (1971), the diamictites originated from piedmont glacier and fluvio-glacial processes. The association of the diamictites with immature sandstones and non-clastic beds (shale and banded iron-formation) in a cyclic fashion argue for the deposition of the material under-water (De Villier and Visser, 1977).

The top-contact between the Makganyene Formation and the overlying Ongeluk Formation is conformable (Nel, 1929; Truter et al.,1938), but it was never actually found exposed within the limits of the area studied by Nel (1929). Even if the actual contact is nearly everywhere covered by sand, the two rock types were seen within a few metres of each other with the field-relationships leaving no doubt that the Ongeluk lava overlies the Makganyene Formation conformably and has exercised a local indurating effect on it (Visser, 1958). According to SACS (1980), the Ongeluk lava overlies unconformably the Makganyene Formation due to the presence of a low angle unconformity (Altermann and Hälbich, 1991; Grobbelaar et al., 1995). However, in the basinal area of Griqualand West, no unconformity is present at the base of the Ongeluk Lava (Beukes, 1983). Volcanic shards are abundant within the upper strata of the Makganyene Formation (De Villier and Visser, 1977; Evans et al., 1997), indicating that volcanism had already commenced during late-stage glacial time. In conclusion, no significant hiatus separates the Ongeluk Lava and the underlying Makganyene Diamictite.

II.1.1.2.2. The Ongeluk Formation

The Ongeluk volcanics are composed of a monotonous succession of greyish-green andesitic lava (Visser, 1958). According to Grobler and Botha (1976), the succession consists from the bottom upwards of a massive andesitic lava unit concordantly overlain by a hyaloclastic unit composed of large, massive lava fragments and smaller angular glass fragments. This unit in turn is overlain along a gently rolling contact by a unit with prominent pillow lava (Visser, 1958; Grobler and Botha, 1976) in which a lens of massive lava is interbedded. The more usual rock types show small pyroxene crystals in hand specimen (Truter et al., 1938), which vary in composition from diopside to pigeonite augite and surround orthopyroxene (enstatite) or occur as irregular intergrowths with feldspar.

Grobler and Botha (1976) consider the mode of formation of the Ongeluk lava as hydrovolcanic due to the following evidence:

* glassy fragments and finer-grained palagonitised fragments are present in the hyaloclastites,
* pillow lava proper overlies the hyaloclastite,
* the presence of the lens of massive lava in the hyaloclastite-pillow lava sequence is a feature which is commonly associated with hyaloclastite.

However the basal unit of the massive lava unit might have cooled on dry land (Grobler and Botha, 1976).

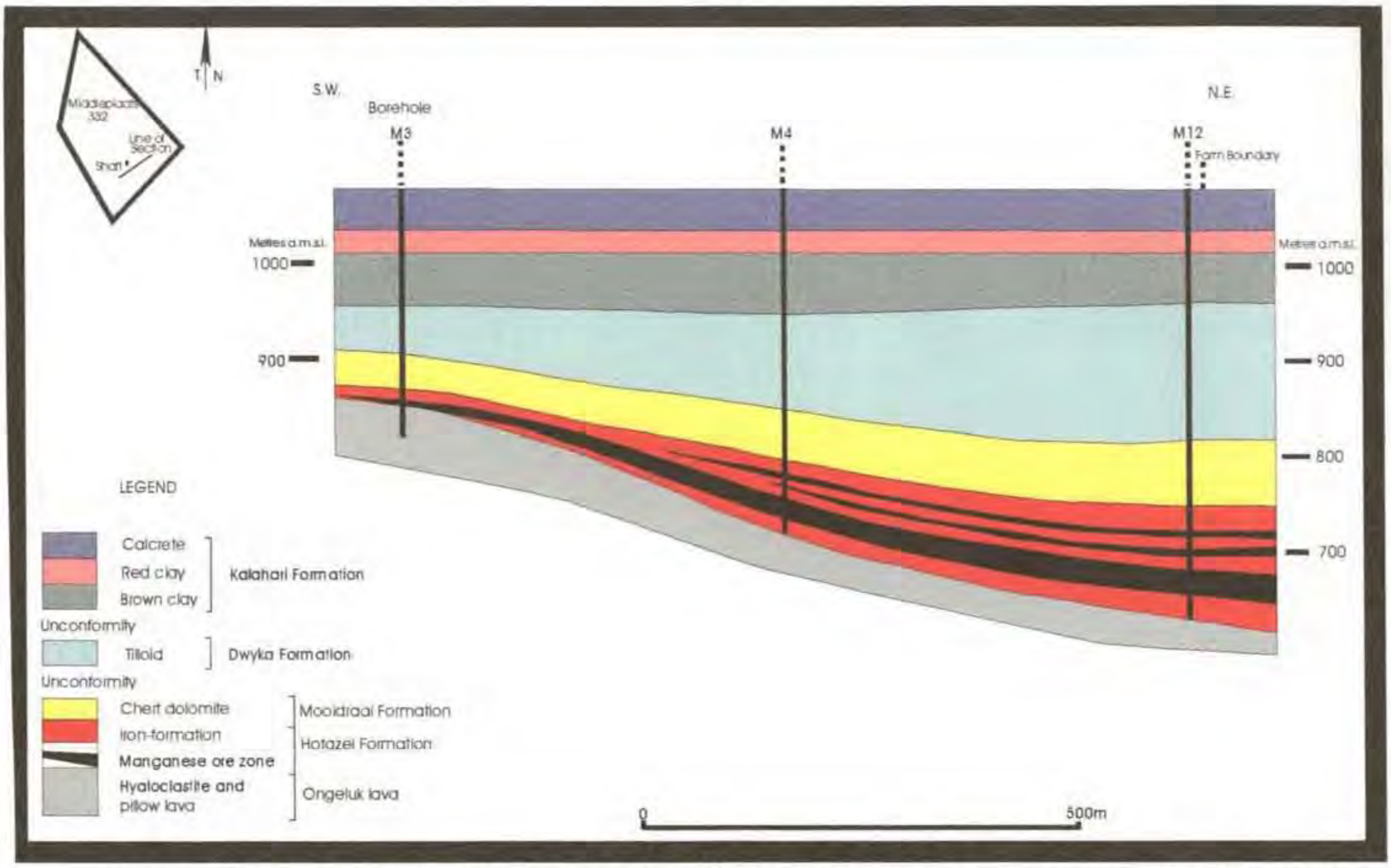


F.8. Southwest-northeast stratigraphic section at the Middleplaats Manganese Mine of the Kalahari manganese field (after Beukes, 1983)

II.1.1.2.3. The Voëlwater Subgroup

II.1.1.2.3.1. The Hotazel Formation

The Hotazel Formation which is the base of the Voëlwater Subgroup, overlies the Ongeluk Formation conformably (Tsikos and Moore, 1998) (see figure 7 after Beukes, 1983). The Hotazel Formation is comprised of three manganese ore beds within iron-formations (Dunn et al. 1980; Beukes, 1983; De Villiers, 1983; Kleyenstüber, 1984; Dixon, 1985; Nel and al., 1986; Miyano and Beukes, 1987; Plehwe-Leisen , 1995; Beukes et al., 1995; Gutzmer and Beukes, 1996; Gutzmer and Beukes, 1996, 1997; Gutzmer et al., 1997; Tsikos and Moore, 1997, 1998, 1999; Tsikos, 1999), but only the lower manganese bed is extensively mined. The manganese horizons attain considerable thickness (the lowermost economic manganese unit ranges from 15 to 45 m in places, the middle and upper units reach 3 and 10 m respectively) (Tsikos and Moore, 1997). The manganese beds and the iron-formations are horizontally interbedded.

The Hotazel Formation reveals evidence of cyclicity on a variety of scales (Beukes, 1983; Kleyenstüber, 1984; Tsikos and Moore, 1997), a typical feature of most Paleoproterozoic banded iron-formations. In the case of the Hotazel Formation, three prominent macro-cycles have the manganese units in their midst. Of importance is the gradational contacts between all the units, forming the Hotazel megacycle (Tsikos and Moore, 1997).

II.1.1.2.3.2. The Mooidraai Formation

The Mooidraai Formation represents the uppermost part of the Postmasburg Group and is comprised of dolomites and limestones (Tsikos, 1999) (see figure 8; after Beukes, 1983). The contact with the underlying Hotazel Formation is gradational.

II.1.2. The Olifantshoek Supergroup

Sink-holes structures in the carbonate are developed beneath the major unconformity between the quartzite of the Olifantshoek Supergroup (from 1.9 Ga to 1.8 Ga; Cheney, 1996) and the Transvaal Supergroup due to some circulation of fluids along this surface. This provided manganese mineralisation along the Gamagara ridge in these dissolution structures and high grade iron-ore when the unconformity runs over the banded iron-formations from the Ghaap Group..

The Olifantshoek Supergroup overlies the Transvaal Supergroup with a regional unconformity. Generally accepted is the thrusting of the Transvaal Supergroup over itself leading to the duplication of the Transvaal Supergroup and therefore misinterpretations of the stratigraphy in this Griqualand West Basin (De Villiers, 1967; S.A.C.S. , 1980). The Gamagara Formation from the Olifantshoek Supergroup is the correlative of the Mapedi and Lucknow Formations

II.2. Tectonic settings of the south-western corner of the Kaapvaal craton

II.2.1. Regional tectonic settings

The study area, which is in the Rooinekke area, is situated on the western west side of the Ongeluk-Witwater Syncline, along the main thrust fault where the Transvaal strata were thrusted over the Gamagara Formation (figure 2; after Grobbelaar et al., 1995). Here, the Transvaal strata were affected by the Kheis and Namaqua orogenies. The Kheis Subprovince, which flanks the western margin of the Kaapvaal craton, is limited to the east by a boundary extending north-eastwards from the vicinity of Marydale and is marked by north-west dipping thrusts near the base of the Matsap Quartzite Formation (Stowe, 1986). The main thrust fault (or "Blackridge Thrust" of Beukes and Smit, 1987) extends from Black Rock Mine southwards to Rooinekke Mine (around 180 km along strike). Further north this boundary follows the unconformable base of the folded Matsap, where décollement is inferred above the relatively undeformed Transvaal Supergroup of the Kaapvaal craton (Stowe, 1986).

According to Stowe (1986) and Schlegel (1988) three main phases of deformation (KD1, KD2 and KD3) affected the Kheis Subprovince between 2-1.8 to 0.9 Ga. Altermann and Hälbich (1990, 1991) recorded 7 phases (D1 to D7) of deformations affecting the Kheis from 2.5-2.4 to 0.9 Ga.

According to Altermann and Hälbich (1990, 1991) the first phase D1 gave rise to a blind $D_1$ thrust which is the oldest deformation recorded on the Kaapvaal Craton in the Northern Cape (age between 2.5 Ga and 2.24 Ga; Altermann and Hälbich, 1991). The $D_1$ blind thrust occurred in the western limb of the Uitkoms Syncline (figure 2; after Grobbelaar et al., 1995) in the Koegas Subgroup resulting in folded features of the Transvaal Strata (Beukes an Smit, 1987) due to the collision of the Zimbabwe craton with the Kaapvaal craton (Clendenin et al., 1988 and Clendenin, 1989). Drag folds, microscopic eye-structures and connecting bands are evidence of pre-Makganyene movements, and are completely recrystallised by quartz and calcite (Altermann and Hälbich, 1991). The $D_1$ explains the unconformity at the base of the Makganyene Formation seen by Altermann and Hälbich (1991). $D_1$ predates the Makganyene deposition.

The next phase of deformation, D2 occurred not long after D1 but D2 is definitely older than the Ongeluk lava. D2 would be responsible for the "low-angle unconformity" only observed by Altermann and Hälbich (1990, 1991) between the Ongeluk and Makganyene Formations. D2 is responsible for slump folds, décollements, and thrusts seem to represent an extended period of movements of D1 (Altermann and Hälbich, 1990, 1991). Therefore correlation between the two is possible, but they should be kept separated.

The presence of Transvaal strata within thrust sheets implies large scale stratigraphic duplication and support for Stowe's model (1986) that a system of thin-skinned tectonic deformation was operative along the western margin of the Kaapvaal craton at one stage in the Early Proterozoic (Beukes and Smit, 1987). Furthermore Stowe (1986) and Beukes and Smit (1987) stated that the Blackridge Thrust is probably related to the Kheis-Korannaberg orogeny which is situated on the western margin of the Kaapvaal craton and is probably reworked $D_1$ blind thrust (Altermann and Hälbich, 1990, 1991). This orogeny is suggested to have taken place between 2000 and 2200 Ma (Beukes and Smit, 1987), but might be younger than 1900 Ma because the Olifantshoek Supergroup (1.9 Ga) has also been duplicated. The main event of the Kheis orogeny D3 correspond to the metamorphic overprint in Marydale Group near Prieska. Furthermore Beukes and Smit (1987) stated that the Transvaal Supergroup lying below the Blackridge Thrust is relatively undeformed.

The next event D4 of Altermann and Hälbich (1990, 1991) deformed the Blackridge thrust, and some re-activation of D1-D2 structures may have occurred. The age of D4 event ranges between 2.07 and 1.88 Ga.

These four deformation events described above correspond to the phase KD1 of Stowe (1986). With the age range from D1 (2.5-2.4 Ga) to D4 (1.88 Ga), it seems that Kheis deformation events started earlier than Stowe (1986) observed. D1 and D2 early deformations from Altermann and Hälbich (1990, 1991) explain the presence of two unconformities, one on top of the Ghaap Group (high-angle unconformity) and one at the top of the Makganyene Formation (low-angle unconformity).

The next deformation events, D5 to D7, are of Namaqua age (1.3 to 0.9 Ga) and redeformed the Kheis Subprovince. According to Stowe (1986), the second event of thrusting KD2 in the Kheis Subprovince is 1.3 Ga old and corresponds to early stage of the Namaqua orogeny. KD2 corresponds to phase D5 of Altermann and Hälbich (1990, 1991). According to Stowe (1986), the second event of thrusting has several hypothesis of occurrence. A gravity mechanism is capable of explaining the thrust features because a weak basal layer materialised as several phyllite zones. The driving force could be uplift of a rearward arc complex or internal thickening at the rear of the thrust wedge complex. The thrust fault may also form in a continental arc convergent setting. If present, an arc would have been situated west of the Kheis belt at about 1300 Ma ago. A thin-skinned thrust belt of this type requires a competent basement at depth less than the brittle-ductile transition (10-15 km), but with the absence of deep seismic profile data this question remains speculative (Stowe, 1986). Therefore no definite model for the formation of the second thrusting event KD2 has been proposed.

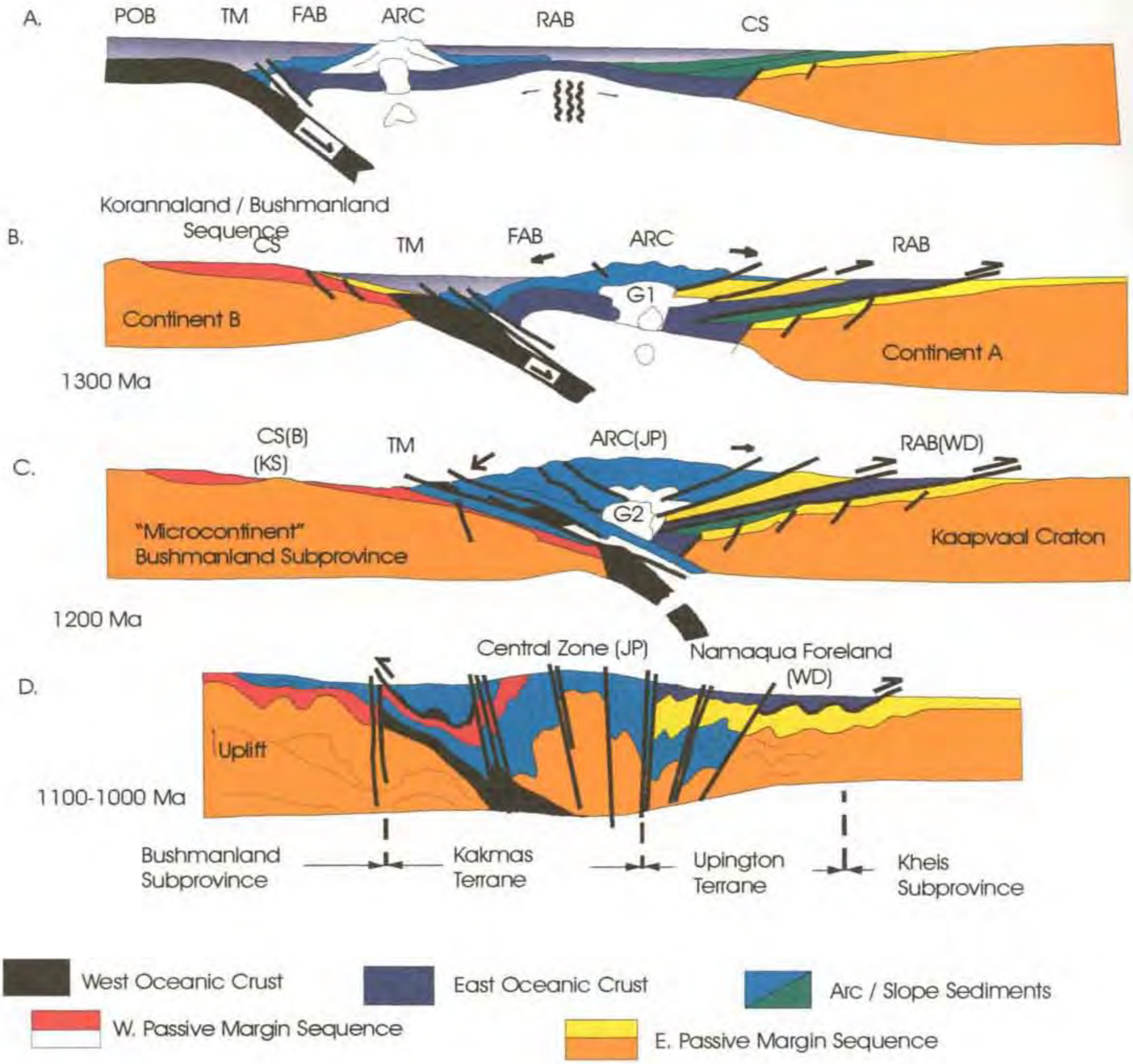


F.9. Model for obduction geometry and their possible relationship to the Wilgenhoutsdrif Formation in eastern Namaqualand. RAB/FAB = Rear/fore-arc basin, POB = Passive ocean basin, TM = Trench melange (after Stowe, 1986).

The Stowe's model (1986) for the Namaqua event is presented in figure 9 (after Stowe, 1986). Most of the present day active subduction zones dip towards the continental margins (as in
figure 9.a) and thrusting spreads outwards, both in the foreland thrust belt towards the continental side of the arc and in the arc-trench gap towards the ocean side. If a continental fragment on the down-going plate arrives at a subduction zone, initial closure and partial obduction of the rear-arc basin may occur (figure 9.b; after Stowe, 1986). Isostatic elevation of this continent/arc-continent complex results in lateral gravity-spreading towards the foreland margins, and subduction will eventually cease (Stowe, 1986). Syntectonic sheets intruding the sub-arc melange and scattered mafic remnants may mark the suture zone, which is situated on the opposite side of the arc complex from the obducted rear-arc basin (figure 9.c; after Stowe, 1986). This model presents the tectonic settings of the deformations of the Transvaal Supergroup on the western margin of the Kaapvaal craton during the Namaqua orogeny.

II.2.2. Local tectonic settings

Field work (mapping) was undertaken in two different tectonic settings. The first setting is located on the autochtonous part of the Transvaal Supergroup (on Vaalwater 84 and Koodooskloof 96) and the second is part of the thrusted section of the Transvaal Supergroup and part of the Olifantshoek Supergroup over themselves (Paauwvlei 190). Maps are shown in figure 10 (Paauwvlei 190 and Koodooskloof 96) and figure 11 (Vaalwater 84).

In the autochtonous part of the Transvaal Supergroup, on the farm Koodooskloof 96, the outcrops display gentle folding forming anticlines and synclines. Their general trend is 160° with a plunge of 14° to the south. The trend and plunge of these folds follow well the general trend of the outcrops rising above the flat lying Kalahari Formation. This fold system provides shelters located in the synclines from weathering of the soft Makganyene Formation relative to the underlying harder formations. Due to the absence of the Ongeluk lava on the farm, the whole succession of the Makganyene is not present. The dipping of the strata is generally between 15/20° and ranges from 5° to 44°. Three major faults were mapped on the farm Koodooskloof 96. The western faults have a strike approximately N-S and the other fault is NE-SW, the three of them

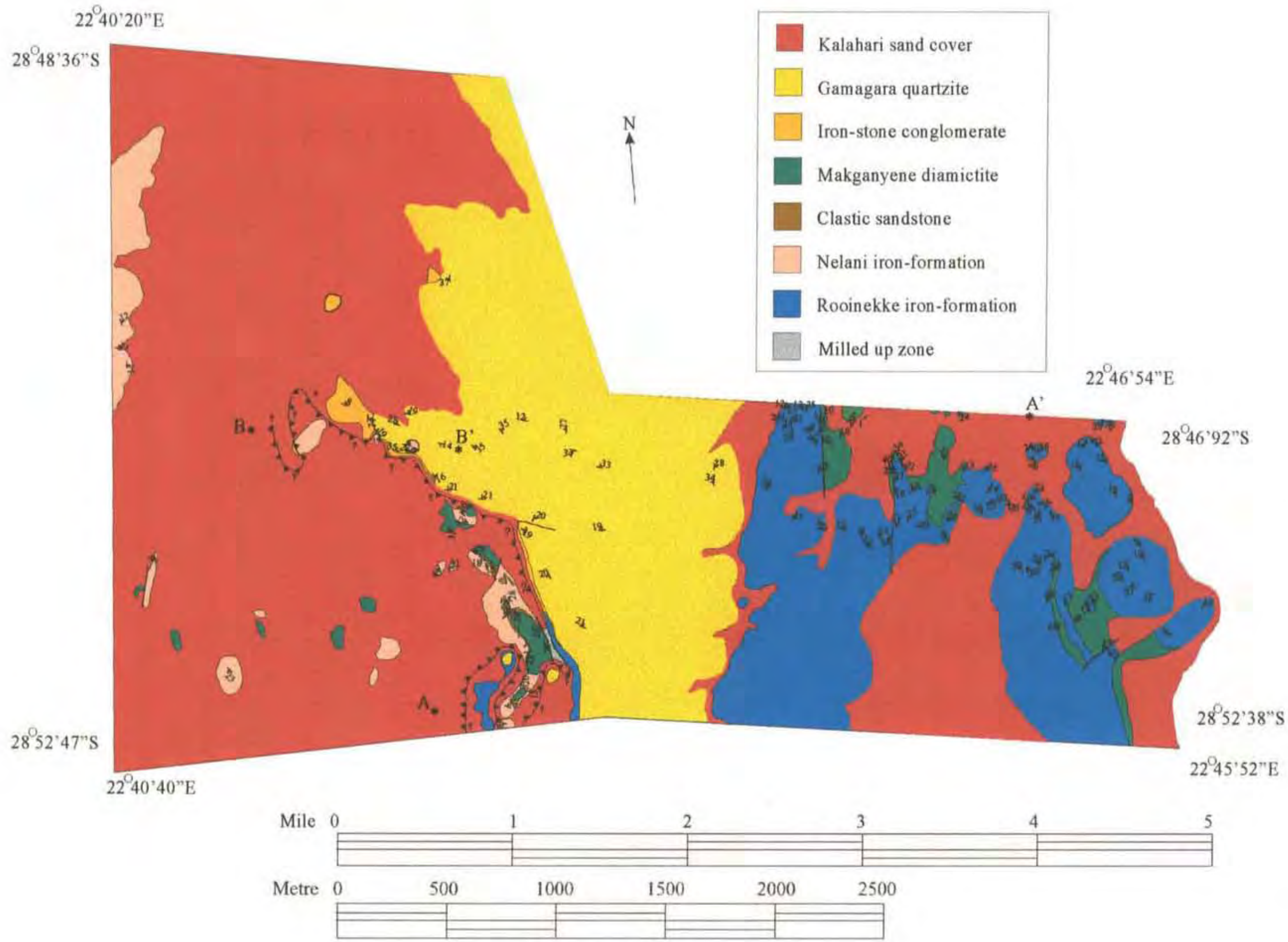


F.10. Geological map of the farms Koodooskloof 96 and Paauvlei 190.

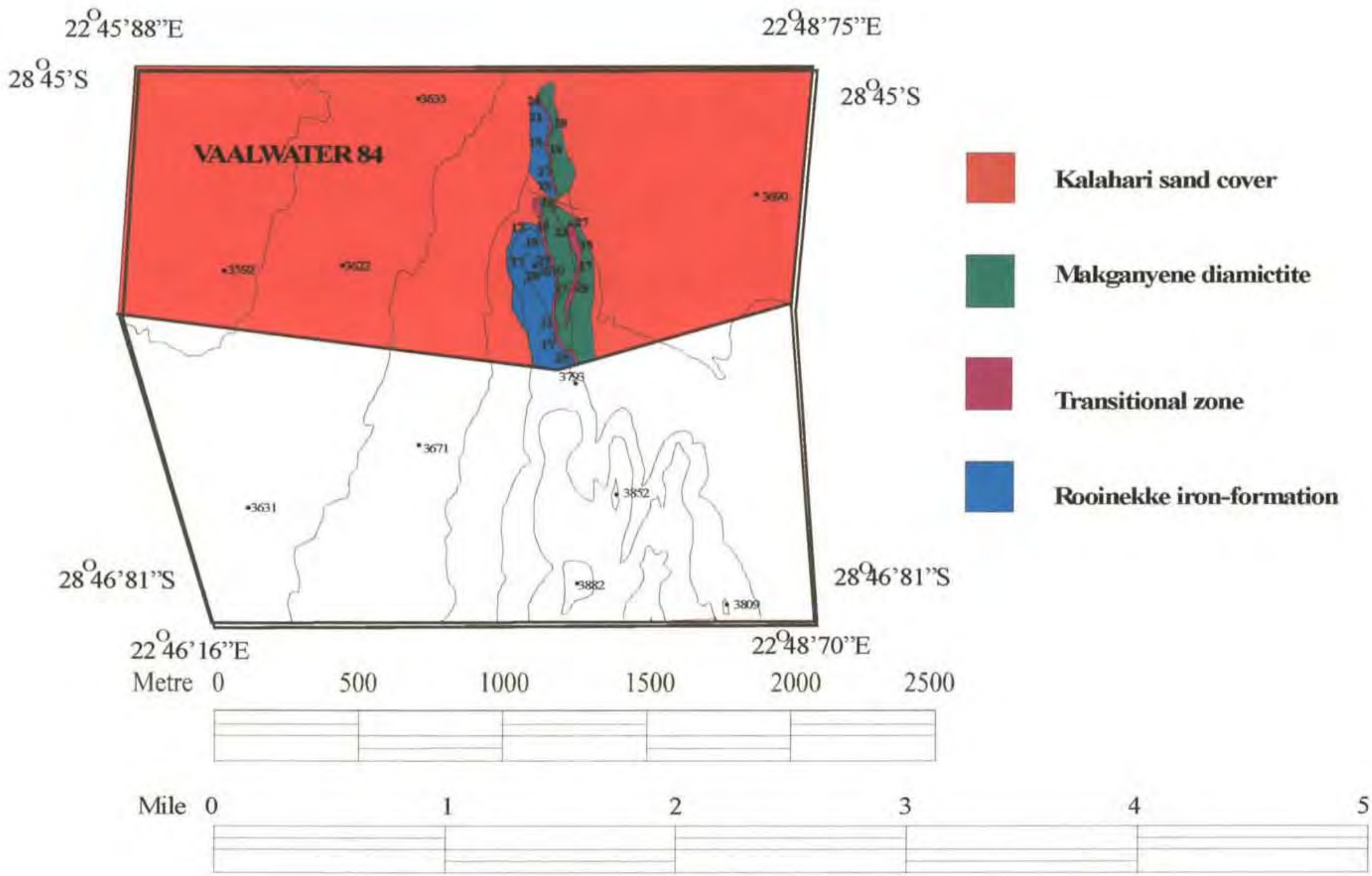


F11. Geological map of the farm Vaalwater 84.

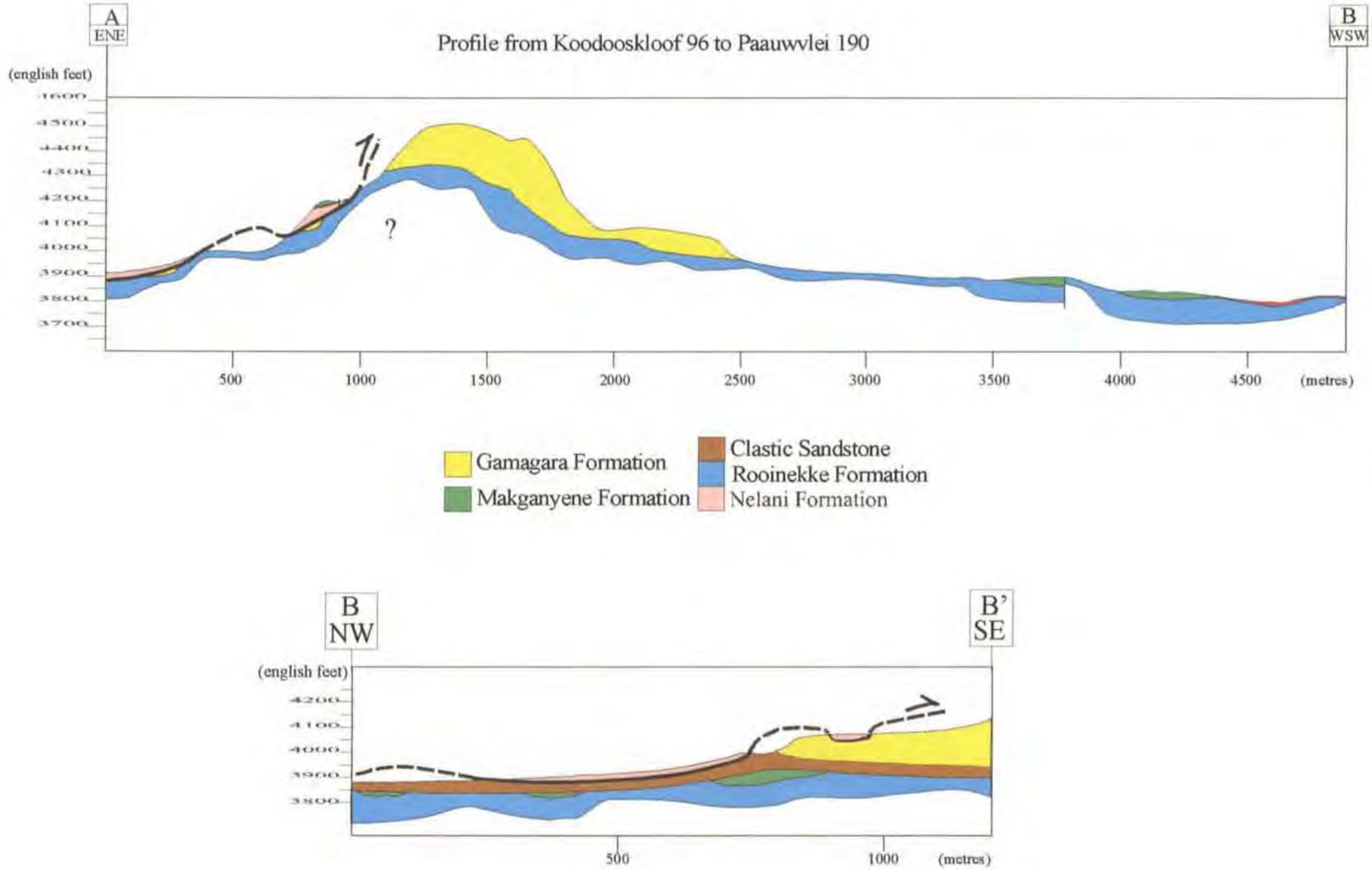


F. 12. Sections from figure 10 where section lines AA' and BB' are located.

dipping steeply almost vertically. The two western faults form a grabben due to normal faulting. Their throw is less than the entire thickness of the Makganyene Formation (about 150 metres) because of the absence of the Ongeluk lava on top. The NE-SW fault is a normal fault. The throw is very small, certainly in the order of few metres. This is easily explained by the progressive changes in facies of the underlying iron-formation towards the Makganyene Formation: the hanging-wall shows facies characteristics of being very close to the contact, and the foot-wall has the contact preserved.

On the farm Vaalwater 84, strata are dipping gently to the east with a very constant value of 18° despite the presence of a fold (anticline) elongated N-S, dipping to the south with an angle of 15°. comparative value found on Koodooskloof 96. Three faults were observed, displacing the zone forming the contact between the Rooinekke and the Makganyene Formation. Their trend is NE-SW and the displacement is small (in the order of a metre or two). A fourth fault was assumed between the two hills (see the figure 11) but covered by the recent Kalahari Formation. The throw is important (one tenth of metres) relative to the other mapped faults.

P. 1. Highly deformed clasts from the Makganyene Formation along the Blackridge Thrust sole.

On Paauwvlei 190, a major thrust fault duplicating the Transvaal is present. This thrust fault is called Blackridge Thrust (Beukes and Smit, 1987). As shown on figure 10 and 12, evidence for this thrust is found by the presence of intense deformation (breccia, highly deformed clasts within the diamictites: see photo 1), of klippes and windows. The klippes are non eroded remnants of the Nelani Iron-Formation sitting on top of the Gamagara quartzite, which are more commonly found where section BB' of figure 12 was drawn. Windows can be observed when autochtonous rocks (Rooinekke Formation and/or Gamagara Formation) are found below the Nelani Formation, and are partly shown in the section AA' of figure 12. The thrust surface is apparently folded by the D4 event of Altermann and Hälbich (1990, 1991), which represents the last event of the Kheis orogeny by folding the previous structures (folds and thrust). Few minor normal faults have a movement of a few tens of centimetres causing duplication of the contact between the Makganyene Formation and the Nelani Iron-Formation. The Makganyene Formation is preserved at the top of an elongated ridge in a syncline. Outcrops are generally localised on topographic heights on Paauwvlei 190, because the low lying terranes are covered by the Kalahari sand, resulting in very localised outcrops.

## II.3 Field work observations

Field work took place in the farms Koodooskloof 96, Paauwvlei 190, and Vaalwater 84 and comprised mapping and description of outcrops with emphasis on the basal contact of the Makganyene Formation with the underlying Koegas Subgroup. Additional observations were made with borehole material provided by ISCOR at Sishen and ASSMANG at Boshoek.

### II.3.1. Lower Contact

In the field the contact looks gradational on Vaalwater 84 where some layers of diamictite, ten centimetres thick, are interbedded with the iron-formations of the Rooinekke Formation with a sharp contact, no brecciation can be seen, so this is unlikely a structural duplication, but a true interlayering of diamictite within the iron formations (see figure 13). Each layer of diamictite is a few metres apart from the other on Vaalwater 84, and it is on this farm that the interlayering of diamictite with the Rooinekke Iron-Formation can clearly be observed. This interlayering is strictly conformable and can be followed on aerial photographs.

On Koodooskloof 96, the underlying rocks are also the Rooinekke Iron-Formation from

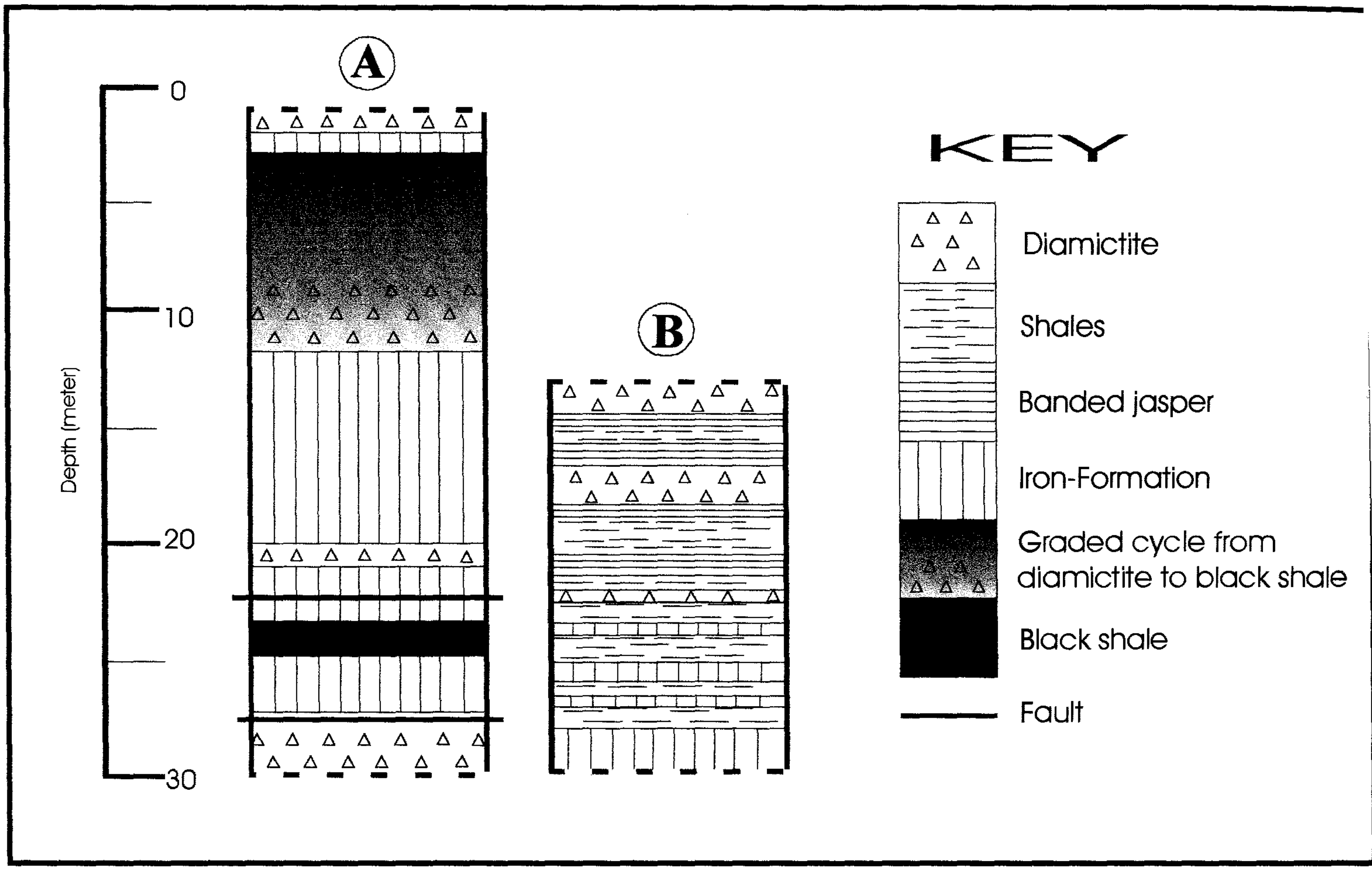


F. 13. log showing the basal contact of the Makganyene Formation (diamictite and shales) with the underlying Rooinekke Formation (iron-formation and banded jasper) at A: Ga171, borehole from Sishen; B: profile from Vaalwater 84.

the Koegas Subgroup. The Rooinekke Formation, far below the contact with the Makganyene Formation looks like a typical banded-iron-formation: alternance of bands of silica-rich and iron-rich bands (see photo 2). By going up in the stratigraphy, i.e. towards the contact of the Rooinekke Formation with the Makganyene Formation, the banded iron-formations become progressively more silica-rich, or banded jasper (see photo 3). The contact between the diamictites and this banded jasper is very sharp, and a conformable relationship is observed (see photo 4) leaving further evidence for the absence of an unconformity at the base of the Makganyene Formation . As occurred in Vaalwater 84, two very thin levels (about 10 cm each) of diamictite are present below the main contact shown on photo 4. On Koodooskloof, this intimate interlayering between diamictites and iron-formations (see photo 5) is not as well developed as on Vaalwater 84. No structural duplication is responsible for this interlayering.

P. 2. Typical Rooinekke Iron-Formation far below its contact with the overlying Makganyene Formation.

P. 3. Typical banded jasper found closer from the base of the Makganyene Formation.

P. 4. Contact between the Rooinekke Iron-Formation and the Makganyene Formation.

P. 5. Level of diamictite within the banded jasper present at the top of the Rooinekke Formation.

On Paauwvlei 190, just on the western side of the Gamagara ridge separating Paauwvlei 190 from Koodooskloof 96, the contact is different, but still looks conformable with the underlying Nelani Iron-Formation. The true diamictites (terrigenous matrix and cherty angular clasts) are underlain conformably by a clastic sandstone unit. The contact between this clastic sandstone and the diamictites is gradational and depends essentially on the grain size of the matrix (sandy in the clastic sandstone, muddy in the diamictites. This clastic sandstone is in turn underlain by a massive iron-stone (iron-rich mudstone) of the top of the Nelani Iron-Formation. The contact with the overlying clastic sandstone is sharp, but not originally represented by a flat surface, but rather by a disturbed level of the underlying iron-rich clay and some tongues of sandstone (see photo 6).

The farms Vaalwater 84 and Koodooskloof 96 are situated east of the Black Ridge Thrust Fault. Here, the Makganyene Formation shows interbedding with the underlying formations shown in figure 13. On the other hand, on the farm Paauwvlei 190, which is located on the main sole thrust, much deeper in the basin relative to the platform, the Makganyene Formation has a layer of clastic sandstone of about 2 to 3 metres thick at its base.

In the cores available at Boshoek (MTP-4 and MTP-9) and Sishen (SA-1977, GA-129 and

GA-171) (see figure 14), the basal contact of the Makganyene Formation cannot be observed due to thrusting. But in these cores, the Makganyene Formation exhibits similar interbedding (banded iron-formations, shale, sandstone interbedded with diamictite) as seen on the field in farms Koodooskloof 96 and Vaalwater 84, which seems to be an important feature of the contact described previously.

P.6. Contact between the Nelani Formation and the Clastic Sandstone from the Makganyene Formation.

II.3.2. Description of the outcrops

On Paauwvlei 190, the formation below the Makganyene diamictite is the Nelani Formation. The lowest part of the Nelani Formation outcropping (10 m below the top contact) is a typical banded iron-formation that is finely laminated (bands up to 2 cm thick). This facies becomes interbedded with iron-rich mudstone, first with 2 cm thick shale bands. The thickness of the iron-rich mudstone (dark reddish to pinkish in colour) gradually increases up to 50 cm, and finally the iron-rich mudstone becomes massive at about 3-4 metres below the contact with the Makganyene Formation. The iron-rich mudstone is the "musdtone unit", often jasperoidal of Thatcher et al. (1993), only present west of/above the Blackridge Thrust.

The base of the Makganyene Formation consists of a coarse clastic sandstone. The clastic sandstone has a regular thickness of approximately 5-10 m. The clasts within this unit show the same characteristics as the diamictite : angular, elongated, and the same composition : cherty (from green to purple to whitish), but some clasts are of intra-clast origin (muddy clasts). The weathering aspect is the same as a granite : well rounded boulders crop out on the surface. The colour is red in general, but can be whitish. This clastic sandstone unit differs from the Gamagara Quartzite which is generally whiter in colour, has smaller and much more rounded clasts, varying in colour from bright red to black, and has a clast composition including iron-formation not present in the clastic sandstone. The latter unit does not show any bedding, graded cycles, or any sedimentary structure, but contains some rare thin lenses (up to 30 cm wide) of grey siltstone with a thin regular planar bedding.

At the field work localities, the diamictite can readily be identified from the presence of angular cherty clasts in a muddy to sandy matrix. The colour of the matrix is reddish to brown, and may be difficult to differentiate with the top of the Nelani Formation (below the clastic sandstone) which have the same colour and same grain size of matrix. The clasts are randomly distributed, with some areas having a very dense clast content and some mainly composed of shaly matrix (see photo 7). On Paauwvlei 190, the diamictite forms beds approximately 2 m thick, each one generally separated from the other one by a thin, up to 30 cm thick shale unit (see photo 8). In this case, each layer may be part of a debris flow where the thin material accumulates on top before the next debris flow.

P. 7. Typical aspect of the Makganyene diamictite, with heterogeneous clast size and distribution.

P. 8. Thickly layered diamictite (about 2 metres thick).

On Vaalwater 84 and Koodooskloof 96, the underlying formation is the Rooinekke Formation. The description of the contact between the Rooinekke Formation and the Makganyene Formation has already been discussed. The Rooinekke formation is a typical banded iron-formation far below the contact (see photo 2). It becomes more silica-rich towards its contact with the Makganyene Formation (see photo 3). At the contact with the diamictite, the jasper of the Rooinekke Formation contains abundant syneresis cracks (Beukes, 1983) (see photo 4).

P.9. a. and b. show two different striated pebbles with angular facets.

The clasts within the diamictite can show a rough orientation. But generally, the clasts are disseminated randomly in the matrix (see photo 7). They show a general angular to sub-rounded shape, with sizes ranging from 0.5 cm to almost 30 cm. Striated clasts can be found through intense searching (see photos 9.a. and 9.b.). Dropstones are also present and are characterised by the clast itself compacting surrounding smaller clasts (see photo 10).

Some outcrops are very weathered : hematised or show the desert varnish.

P. 10. Dropstone compacting the surrounding smaller clasts.

The borehole samples show the intimate relationships between the clastic diamictite and the chemically precipitated banded iron-formation within the Makganyene Formation (see figure 13 and 14). The banded iron-formations are of two types, one is found in Sishen area and is well banded to slumped with a thickness up to 12 metres. The second type is found in the Matsap Hill area where the banded iron-formations are up to 1 metre thick with incorporated clastic material such as dropstones (3 cm diameter) or completely slumped (2 to 10 cm thick). It is important to emphasise on the distribution of the banded iron-formation within the core. They are present throughout the boreholes, but thicker towards the base.

The Sishen type can be divided into three categories. The first group represent the regularly well banded iron-formations which are strongly magnetic. Black magnetic bands of generally 3 mm thick alternate with red-brick coloured hematitic bands. The second group is

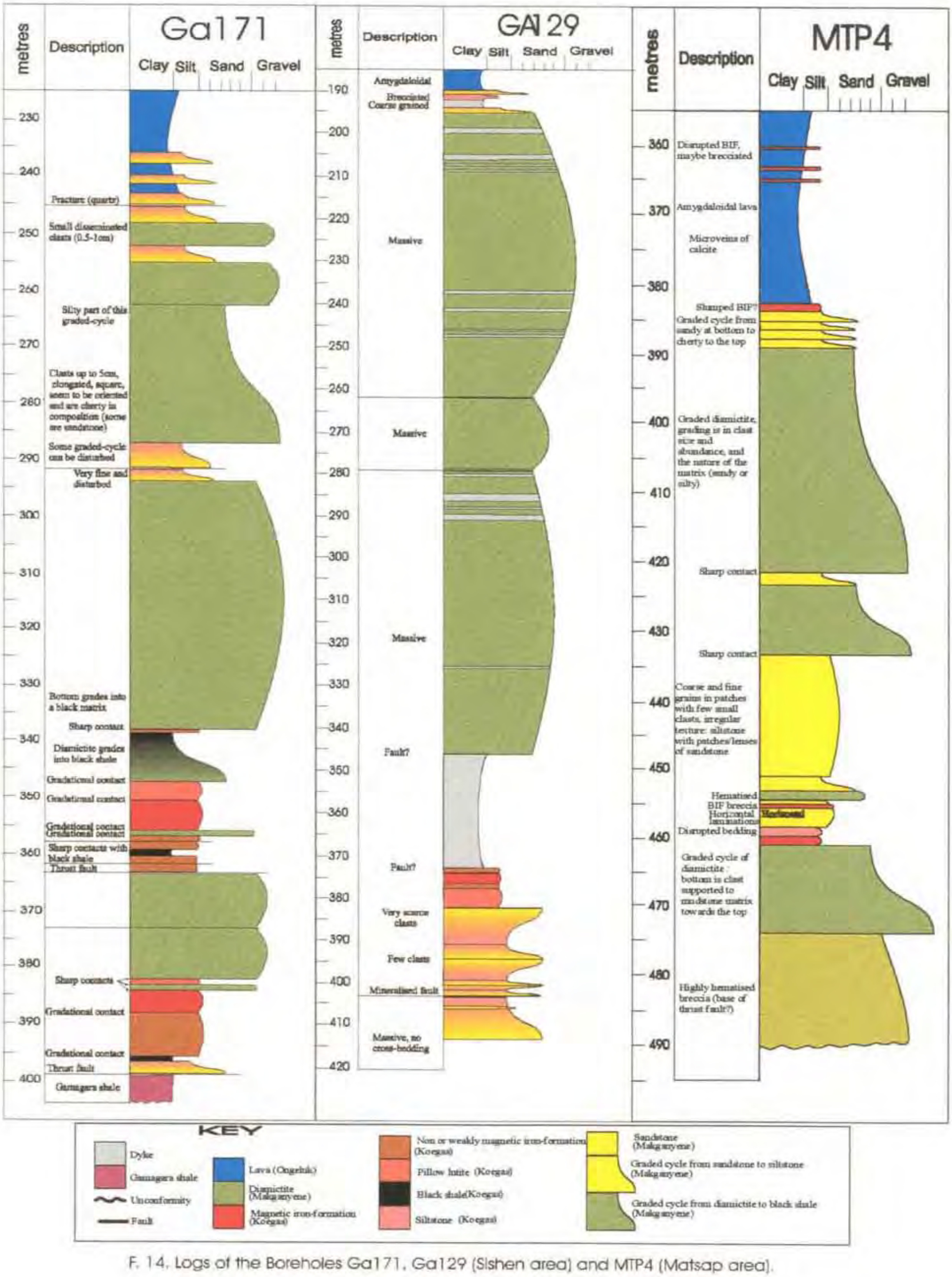


F. 14. Logs of the Boreholes Ga171, Ga129 (Sishen area) and MTP4 (Matsap area).

similar to the first, but intense syn-sedimentary deformation (slumping) occurred. The samples are less magnetic. The third group is also similar to the first group, but the bands contains elongated pillows composed of chert. The contacts between each type are gradational. In borehole GA171, diamictite grades into black shale which in turn grades into banded iron-formation, or banded iron-formation grades into black shale to in turn grade back into banded iron-formation.

Sandstone units are present in boreholes, especially towards the base of the Makganyene Formation (borehole GA171 and GA129). The sandstone is massive and white in colour with rounded grains (15 metres thick) or can grade into siltstone. Inverted graded cycles occur in borehole GA129, from siltstone to sandstone. Shale units are also present, black shale may grade from banded iron-formation and diamictite, or grade into banded iron-formation.

II.3.3. Upper Contact

Field and core observations

The upper contact between the Makganyene and the Ongeluk Formations has not been observed in the field. However within borehole cores available at Boshoek (MTP-4 and MTP-9) and Sishen (SA-1977, GA-129 and GA-171) (for locations see annexe A1), the upper contact is well observed and described. The top of the Makganyene Formation, in the cores, is composed of fine normal graded cycles. Each cycle measures about seven centimetres in thickness, starting with a fine sandstone (silty-sandstone) and finishing with very fine silty laminations of less than 1 millimetre in thickness. These graded cyclic units contain some interbedded levels of amygdaloidal lava with sharp bottom and upper contact. These graded cycles can be interpreted as volcanic tuff. Volcanic eruptions provided the Griqualand West Basin with ashes which accumulated prior to the appearance of the Ongeluk Lava. One cycle represents slumped material for the volcanic eruptions and settled down in the basin in the way observed today, i.e. coarse base and very fine top part. These graded cycles lie conformably on the coarse diamictites and are also interbedded within the diamictites. Therefore the upper contact between the Makganyene and the Ongeluk Formations is not a sharp contact, but rather gradational from a sedimentary to a volcano-sedimentary to exclusively volcanic environment. The Ongeluk Formation is composed of a monotonous succession of greyish-green andesitic lava (Visser, 1958). In all localities hand-specimens at the contact commonly show small pyroxene crystals varying in composition from diopside to pigeonite augite and surround orthopyroxene (enstatite) or occur as irregular intergrowths with feldspar (Truter et al., 1938).

This gradational upper contact shows that there was no significant time gap between the Makganyene Formation and the Ongeluk Formation of the Postmasburg Group, but rather a continuous process in the stratigraphy.

## II.4. Conclusion

The observations made in the field and in the boreholes show close relationships between banded iron-formations and glacigenic rocks from the Makganyene Formation. The basal contact is generally represented by interbedded iron-formations of the Rooinekke Formation of the Koegas Subgroup with clastic rocks (sandstone, siltstone, diamictite) from the Makganyene Formation. Another type of contact is characterised by a 2 m thick layer of clastic sandstone on Paauvlei 190 lying conformably between the underlying Nelani Formation of the Koegas Subgroup and the Makganyene Formation. This clastic sandstone forms the base of the Makganyene Formation in this location. The first conclusion is that the Makganyene Formation is broadly conformable with the underlying banded iron-formations of the Koegas Subgroup. The top contact, only observed in boreholes, is also conformable. These gradational lower and upper contacts of the Makganyene Formation with the surrounding formations show that there was no significant time gap between the Ghaap Group and the Postmasburg Group depositions.

The characteristics of the different facies of the diamictite show that water was present during the glacial period. This important conclusion assists determinations of the type of glacial front in the depositional model of the Makganyene Formation.

# III Petrography and geochemistry of the Makganyene Formation

## III.1. Petrography

### III.1.1. Introduction

Basic petrographic studies of the different rock types (i.e. diamictite, banded iron-formation, shale, sandstone, siltstone) of the Makganyene Formation were undertaken during this project. Both microscope and X-Ray Diffraction (XRD) methods were used for identification of the mineral phases.

### III.1.2. Methods

The main characteristic of the clastic facies of the Makganyene Formation is the very fine grained matrix which contains clasts of different sizes. The characteristic of the iron-formations interbedded within the diamictite and of virtually all unmetamorphosed Proterozoic iron-formations, as far as mineralogical studies are concerned, is their extremely fine grained nature, and the iron-formations present are not an exception.

Identification of minerals by XRD was done on powder patterns which were obtained using a Philips Standard Water-Cooled Diffractometer. The powdered samples were packed onto aluminium slide holders. CoK$a_1$ radiation was used with variable instrumental settings (30-40 kV, 20-30mA) and a scan rate of 1°/30 sec. Minerals were identified by comparison with the values of d-spacing given in the Powder Diffraction Data File, published by the International Centre for Diffraction Data (JCPDS, 1974, 1980).

### III.1.3. Mineralogy

The Makganyene Formation contains several types of lithologies : diamictite, sandstone, siltstone, black shale and iron formations. For each of the rock types, the mineralogy is presented in table 1.

As shown in the table 1, no plagioclase has been determined using the XRD method, minimising the influence of any igneous input to the Makganyene clastic rock types. The mineral assemblage found does show a diagenetic to low metamorphic facies. The groups of minerals defined by James (1969) for iron-formation mineralogical descriptions, including silicates, carbonates, oxides and sulphides, are used here not only in banded iron-formations, but also on the other rock types for a clear systematic.

Slight differences in mineralogy can be seen in table 1. The mineralogy of the diamictite and all the clastic rock types depends essentially on the type of the source, the weathering processes (either mechanical or chemical) and on the different sedimentary processes, such as sorting during transport. Diamictite and iron-formation contain similar mineral assemblages. The difference between the two is the presence illite and the absence of magnetite and chalcopyrite. The sandstone and siltstone must have undergone high degrees of sorting during transport to the site of accumulation, explaining the differences in mineralogy : only the hardest mineral (quartz), the diagenetic to low-grade metamorphic minerals (siderite and chlorite) are present.

| Minerals | Diamictite | Sandstone | Siltstone | Black shale | Iron formation |
|---|---|---|---|---|---|
| silicates | | | | | |
| Illite | X | X | | | |
| Chlorite | X | X | X | X | X |
| Greenalite | (X) | | | | X |
| Stilpnomelane | (X) | | | X | X |
| Chert, quartz | X | X | X | X | X |
| carbonates | | | | | |
| Dolomite-ankerite series | X | | | X | X |
| Siderite | X | X | X | X | X |
| oxides and sulphides | | | | | |
| Magnetite | | | | | X |
| Hematite | X | | | | X |
| Pyrite | X | | | X | X |
| Chalcopyrite | | | | | X |

T.1. Mineralogy of the different rock types of the Makganyene Formation determined by XRD.

A difference in the mineral composition between the iron-formations present in the Makganyene Formation and other iron-formations in the Transvaal Supergroup is the absence of minnesotaite and riebeckite. According to Beukes (1978, 1983), Beukes et al. (1982) and Tsikos (1994), minnesotaite is one of the most common minerals in diagenetic to low-grade metamorphic banded iron-formations. According to Tsikos (1994), minnesotaite is common throughout the stratigraphic column in certain boreholes in the Voelwater Formation, and may be virtually absent in others. This indicates a vertical consistence as well as a lateral impersistence in its occurrence, and that the absence of the minnesotaite in the samples of the present study does not rule its absence in the entire area.

Riebeckite is also a major constituent in banded-iron formations of the Griqualand West Basin (Beukes, 1978, 1980, 1986, Tsikos, 1994). But its absence in the Makganyene Formation continues in the Voelwater Formation where riebeckite is an uncommon mineral of diagenetic origin (Tsikos, 1994).

The following paragraphs are dealing with the petrography of the different rock types which are diamictite, iron-formations, sandstone, siltstone, shale, and the graded cycles towards the top of the Makganyene Formation.

III.1.4. Petrography of the Makganyene Formation

III.1.4.1. Introduction

The different rock types of the Makganyene Formation have been observed under transmitted light. Six different rock types can be distinguished : diamictite (or poorly sorted mixture of rock fragments within a clay matrix), iron-formation, sandstone, siltstone, shale and graded cycles. Since outcrop descriptions have already been made in the chapter II, just microscopic observations follow. A total of 28 thin sections were examined during this study.

III.1.4.2. Petrography of the diamictite

Under the microscope, the diamictites follow the same trend as in the outcrops. They are constituted of poorly sorted angular rock fragments inside a matrix. These rock fragments can be of two types : chert and/or quartz grains and intraclasts (or clasts of matrix).

Chert is the most abundant clast present in the Makganyene Formation and is therefore one of the major constituent of the diamictite . Chert is composed of very fine grained quartz. But single quartz grain clasts are also present. On photos 11.a. and 11.b, different clasts can be distinguished:

- the common angular to subrounded chert, composed of very fine grained quartz,
- angular to subrounded banded chert, where the bands are hematite-rich within a cherty matrix,
- angular quartz grains.

Some anhedral carbonate aggregates could be mistaken for clasts, but these are clearly late diagenetic due to their recrystallisation in their euhedral shape (rhombohedral). But some carbonate clasts have been observed during the present study, having the same average shape as the cherty clasts, maybe more rounded, but this type of clast is very scarce (see photos 11.a and 11.b). The relationships between clasts and carbonate minerals are easy to see under microscope in fresh samples : the carbonate minerals tend to replace the clast (see photos 12.a and 12.b).

As stated before in the definition of a diamictite, the clast size is heterogeneous, and could even become so fine that the clasts could be included in the matrix. This is due to the glacial processes, supplying clasts from up to 30 cm in diameter to rock flour. And it is the latter which will constitute the major part of the matrix. Some hand-specimens show an orientation of clasts which could be interpreted as an orientation under the influence of submarine currents. But in thin section, this apparent sedimentary structure represents a soft sediment deformation due to shearing which induced rolling structure of clasts (see photo 13).

The matrix of the diamictite is made out of very fine quartz, chlorite and early diagenetic carbonates. Stilpnomelane and greenalite have been identified optically in a very disturbed diamictite-iron-formation like (because of the presence of clastic input : quartz grains and chert) (see photo 14). These two silicate minerals are absent in the more common type of diamictite. Some clasts are intraclasts, certainly due to the remobilisation of the sediments which have undergone further sedimentary processes after deposition. Since the matrix is fine grained, XRD means for identification were indispensable. Greenalite, in the disturbed iron-formation, as shown on photos 15.a and 15.b, replaces the chert clasts from the margins, developing needles pointing towards the centre of the grain (or clast).

The easiest minerals to identify are the rhombohedral carbonate minerals . The carbonate minerals are from the dolomite-ankerite series and siderite (positively identified by XRD means). Distinction between the carbonates is not evident under microscope, but the members of the dolomite-ankerite series have a rhombohedral shape with a "cloudy" centre (Tsikos, 1994). These carbonate minerals are disseminated evenly within the matrix, but could show a higher concentration near a quartz/carbonate vein.

Late veining is also present. The veins consist of quartz/carbonate or hematite.

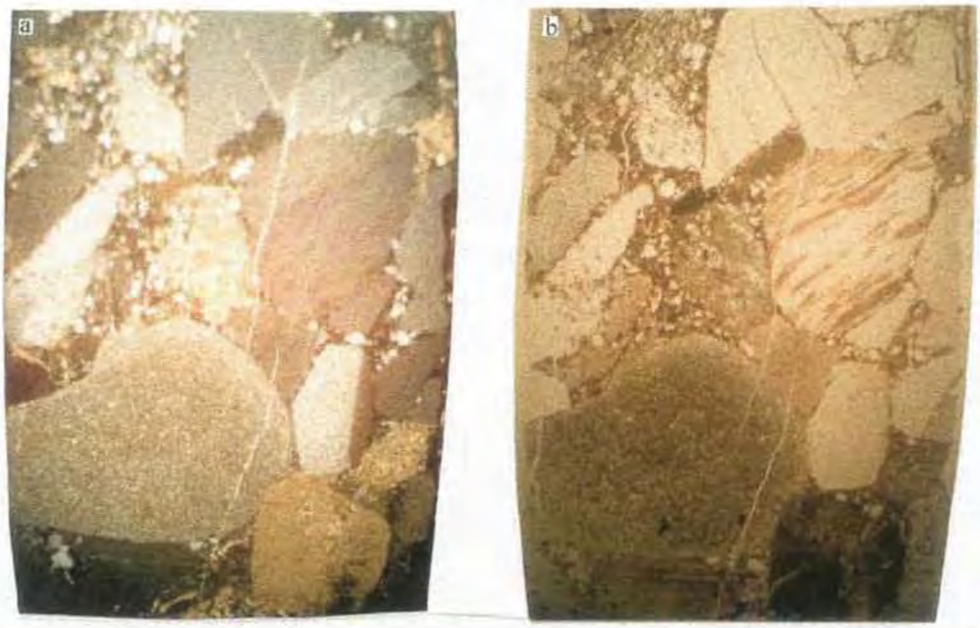


P. 11. Clasts present within the Makganyene diamictite : chert, banded jasperoid, carbonate (bottom right), 13 mm across. a : cross-polar; b: plain polar.

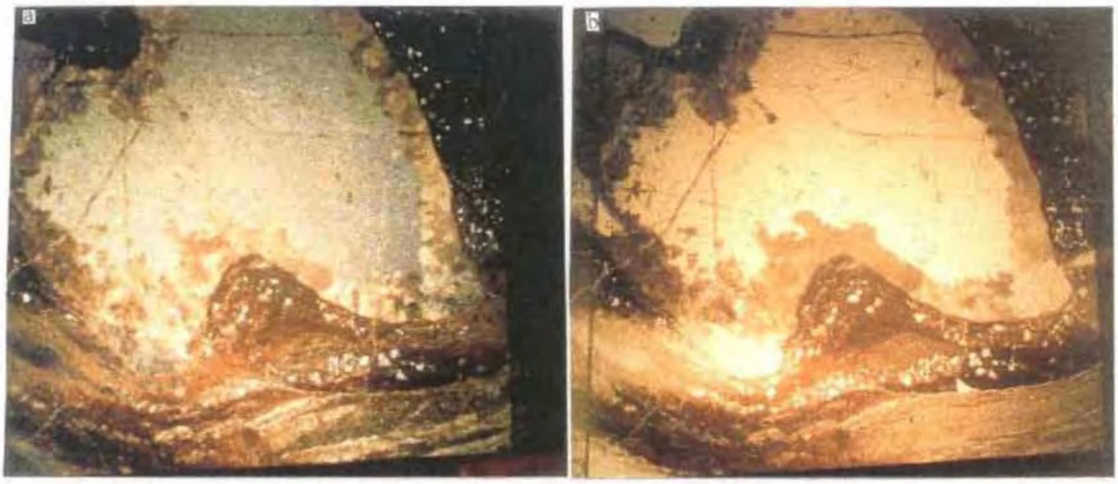


P. 12. Dropstone being replaced by carbonate in banded iron-formation from the Makganyene Formation, 24 mm across. a: cross-polar; b: plain polar.

P. 13. Evidence of searing in soft sediments (plain polar), 8 mm across.

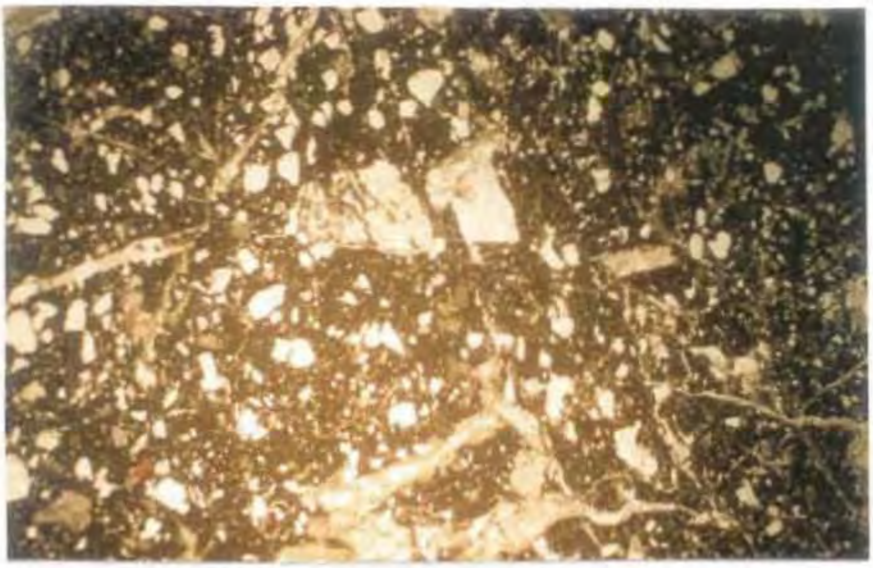

P. 14. Diamictite having the same composition as an iron-formation, 24 mm across.

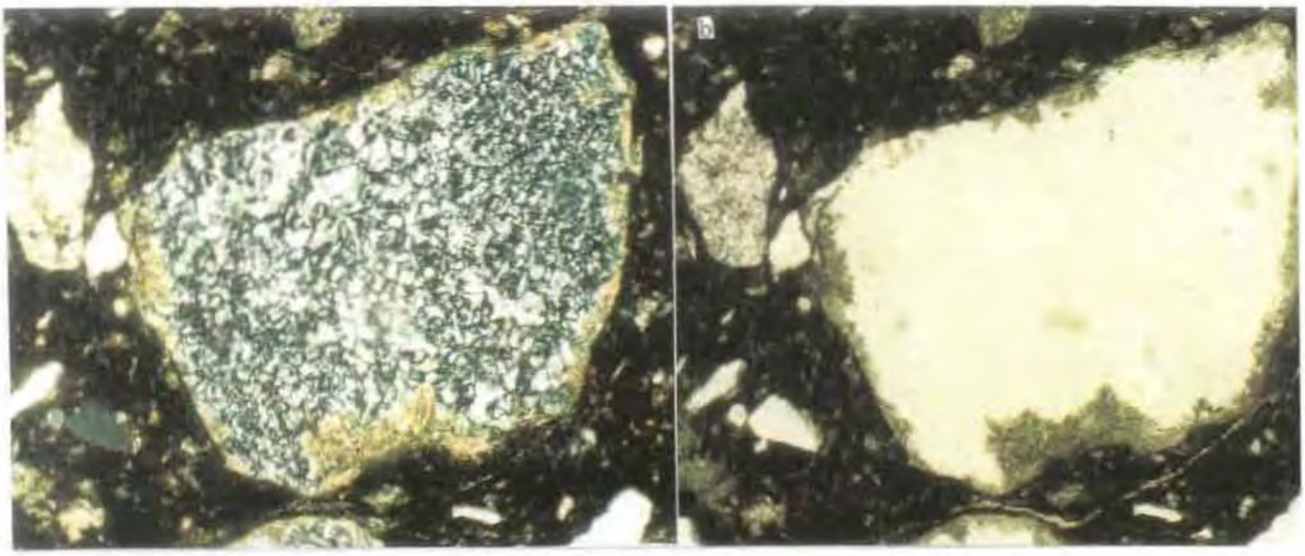


P. 15. Clast of chert being replaced by greenalite, 4 mm across. a: cross-polar; b: plain polar.

III.1.4.3. Petrography of the iron formations

Different types of iron formations have been identified during the present study :

- the common highly magnetic, well banded iron formation from Sishen,
- the iron formation containing pillows from Sishen,
- disturbed iron formations (slumped, having dropstone...) from Sishen and Matsap.

The iron-formation criteria in this study was the presence of alternating bands of hematised chert with bands of magnetite. A very disturbed iron formation showing no banding and presence of clasts was classified in the diamictite class. But in this section, a banded iron-formation can have clasts if the banding is still evident. The mineral phases present in the Makganyene Formation are summarised in table 1.

The well-banded and strongly magnetic iron-formation from the Makganyene Formation contains bands of pyrite and/or magnetite-rich which are developed, giving the typical banded aspect of the iron-formation. Magnetite and Pyrite are mainly primary minerals, including chert. Hematite is extensively present in the samples, giving a distinctive reddish to pinkish colouration of the altered minerals (from carbonate to magnetite to chert). The matrix is invariably composed of a background made out of chert with some early diagenetic to low-grade metamorphism fine euhedral carbonate grains which are generally more concentrated within veins, but present throughout this chert matrix. Late Carbonate and quartz micro-veining (less than 1 mm thick) which are inter-related to each other, forming a hair-like network. This network is not as developed as it could be in some samples. These veins display coarse grained size compare to the matrix.

The well banded iron formations containing pillows have the same features as the well banded and strongly magnetic iron-formations of the Makganyene Formation. The difference is the presence of pillows (Beukes, 1983). The pillows observed are composed mainly of chert with very minor fine grained patches of carbonates. The shape of a pillow is ellipsoidal with a length of the long axes ranging from 7 to 3 centimetres. The banding around them follows the margins of the pillows. This means that the pillow formation was early diagenetic. A pillow displays generally replacement features from the margins to the centre by coarse grained carbonate The latter is partly replaced by greenalite and stilpnomelane (see photos 16.a and 16.b). In places the lutite matrix is intensively replaced by stilpnomelane, and this is occurring next to the pillow.

In the disturbed iron-formations, having generally been slumped or containing dropstones, the characteristics described for the first type of iron-formation are the same, except that the sample is not well banded. The amount of clastic detrital quartz grains is not negligible (see photos 17.a and 17.b and 12), and generally the largest dropstones display the same carbonate rim as a pillow. The dropstones clearly disturb the banding, indicating emplacement in an unsolidified stratified mud.

By comparison with all the banded iron-formations from the Transvaal Supergroup, only the iron-formations from the Makganyene Formation contain dropstones. This is a fundamental evidence for deposition and accumulation of banded iron-formation under ice (iceshelf or iceberg) in cold climate. The presence of pillows have been observed by Beukes (1980) at the topmost parts of both Kuruman and Griquatown Iron-Formations. In the Pietersberg Member, topmost part of the Griquatown Iron-Formation, pillowlutites are present (Beukes, 1980). Overlying the Pietersberg Member is the Makganyene Formation which also displays pillows towards its base. The Rooinekke Formation is also stratigraphically situated below the Makganyene Formation. The Rooinekke Formation consists predominantly of orthochemical iron-formations with relatively thin interbedded shales, mudstones and siltstones (Thatcher et al., 1993). The iron-formations from the Rooinekke Formation contain also pillows. The similarities between the Griquatown (topmost part of the Ghaap Group), Rooinekke and Makganyene iron-formations are striking. Are these iron-formations from the same stratigraphic level, meaning that they are interbedded? This sensitive point will be discussed in the last chapter.

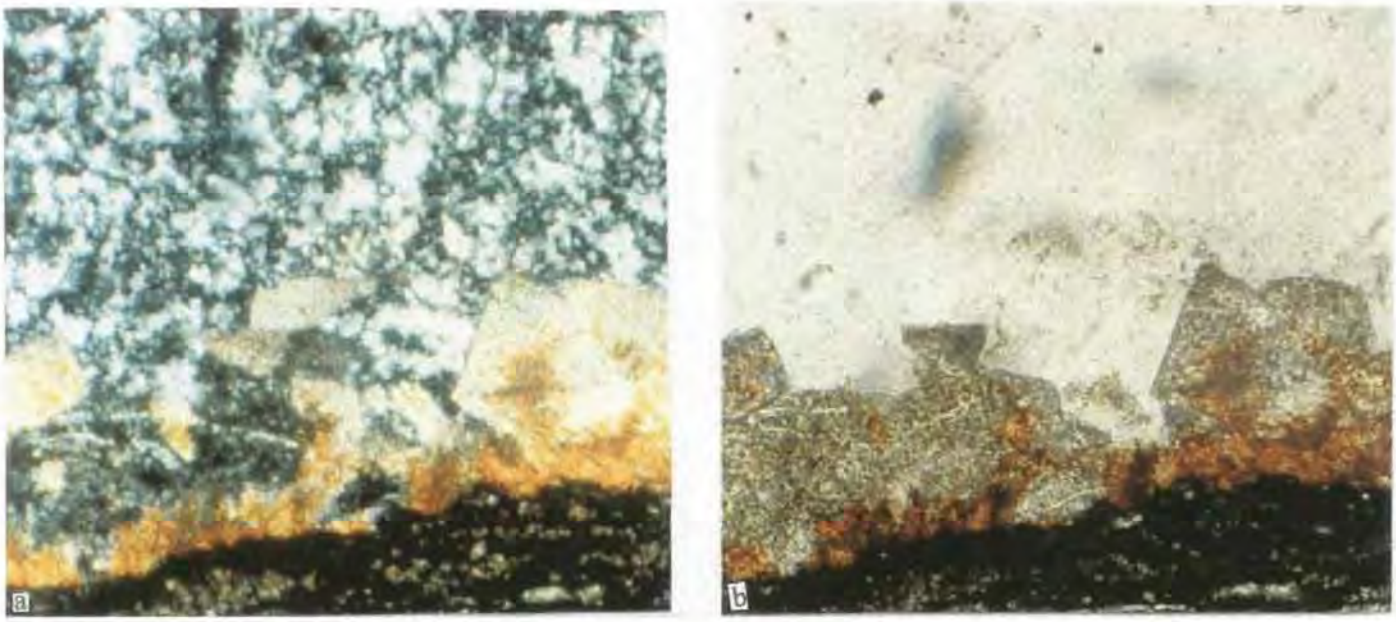


P. 16. Late stilpnomelane replacing carbonates (same carbonate as photo 12), 4 mm across. a: cross-polar; b: plain polar.

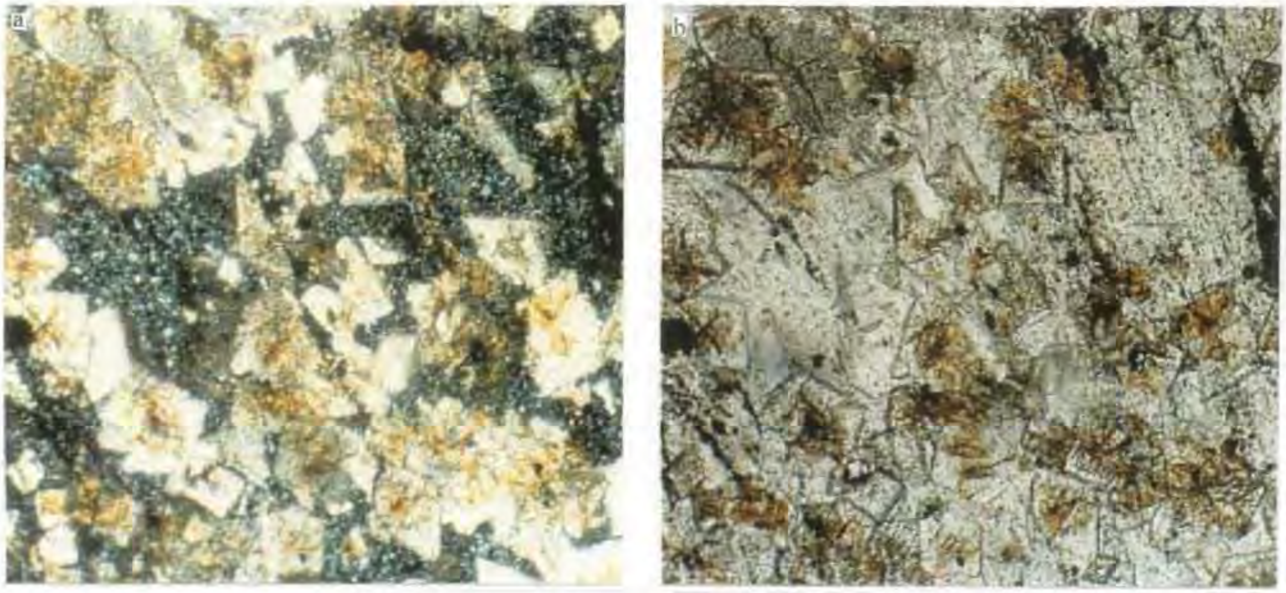


P. 17. Stilpnomelane replacing euhedral carbonate (ankerite?), 4 mm across. a: cross-polar; b: plain polar.

After a brief description of the three different types of iron-formations present in the Makganyene Formation, a description of the occurrence of the mineral phases follows, using the order from silicate minerals to carbonates and then to sulphides and oxides, only if optical positive identification was possible. Other mineral phases not observed under microscope are not described, but are listed in table 1.

Greenalite is a relatively common silicate mineral in diagenetic to low-grade metamorphic Proterozoic iron-formations (Klein, 1983; Tsikos, 1994). Greenalite is most commonly microcrystalline, with a grain size always many orders finer than of any coexisting mineral (Tsikos, 1994), and because of its poorly crystalline texture, it is considered as one of the most possible primary mineral in banded iron-formations (Klein, 1983; Tsikos, 1994).

Stilpnomelane is also one of the most abundant silicate mineral in late diagenetic to low-grade metamorphic banded iron-formations, virtually present in all the major Paleoproterozoic iron-formations of the world (Klein, 1983) in the form of thin needles in coarse-grained sprays and irregular patches. According to Beukes (1983), stilpnomelane is considered to be a product of fumarolic activity and subsequent ash flows, which took place simultaneously with the deposition of the Kuruman Iron-Formation in the Griqualand West Basin. Stilpnomelane is positively identified with its characteristic high birefringence and strong pleochroism (yellowish to dark brown). Stilpnomelane could be present in the ground mass, but also shows evidence of replacement origin. In photos 17.a and 17.b, rhombohedral carbonate (ankerite or siderite) are being replaced by stilpnomelane. This replacement also occurs along the rims present around dropstones or pillows. In the rhombohedral carbonates, the replacement is from the centre to the edges, but in the carbonates coating dropstones or pillows, the replacement is inward (see photos 18.a and 18.b).

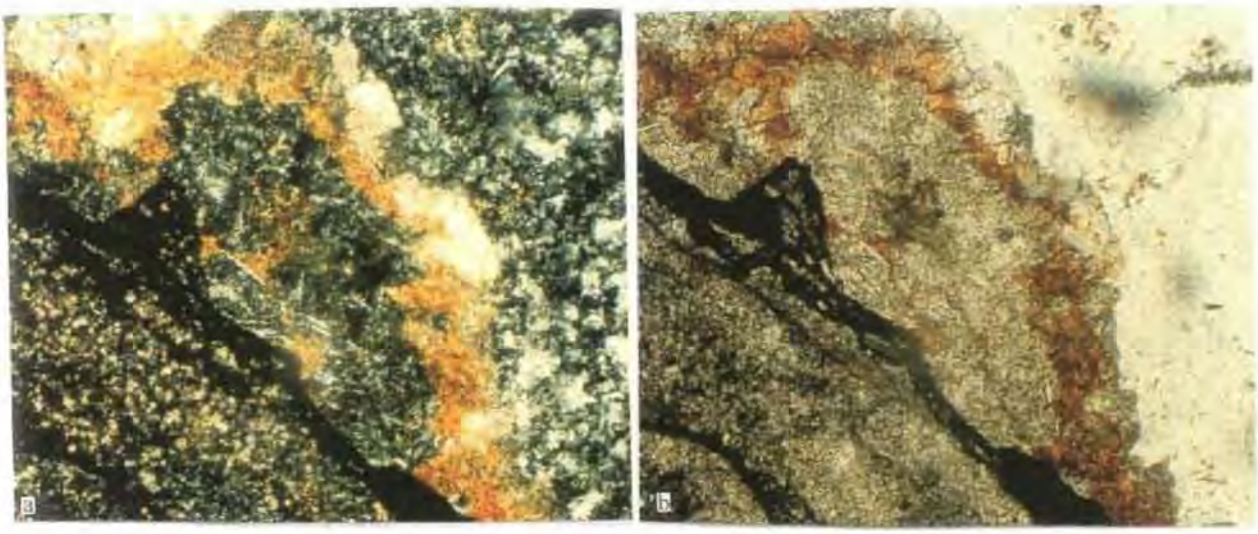


P. 18. Stilpnomelane replacing carbonate (which replaces chert of the pillow) in a pillow of a Makganyene banded iron-formation, 4 mm across. a: cross-polar; b: plain polar.

Chert is a major constituent of the Makganyene iron-formations. Variations in grain size may be an indicator of change in the conditions during metamorphism, on the assumption that any increase in the metamorphic grade would be followed by recrystallisation of $SiO_2$ to form coarser chert (Tsikos, 1994).

The carbonate minerals are from the dolomite-ankerite series and siderite. Distinction between the two under the microscope is not evident, but the members of the dolomite-ankerite serie have a rhombohedral shape with a "cloudy" centre. This cloud is a replacement feature by late diagenetic stilpnomelane (see pictures 17.a and17.b). The carbonates are disseminated throughout. A second generation of carbonates occurs in veins associated with quartz. In this case, the carbonates are anhedral and have not undergone replacement by stilpnomelane. No pure calcite has been identified by XRD means. The siderite is difficult to distinguish from ankerite, but according to Klein and Beukes (1989), Beukes and Klein (1990), recrystallised varieties are relatively rare and are more present as very fine-grained blebs, irregular patches, granules microspheres, intraclasts, dark microlaminae. Positive identification of siderite and ankerite was only possible by XRD means.

Sulphides and oxides (magnetite, hematite and pyrite) have been observed under reflected light. Magnetite is present in the Makganyene iron-formations, and it is commonly medium- to coarse-grained, well-crystallised (subhedral to euhedral habits) and occurs in generally continuous bands and laminations : overprinting growth of magnetite in hematite-rich bands. Hematite is present as elongated patches parallel to the main banding, but hematite is also present as inclusions within the magnetite phase. These hematitic bands are present throughout the samples, but are wider within the magnetite/pyrite bands. Hematite typically overprints magnetite, which strongly suggests that magnetite might be one of the primary features and that the hematite phase crystallised under diagenetic and/or very low grade metamorphic conditions replacing magnetite. Pyrite present in the Makganyene iron-formations is a minor constituent, well crystallised (subhedral to euhedral habits), medium- to coarse-grained compared to the magnetite.

Chalcopyrite occurs scarcely, and is euhedral to subhedral. Chalcopyrite is associated in late magnetite veins, but also occurs as inclusions in pyrite. Chalcopyrite is a very minor constituent in the banded iron-formations of the Makganyene Formation.

III.1.4.4. Petrography of the graded cycles

The graded cycles are found in the top most part of the Makganyene Formation where they are interbedded with the diamictites and also with the overlying Ongeluk volcanics, as shown in the figure 14 displayed in chapter II. They are generally about 10 cm wide, but they can be shorter (1 centimetre or less) and longer (up to 30 centimetres). They have sharp bottom contacts, and sometimes grade into very fine silt which, if present, shows very fine laminations (see photo 19, note the load-cast on top of the graded cycle and photo 22 for fine laminations). Scarce cross-beddings can be seen, but the scale of the cross-beds is few millimetres (see photo 20). The graded cycles can make sometimes up to 6 metres long stacked cycles. Their mineralogy is simple, corresponding in table1 to the siltstone column.

Their base is usually constituted of coarse siltstone to sandstone, and also may contain oriented coarse flakes of chlorite. The size of the anhedral/euhedral carbonate grains is also following the graded trend (i.e. fining upward) (see photos 21.a and 21.b; 22.a and 22.b). The coarse base is generally thin, about 2 cm at most.

Towards the top of a graded cycle, the matrix becomes finer grained very quickly to become a very fine silt where carbonate grains are more scattered and chlorite flakes are finer and also dispersed. Carbonates may also be present in bands towards the base of some graded cycle (see photo 21.a. and photo 21.b).

P. 19. Graded cycle with top-dark part showing a load-cast (plain polar), 18 mm across.

P. 20. Cross-bedding in graded-cycle (plain polar), 14 mm across

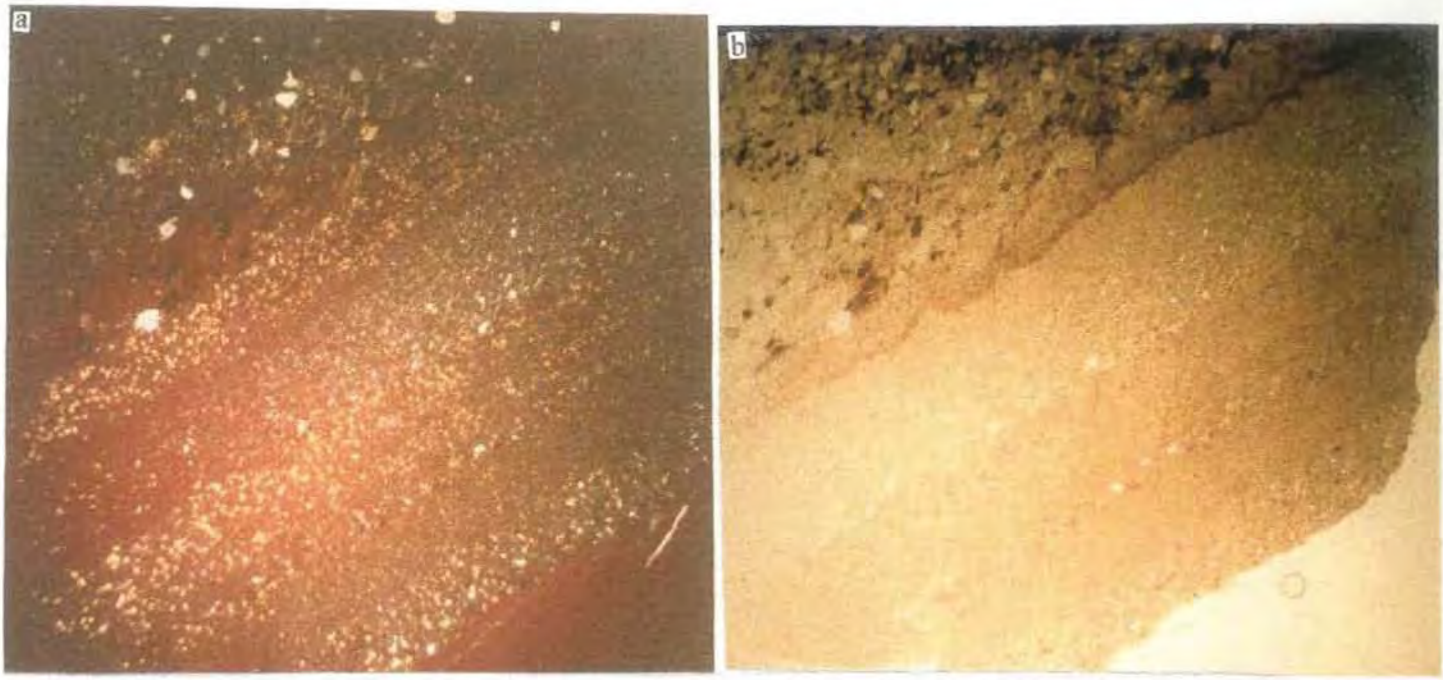


P. 21. Graded cycles showing carbonate-rich bands concentrated at the base of small cycles, note that the carbonate minerals are also fining upward. The next cycle (at the top) has coarse chlorite flakes at its base. a: cross-polar; b: plain polar, 10 mm across.

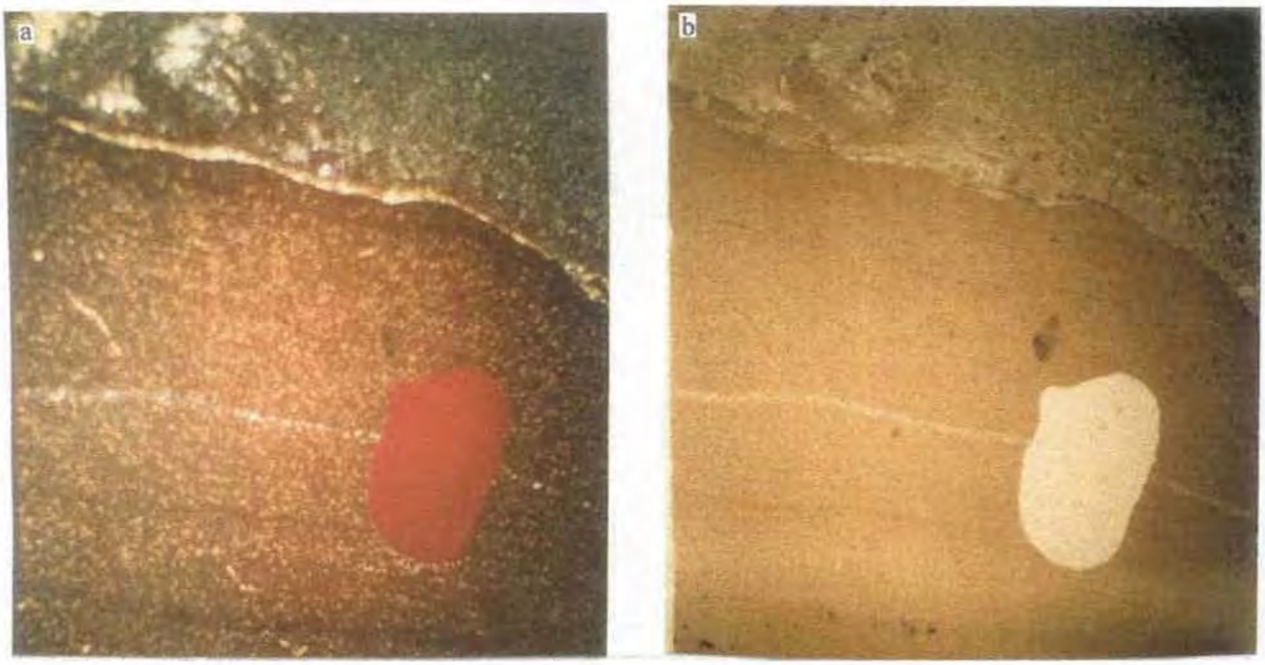


P. 22. Top part of a graded cycle may be very fine-grained, showing thin laminations of dark minerals, while carbonates are disseminated throughout, 17 mm across. a: cross- polar; b: plain polar.

III.1.4.5. Petrography of the shale, siltstone and sandstone

The black shale from table 1 has not been observed under microscope due to its crumbly properties when preparing the thin section.

Sandstone has quartz and chert grains rounded to angular. Chert grains are more abundant and generally larger than quartz grains. The grains can be partly or totally replaced by hematite. The replacement of the grains by hematite starts from the margins. The matrix contains quartz, chlorite, rhombs of carbonates, and hematite. The quartz is usually very fine-grained, but evidence of recrystallisation is present (patches of coarser quartz grains with 120° triple junction) and replacement by hematite occurs. Chlorite, when present, shows preferential direction of elongation. Chlorite is also replaced partly by hematite. The latter tends to replace chlorite along the clivages. Rhombohedres are the only evidence of presence of carbonate because the hematite completely replaced them. Hematite is clearly a late feature and overprints almost all the samples.

The siltstone is very fine grained. Similarly with the sandstone, the very fine quartz grains have also been recrystallised (coarser quartz grains with common 120° triple junction).

## III.2. Geochemistry

### III.2.1. Introduction

Geochemistry applied to clastic sediments is used for provenance studies (Wronkiewicz and Condie, 1987; Johnsson et al., 1988; Nesbitt et al., 1996, 1997; Fedo et al., 1997), for paleoclimate ( Andrews et al., 1996; Fedo et al., 1996, 1997) for tectonic settings determination (Bathia and Crook, 1986; Condie, 1986; Feng and Kerrich, 1990; Rollinson, 1993), and for the evolution of the crust (Taylor and McLennan, 1985, 1991; Wronkiewicz and Condie 1989; McLennan et al., 1995).

A number of recent studies on sediments (Johnsson et al., 1988; Nesbitt et al., 1996, 1997; Fedo et al., 1997) clearly stress the importance of weathering conditions, measured by the degree of effectiveness of chemical weathering, as the major control on the composition of siliclastic detritus. It must be emphasised that the Makganyene Formation is supposed to be of glacial origin and thus the major weathering process of the source rock was mechanical abrasion. Very few studies have been made to assess the effects of specific physical processes on the bulk chemical compositions of fine- and coarse-grained sediments (Nesbitt and Young, 1996).

### III.2.2. Methods of study

Three boreholes (MTP4, GA129 and GA171) situated at Matsap (for the MTP4) and around Sishen Mine (for the GA129 and GA171) were sampled. These boreholes do not show the bottom contact between the Makganyene Formation with the underlying iron-formations due to thrusting in the area. Their selection was based on two facts :

- the boreholes exhibit significant thickness of the Makganyene Formation,
- the boreholes provide significant facies changes within the Makganyene Formation.

A total of 24 samples were selected out of the 3 cores. These 24 samples represent the most homogeneous and at the same time are the most representative of each rock type. They were crushed, ground in two stages (swing mill and automatic agate pestle and mortar) and analysed for major and trace elements using X-Ray Fluorescence (XRF) procedures.

Major elements (except Na) were determined on fused duplicate lithium tetraborate glass discs prepared after the method of Norrish and Hutton (1969); trace elements and Na were determined on pressed powder pellets. The analyses were done on a Philips PW 1480 X-Ray spectrometer at Rhodes

University and the results are summarised in tables A2 (clastic sediments)and A3 (banded iron-formations). Also follows in A4 (MTP4) and A5 (GA129, GA171) descriptions of the collected samples with highlighted analysed samples.

All analytical runs were calibrated using a variety of international and in-house standards. Corrections for dead time, background, spectral line interference, instrumental drift and mass absorption were made in all determinations.

III.2.3. Bulk geochemical composition

III.2.3.1. Geochemistry of the Makganyene diamictite

Vertical profiles of major elements were made to facilitate correlations between different elements (see A6, A7, and A8). Differences in bulk geochemical compositions from the two different localities (i.e. Matsap and Sishen) are observed:

* Sishen samples enriched in CaO, MgO, $Na_2O$ relative to the Matsap diamictite samples;
* Sishen samples are depleted in $Fe_2O_3$, $Al_2O_3$, MnO relative to the Matsap diamictite samples;
* The lowest iron-formations located at the base of the Makganyene Formation have MnO values approaching 1 wt%, and this value drops to 0.2 wt% in the iron-formations situated above.

A better understanding of the inter-element associations between Fe, Si, Ca can be obtained by means of the diagrams 15.a, 15.b and 15.c (for iron-formations) and 15.c, 15.d and 15.e (for clastic sediments). The composition of the three elements is variable, with a range of 2.5 to 11 wt% (CaO), 10 to 46 wt% ($Fe_2O_3$) and 42 to 60 wt% ($SiO_2$) in the iron-formations, and 0 to 12 wt% (CaO), 6 to 27 wt% ($Fe_2O_3$) and 40 to 77 wt% ($SiO_2$) in the clastic sediments. As shown on the diagram 15.e, a positive correlation and constant values of CaO occur between CaO and $Fe_2O_3$ verifying the presence of two different populations of diamictite. The CaO-rich population is from Sishen, the other from Matsap. Diagram 15.d shows the same differentiation between these two populations of different localities.

The rocks of this study generally show high values of $SiO_2$ (from 40.4 to 70.89 wt%) and total Fe as $Fe_2O_3$ (from 11.908 to 26.693 wt%). The $Al_2O_3$ values range from 3.065 to 9.05 wt%, the CaO from 0.081 to 10.534 wt%, the MgO from 1.532 to 7.316 wt%, the MnO from 0.107 to 2.559 wt%. The $K_2O$, $Na_2O$ and $P_2O_5$ show very low values generally under 1 wt%.

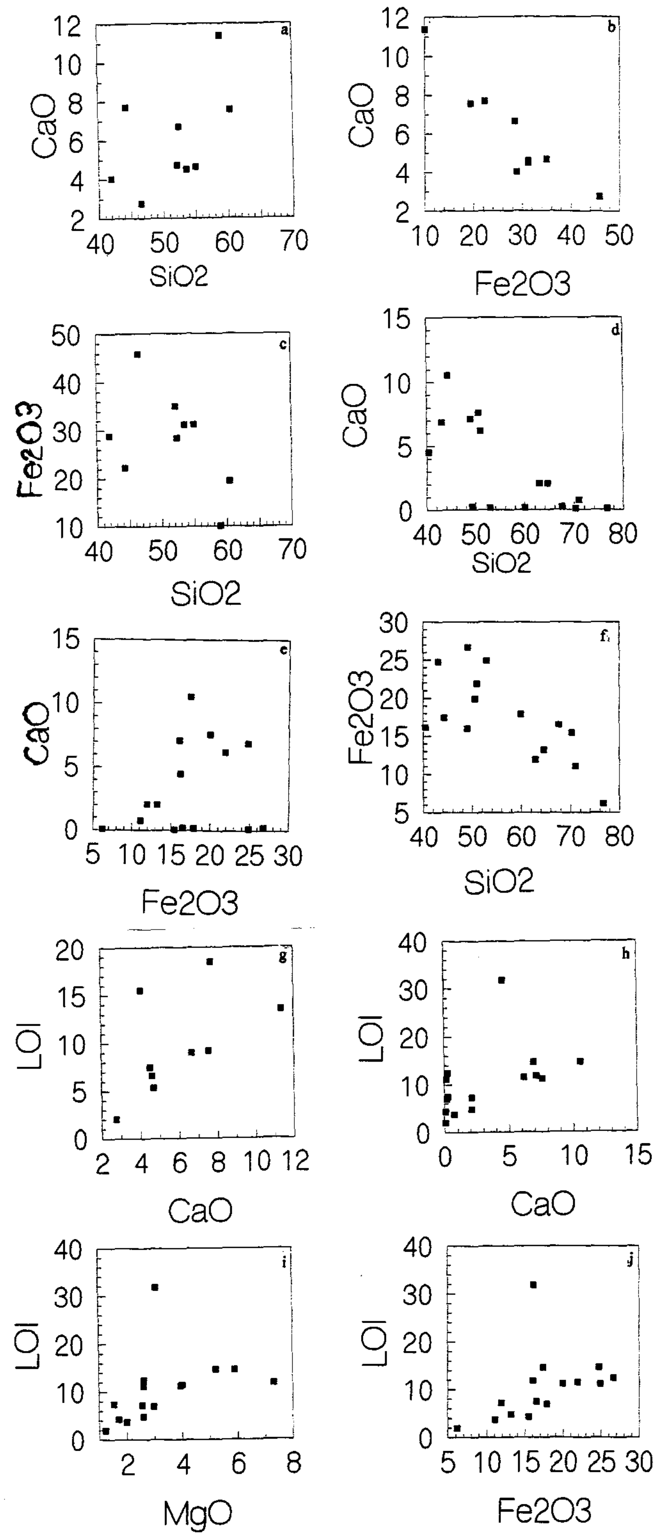


F. 15. Bivariate plots of (a) CaO vs $SiO_2$ (BIF), (b) CaO vs $Fe_2O_3$ (BIF), (c) $Fe_2O_3$ vs $SiO_2$ (BIF), (d) CaO vs $SiO_2$ (diamictite), (e) CaO vs $Fe_2O_3$ (diamictite), (f) $Fe_2O_3$ vs $SiO_2$ (diamictite), (g) LOI vs CaO (BIF), (h) LOI vs CaO (diamictite), (i) LOI vs MgO (diamictite), (j) LOI vs $Fe_2O_3$ (diamictite).

One additional diagram (15.g) has been included, emphasising the presence of carbonates in the iron-formation, by means of the positive correlation between CaO and LOI (Loss Of Ignition). Regarding diamictites, the LOI depends not only on CaO (see diagram15.h), but also on MgO and $Fe_2O_3$ (see diagrams15.i and 15.j). One abnormal sample has a very high LOI (30 wt%), this sample is a diamictite (sample number MTP4-P11). Due to the oxidation of $Fe^{2+}$ to $Fe^{3+}$ during sample preparation, the $CO_2$ and $H_2O$ contents are not truly represented by LOI in analytical data derived from XRF techniques.

III.1.3.1.1. Chemical Index of Alteration (CIA)

The CIA is usually used on clastic rocks having, as a source, igneous rocks (granite, granodiorite, gneiss, dolerite, basalts, gabbros) to determine the most important weathering effect, i.e. mechanical or leaching of the elements. Andrews et al. (1996) gave an example for an average upper-crustal granodiorite. In this type of rock, it is mainly feldspars that weather to form clay minerals. Since feldspars are framework silicates, the production of sheet silicates must involve an intermediate step. This step involves the release of silica, aluminium and other cations, followed by their recombination into a sheet silicate structure. Since this intermediate step involves ions in soil solutions, then ionic composition, soil water pH and the degree of leaching (water flow rate) will influence the type of clay mineral formed (Andrews et al., 1996).

Aluminium and iron precipitate as insoluble oxides or oxhydroxides over normal soil pH range. Other soil cations and $H_4SiO_4$ are quite soluble and thus prone to transport away from the weathering site. This difference in cation behaviour has been quantified as the CIA; using molecular proportions:

$$\boxed{CIA = \frac{Al_2O_3}{Al_2O_3 + CaO^* + Na_2O + K_2O} * 100}$$

$CaO^*$ included in silicate minerals.

Thus, CIA values approaching 100 are typical of material formed in heavy leached conditions where soluble calcium, sodium and potassium have been removed. Kaolinite clays attain such values, whereas illites and smectites have CIA values around 75-85 (see table 2, after Andrews et al., 1996). In comparison, unleached feldspars have CIA values around 50.

In the case of the Makganyene Formation which is strongly believed to have a glacial origin due the presence of dropstones and striated pebbles, the CIA is expected to have values around 50 to 75. In glacial environments, mechanical weathering predominates on chemical weathering, limiting the amount of soluble ions Ca, Na, and K to go in solution. But as shown on table 2 (after Andrews et al., 1996), two different sets of values are present :

* the first from Matsap displays high values between 78 to 96% with a mean value of 88.62%;
* the second from Sishen displays extremely low values between 36 to 65% with a mean value of 43.32%.

| Material | CIA (%) |
|---|---|
| *Clay minerals* | |
| Kaolinite | 100 |
| Chlorite | 100 |
| Illite | 75-85 |
| Smectite | 75-85 |
| *Other silicate minerals* | |
| Plagioclase feldspar | 505075 |
| Potassium feldspar | |
| Muscovite mica | |
| *Sediments* | |
| River Garonne (southern France) suspended load | 75 |
| Barent Sea (silt) | 65 |
| Mississipi delta average sediment | 64 |
| Amazon delta muds | 70-75 |
| Amazon weathered residual soil clay | 85-100 |
| *Rocks* | |
| Average continental crust (granodiorite) | 50 |
| Average shales | 70-75 |
| Basalt | 30-40 |
| Granite | 45-50 |
| *Makganyene Formation* | |
| Matsap samples (mean value from 7 samples) | 88.62 |
| Sishen samples (mean value from 8 samples) | 43.32 |

T.2. Chemical Index of Alteration (CIA) values for various crustal materials (after Andrews et al., 1996).

These CIA values can be explained easily by looking at the bulk composition of the Makganyene diamictite (see paragraph III.2.3.1.). This bulk composition is strongly similar to the composition of an iron formation due to the amount of silica, iron and manganese present in the samples. A second rock type which might have acted as a source is dolomite which supplied the calcium and magnesium. The amount of aluminium present could be accounted to a minor igneous influence (granite basement) providing sodium and potassium.

Because the Makganyene diamictite does not have an igneous source, but rather that of chemically precipitated sediments, the CIA cannot be applied to the rocks of the present study.

An interesting feature in the CIA values are low values in the Sishen samples compared to higher values of the Matsap sample. This is due to an increase in carbonate input to the Makganyene diamictite, lowering the CIA under generally a value of 40%. Ca and Mg values are higher at Sishen than at Matsap to the detriment of Fe, Al, Mn. This shows that the source was very localised, and can vary from place to place. This is one characteristic of a glacial deposit, depending on where the ice is eroding the pavement.

The use of the CIA is generally applied to measure the degree of weathering of silicate rocks, whereas the the Makganyene source rocks were mainly oxides. Provenance studies for identification of source rocks is important and is presented in the following section (III.2.3.1.2.).

III.2.3.1.2. Provenance studies

One diagram very useful is a triangular diagram where each apex represent one type of source (see figure 16)

* the apex $Al_2O_3 + Na_2O + K_2O$ represents the igneous source,

* the apex $SiO_2 + Fe_2O_3 + MnO$ represents the iron formation as a source,

* the apex $CaO + MgO$ represents the carbonate source.

Of course in this diagram, all samples plot very close to the iron formation apex, and two groups can be distinguished: the Matsap samples showing lower values in carbonate component than the Sishen samples, and in both sampled areas, the igneous input is very low.

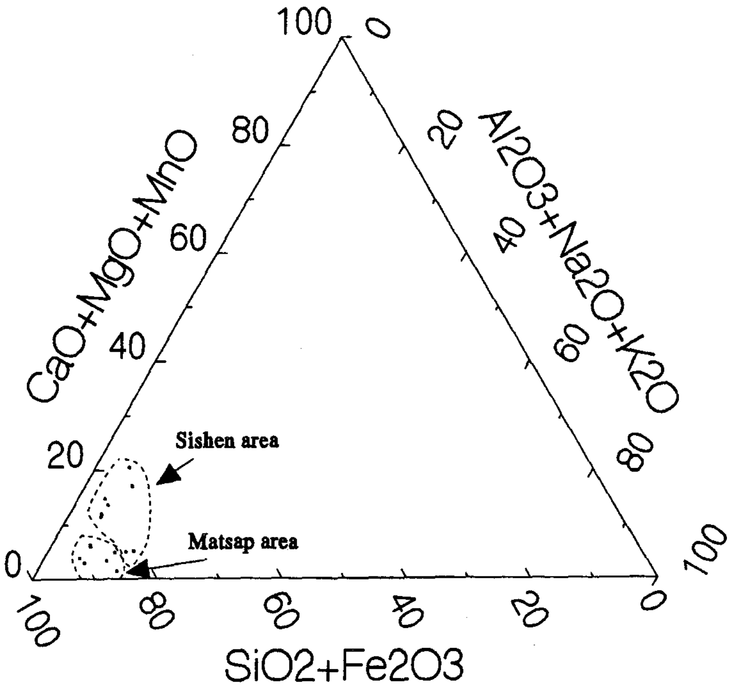


F. 16. Triangular diagram representing the three hypothetical source rock constituting the bulk composition of the clastic portion of the Makganyene Formation.

Some trace elements ratios are commonly used for provenance studies (McLennan and Taylor,1985, 1991; Condie and Wronkiewicz, 1990; Fedo et al., 1997), like the Cr/Th, Th/Sc and Co/Th.

According to Condie and Wronkiewicz (1990), Th, Sc and Cr distributions in fine grained sediments have been proposed as indicators of the composition of the upper continental crust. McLennan and Taylor (1985) stated that these elements not only have low seawater/crust distribution coefficients and sea water residence times, but their ratios are also relatively insensitive to weathering, alteration and metamorphism. According to Condie and Wronkiewicz (1990), some ratios of these elements in Precambrian sediments of the Kaapvaal Craton change with their stratigraphic position, certainly due to a change in source rocks.

However, Cr is susceptible to the effects of weathering and sedimentation. Enrichment of Cr by adsorption in shales may be caused by its adsorption on clay minerals during weathering or deposition. This implies that the Cr/Th ratios in pelites may not monitor sediments provenance. But to appreciate fully the usefulness of the Cr/Th ratio as a provenance indicator, it is plotted against Sc/Th and Th/Sc.

According to Condie and Wronkiewicz (1990), all pelite compositions from the Kaapvaal

Craton can be obtained by using mixing softwares having granite, tonalite, basalt and komatiite as source rocks in various proportions.

These ratio can be useful in the Makganyene Formation to determine the potential type of igneous rocks which acted as a source. The Cr/Th ratio plotted versus the age for the Makganyene diamictite is in the Pretoria Group (Timeball Hill Formation, see figure 17, after Condie and Wronkiewicz, 1990) has values which are close from the tonalite values. This ratio means that the igneous component present in the Makganyene diamictite is felsic and not mafic in composition. The figure 16 shows clearly that the igneous component as a source in the rocks of the present study is very minor. So the use of trace element ratio for provenance studies are commonly made to discriminate the type of igneous rock (i.e. either mafic or felsic) which acted as a source.

When looking at the Th/Sc versus Sc (Fedo et al., 1996, 1997), all the samples plot in a restricted field, indicating that the Th/Sc ratio is not affected by hydrodynamic sorting. That means that Th and Sc are not contained in minerals that are easily separated during sedimentary processes and supports the findings of Taylor and McLennan (1985, 1991) who suggested that the Th/Sc ration may be one of the best overall indicators for provenance. On such diagram, it is possible to demonstrate the effects of chemical mixing, if the end-member compositions are known igneous rocks. But, as in Fedo et al. (1996, 1997), this type of provenance study is applied on rocks derived mainly from tonalitic and granitic source rocks.

As shown in figure16 , in combination with the figure18, it is not questionable that the diamictite itself is very similar to the composition of any iron formation from the Transvaal Supergroup in the Northern Cape Basin. The only difference is the presence of a detrital input characterised by higher aluminium and quartz content in the bulk geochemical composition of the diamictite.

In conclusion, rock types responsible for the geochemical composition of the Makganyene diamictite are mainly the underlying banded iron formations, and to a minor extent dolomites (from the Campbellrand Subgroup) and basement (Ventersdorp). Therefore no crustal evolutionary model could be drawn due to the fact that the source for the Makganyene diamictite is mainly chemical sediments and not igneous rocks.

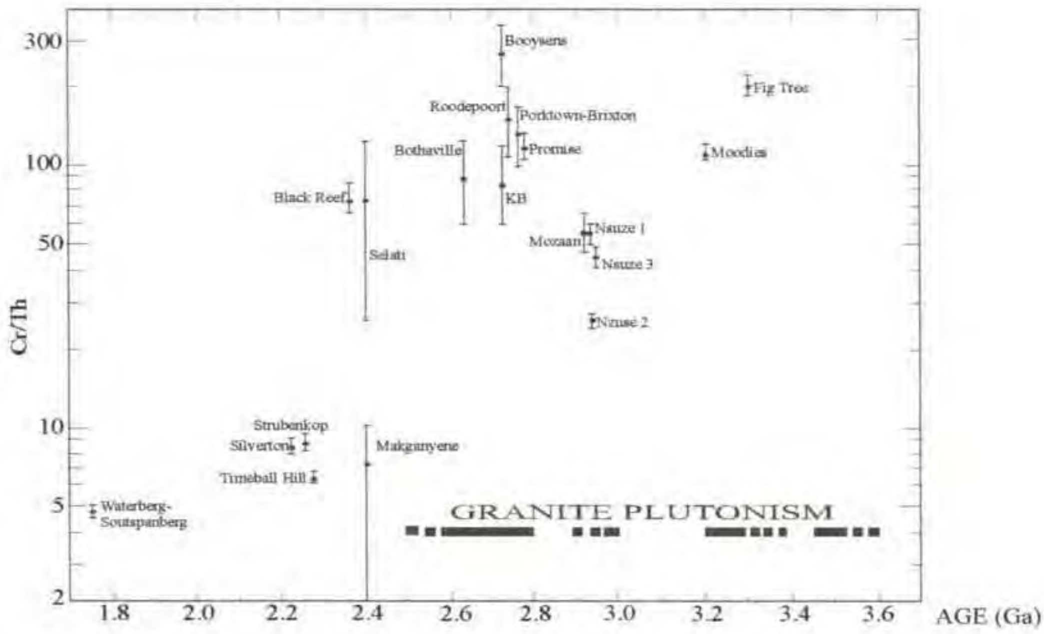


F. 17. The position of the Makganyene Formation depending on the Cr/Th ratio (after Condie and Wronkiewicz, 1990).

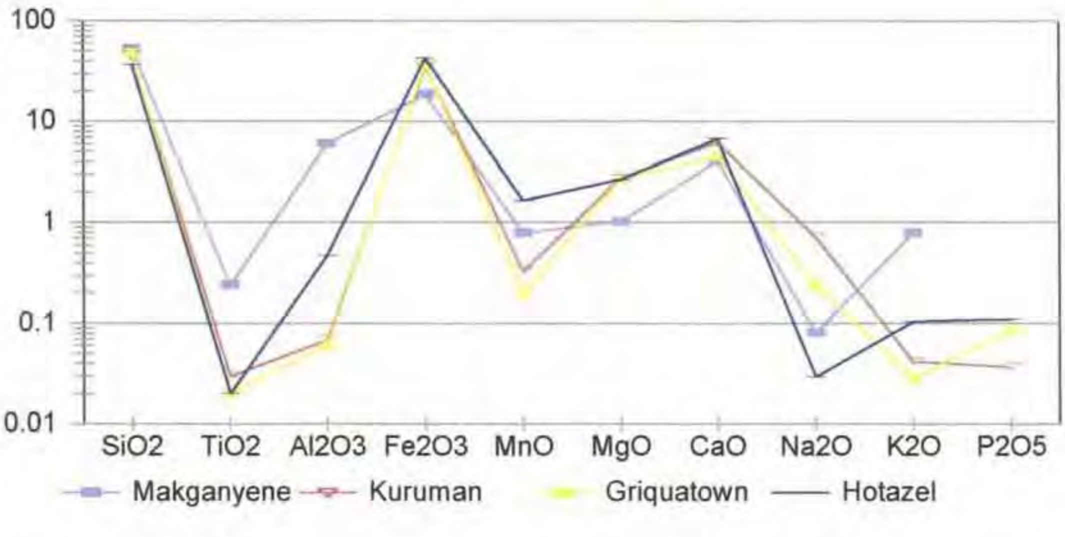


F. 18. Comparison between the average elemental compositions of Makganyene diamictite, Griquatown, Kuruman and Hotazel Iron Formations (Values from Tsikos, 1994; Beukes and Klein, 1990; Klein and Beukes, 1989).

III.2.3.1.3. Ternary diagrams applied on the diamictite

In this brief paragraph, three ternary diagrams where used :

*A-F-K ($Al_2O_3$-$Fe_2O_3$-$K_2O$),

*A-CN-K ($Al_2O_3$-$CaO$+$Na_2O$-$K_2O$), and

*A-CNK-FM ($Al_2O_3$-$CaO$+$Na_2O$+$K_2O$-$Fe_2O_3$+$MnO$)

These three ternary plots are shown in figure 19(a,b,c) respectively.

The first plot shows a difference in composition between diamictite and fine diamictite. Fine diamictites are enriched in aluminium, and potassium, but depleted in iron, relative to the "true" diamictite. This difference in composition, shown in the plot from the figure 19.a displays a linear evolutionary trend (shown with the arrows) corresponding to sorting processes. The information that one could extract from this diagram is that the diamictite and the fine diamictite are both trending towards the illite

The second ternary diagram (see figure 19.b) shows the same separation between the two types of diamictites on Al and CN contents. The difference is that the diamictite and the fine diamictite are widely separated from each other on two distinct fields depending on CN content. Sorting processes are not progressive as on diagrams 19.a and 19.c, certainly resulting in a barrier keeping the diamictite from getting differentiated deeper into the basin. The arrows materialise the compositional link and sorting processes (increasing towards the kaolinite and illite plots) between the two types of diamictite.

The third ternary diagram (see figure 19.c) is very similar to figure 19.a. But the information that one could extract from it is that the diamictite has very constant values of $Al_2O_3$, and is rich in heavy minerals (containing iron and manganese). The fine diamictite evolves rapidly towards the kaolinite and illite plots, following the trends of the arrows. This proves again that the grain size of the two types of diamictites is correlated with their compositions, and must depends on the distance away from the source. The paleo-environment of deposition of the diamictites strongly controls these differences in grain size and composition.

These three ternary diagrams emphasise the sorting processes which induced differences in bulk composition. A passive margin could have controlled the relatively constant composition and grain size of the diamictite. On the other hand, the continental slope facilitated rapid sorting and increased clay minerals contents of the fine diamictite on short transport distances into the basin.

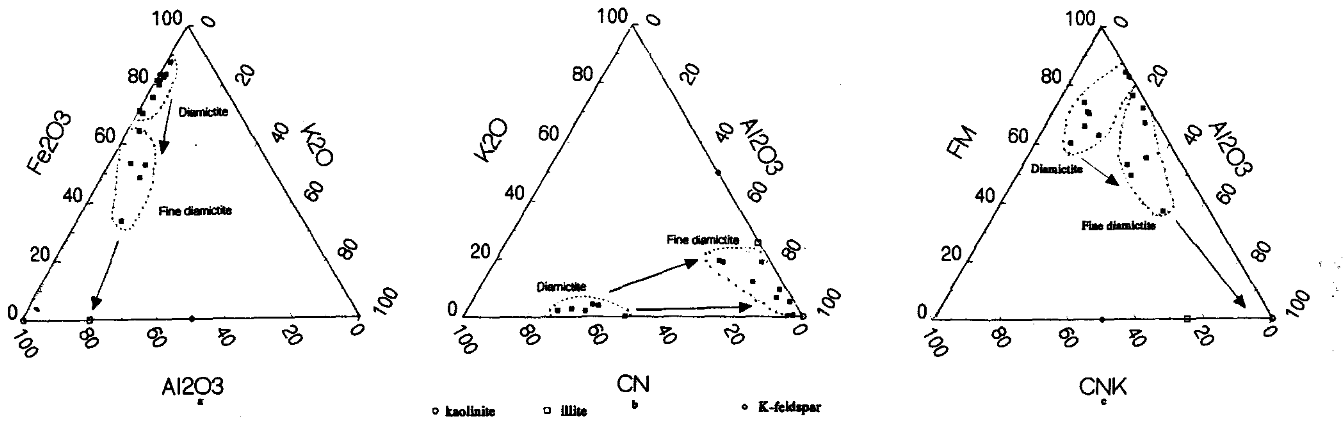


F. 19. a :A-F-K ($Al_2O_3$-$Fe_2O_3$-$K_2O$), b : A-CN-K ($Al_2O_3$-CaO+$Na_2O$-$K_2O$); c : A-CNK-FM ($Al_2O_3$-CaO+$Na_2O$+$K_2O$-$Fe_2O_3$+MnO).

III.2.3.2. Geochemistry of the iron formations of the Makganyene Formation

III.2.3.2.1. Introduction

According to chapter II, the Makganyene Formation is sandwiched conformably between underlying banded iron-formation and overlying Ongeluk volcanics. Therefore, due to this constant sedimentary accumulation, the features of the iron-formations within the Makganyene Formation should be similar in geochemistry and petrography with under- and overlying iron formations and show an evolutionary trend due to the symmetrical setting of the Northern Cape Basin where the Makganyene Formation is the centre of this symmetrical sedimentary cycle.

In the next paragraphs, the geochemical characteristics of the Makganyene iron-formations will be described and compared to the other iron formations belonging to the Transvaal Supergroup in the Northern Cape Basin.

The iron-formations from the Makganyene Formation analysed in this study come from the Sishen area. The reason is that in the Sishen area, the iron formations are regularly banded, or slightly disturbed. In the Postmasburg area, the iron formations where very thin, very disturbed, slumped, and some even contain dropstones. These inhomogeneous features do not allow for reliable bulk geochemical analyses.

III.2.3.2.2. Major elements

One of the most striking feature of the iron formations interbedded within the diamictite of the Makganyene Formation is that, when the values are compared to the underlying Griquatown and Kuruman Iron Formations and to the overlying Hotazel Formation, all the iron formations from the Transvaal Supergroup in the Northern Cape Basin are very similar in major element content (see figure 20). $SiO_2$, $TiO_2$, $Fe_2O_3$, MgO and CaO contents in the Transvaal banded iron-formation are very similar. The Makganyene iron-formations are the most enriched in $Al_2O_3$ and most depleted in $Na_2O$ than the other iron-formations from the Transvaal Supergroup. The MnO content of the Makganyene Formation is identical to the ones of the Kuruman and Griquatown Formations while the Hotazel Formation values are above 1 wt%.

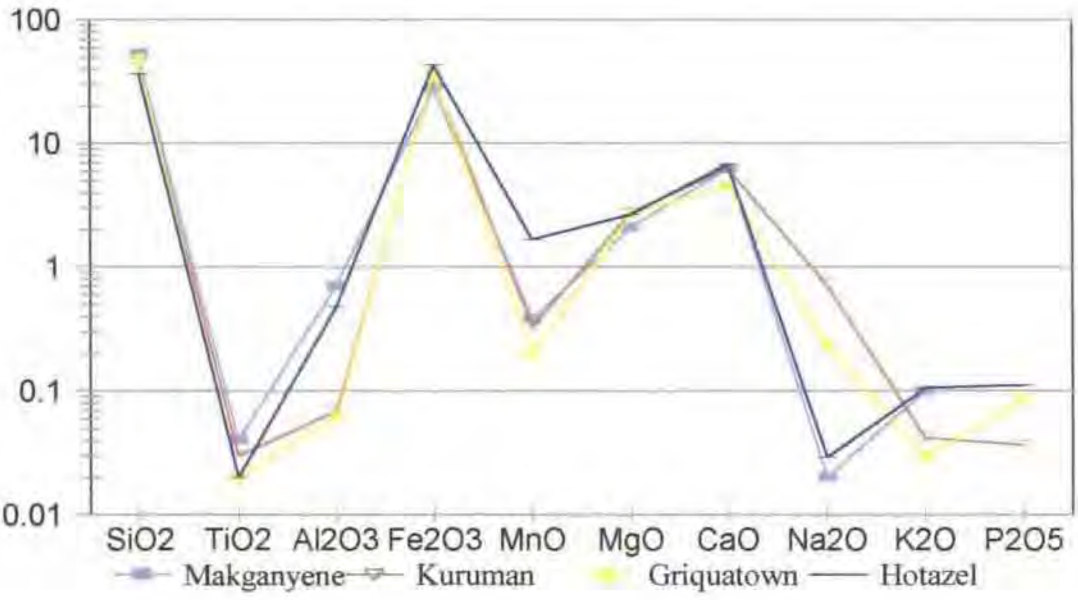


F. 20. Comparison of major element contained in the iron-formations within the Transvaal Supergroup (Hotazel iron-formation values from Tsikos, 1994; Griquatown Iron-Formation from Klein and Beukes, 1989; Beukes and Klein, 1990, Kuruman Iron-Formation from Klein and Beukes, 1989; Beukes and Klein, 1990; and Makganyene iron-formations from this study).

James (1969) proposed a ternary diagram for the geochemical distinction between banded iron-formations and Phanerozoic ironstones. The difference between ironstone and iron-formation is the mode of formation where banded iron-formations are chemically precipitated and whereas ironstones are detrital in origin. This difference in formation is reflected in their mineralogy. The iron-formation contains Fe-bearing silicate minerals and ironstone Al-bearing silicate minerals. Therefore in the figure 21.a, the iron-formations present in the Makganyene Formation belong to the field iron-formation, but this field should be redefined as suggested by Tsikos (1994), since not all the data of the present study and Tsikos's diagram are included in it.

A second diagram could be plotted for the distinction between iron-formations and ironstones. This diagram plots the Ca/Mg ratio against Fe/Al ratios. The ironstones correspond to high Ca/Mg and low Fe/Al ratios which represent Phanerozoic lithologies (Tsikos, 1994), (field 1) and the iron-formations correspond to low Ca/Mg and high Fe/Al ratios from Proterozoic iron-formations (field 2). The figure 21.b displays this diagram (after Tsikos, 1994), and the iron-formations present in the Makganyene Formation belong to the same field as the iron-formations except one sample. This sample (Ga129-24) is a pillowlutite and has a CaO value of 11.37 wt% which is the highest value of the iron-formations analysed during this study. The LOI for this sample is 13.46 wt%.

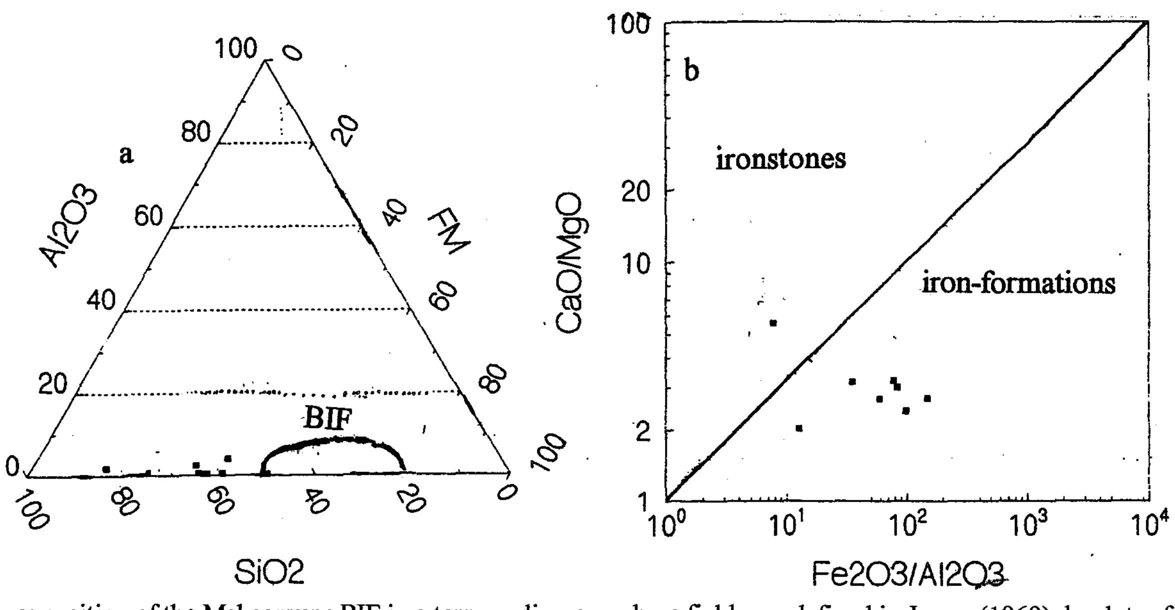


F. 21. a: position of the Makganyene BIF in a ternary diagram where fields are defined in James (1969); b: plots of the Ca/Mg ratio against Fe/Al ratio for the Makganyene iron-formation, fields from Tsikos (1994).

III.2.3.2.3. Trace elements

Dymek and Klein (1988) proposed a diagram to assess the clastic input in the banded iron-formations from Isua Supracrustal Belt, West Greenland. They emphasised the fact that is important to discriminate chemically precipitated components and those which could represent clastic material, including fall of volcanic debris. The iron-formations present towards the base of Makganyene Formation have undergone very little deformation accompanied with low-grade metamorphism. Therefore in the rocks of the present study, standard petrographic techniques could have been used to give a sedimentary features of any clastic input. Although volcanic shards are interpreted by Beukes (1983) as have been replaced by stilpnomelane, little evidence of volcanic input has been observed during the petrographic studies. Figure 22 (after Dymek and Klein, 1988) plots $TiO_2$ versus $Al_2O_3$ (wt%). When the concentrations of the two oxides of figure 22 increase, clastic contaminations also increase. It is clear in the figure 22 that there are two distinct fields, emphasising that the iron-formations of the Makganyene Formation have very little contamination components. It is important to note that the positive trend shown by the iron-formations towards the clastic metasediments and amphibolites is accentuated by the log-scale, but still shows degrees of contaminations.

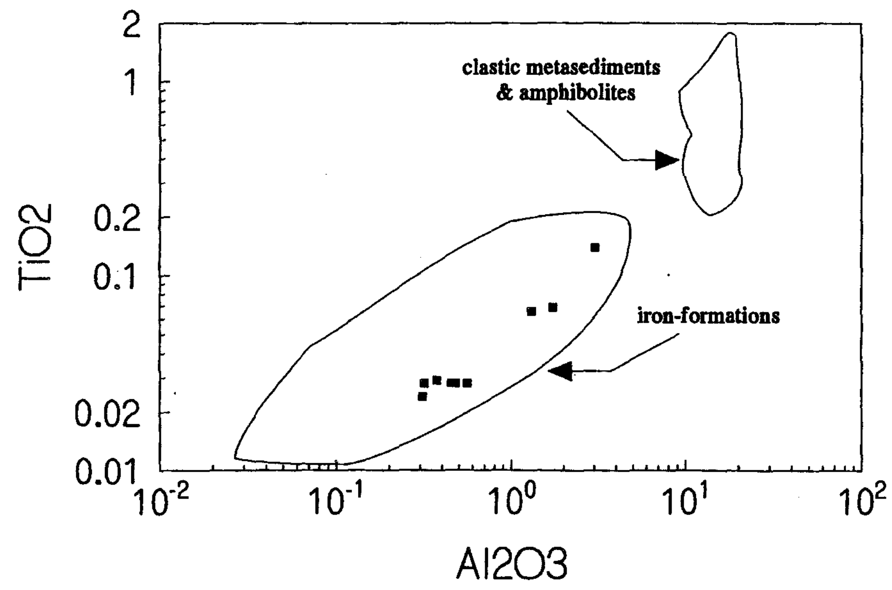


F. 22. Plot of wt% $TiO_2$ vs. $Al_2O_3$ in analysed samples from the Iron-formations of the Makganyene Formation. Fields are defined by Dymek and Klein (1988).

Figure 23 shows concentrations of La and Sc for the same samples evaluated in terms of $Al_2O_3$ and $TiO_2$. The fields have been defined by Dymek and Klein (1988). All the samples analysed from the iron-formations of the Makganyene Formation belong to the field where, according to Dymek and Klein (1988), the samples have more than 1 ppm of Hf (not analysed in this study). This field shows that some minor contamination has occurred in the iron-formations of the Makganyene Formation.

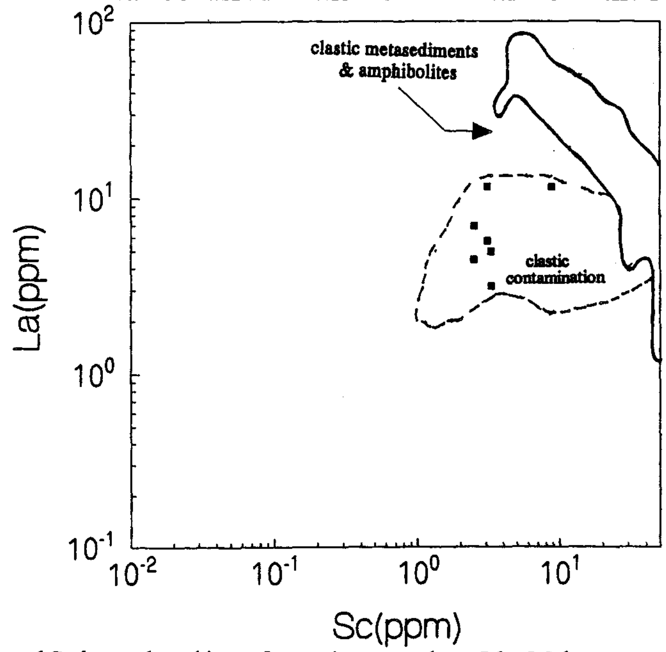


F. 23. Concentrations of La and Sc in analysed iron-formation samples of the Makganyene Formation. Fields have been defined by Dymek and Klein (1988).

The figures 22 and 23 are supporting the same conclusion : the iron-formations of the Makganyene Formation have undergone clastic contamination. Figure 22 shows minor contamination of the samples by clastic input accentuated by the positive trend of the samples, whereas figure 23 shows an overall contamination. The use of logarithmic scales has reduced the separation between the clastic metasediments and amphibolites field (figure 23) with the samples of the Makganyene Formation. It is evident that by using linear scales this separation would be dramatic. Therefore minor clastic contamination occurs in the iron-formations of the Makganyene Formation.

The figure 24 plots La versus Ce normalised on chondrite. This diagram allows one to deduce the presence or absence of a Ce anomaly. Ce is a light rare-earth element (LREE) and its relative depletion is due to selective scavenging of sea water during the formation of metal-rich sediments

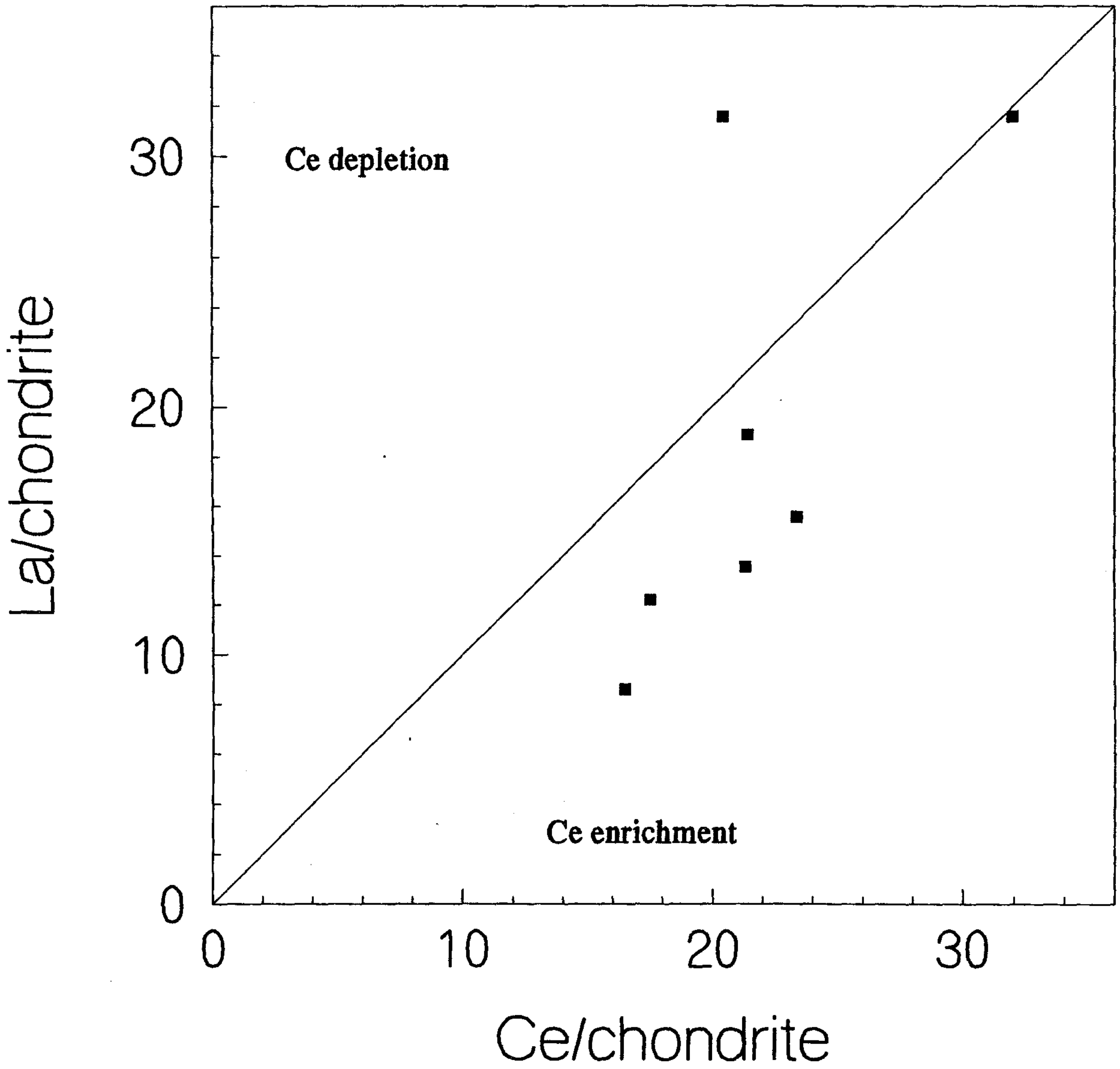


F. 24. La vs Ce normalised to chondrite plot of the banded iron-formations of the Makganyene Formation.

such as Mn nodules (Dymek and Klein, 1988). Thus concentration of Ce relative to the other LREE would allow distinction between hydrothermal (Ce depletion) with hydrogenous sediments (high Ce concentration due to the rapid precipitation of Ce from seawater). In figure 24, all the samples plot in the field of Ce enrichment, except sample GA129-24. The figure 24 shows that the iron-formations from the Makganyene Formation are hydrogenous sediments because all samples (except sample GA129-24) plot in the Ce-enriched field. Because of the general depletion in LREE in the samples, hydrogenous origin for the Makganyene banded iron-formation is excluded.

A potential hydrothermal source for the iron-formations of the Makganyene Formation could not be ruled out. Figure 25.a plots each sample of the iron-formations from the present study, chondrite-normalised. All samples (except GA129-24) are enriched in Ce. Figure 25.b compares La-Ce-Nd averages between the banded iron-formations of the Transvaal Supergroup. No prominent Ce depletion is observed. By comparison with the other iron-formations of the Transvaal Supergroup, similar patterns are observed (for the Asbesheuwels iron-formations, Nd was below limit detection). According to Tsikos (1994), such patterns are characteristic of shallow-water environment where the LREE fraction of the studied rocks does not come from typical processes of chemical sedimentation, but rather from normal continental drainage.

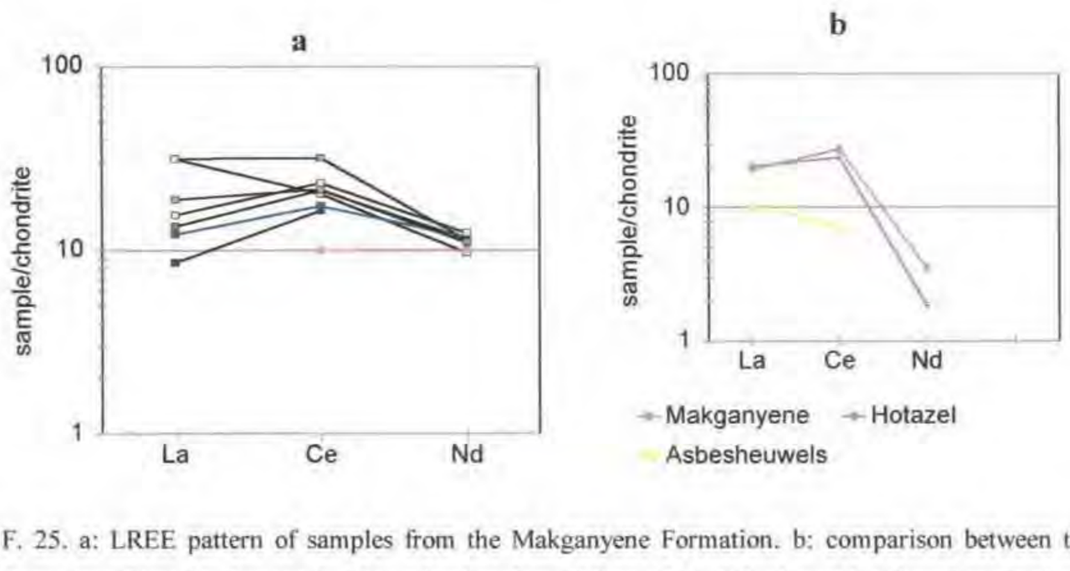


F. 25. a: LREE pattern of samples from the Makganyene Formation. b: comparison between the different iron-formations from the Transvaal. (Hotazel values from Tsikos, 1994; Asbesheuwels values from Beukes and Klein, 1990; Makganyene values from the present study).

III.2.3.3. Stable isotope geochemistry of the Makganyene Formation

III.2.3.3.1. Methods

A total of five samples were analysed, comprising three iron formations, one overlying diamictite and one underlying diamictite. These five samples come from the same borehole GA171 from Sishen. This was done to display possible variations in isotope compositions ($\delta^{18}O$ and $\delta^{13}C$) between the iron-formations and the clastic sediments of the Makganyene Formation. Whole rock samples were used, discarding the late carbonate veining under microscope to obtain reliable results. Then the samples were finely crush using a swing mill. Carbon dioxide was evolved from carbonates (ankerite and siderite) by treatment with $H_3PO_4$ ($\rho > 1.89$ g.ml$^{-1}$) at 100°C for 48 h (Rodembaum and Sheppard, 1986) in evacuated reaction Y-tubes. Carbon dioxide was subsequently isolated by cryogenic distillation. Isotopic compositions of $CO_2$ were determined by conventional mass spectrometric techniques (Santrock et al., 1985) and are expressed relative to the PDB and SMOW standards. Isolation of $CO_2$ gazes by chemical means were done by Harilaos Tsikos at the University of Cape Town (UCT).

III.2.3.3.2. Results

The results are consistent throughout the samples. Variation in the rock types does not seem to change the isotopic composition (see table 3). The average isotopic compositions for the analysed samples are $\delta^{18}O$ (SMOW) averages of 15.2‰ for the diamictite and 16.6‰ for the iron-formations; and $\delta^{13}C$ (PDB) averages of -9.35‰ for the diamictite and -8.7‰ for the iron-formations. Because only five samples from one borehole were analysed, the results are consistent as well as independent of the rock types, and the sampled core section is restricted, the averages will be used and compare with the other iron-formations present in the Transvaal Supergroup of the Griqualand West Basin. This is, from a stratigraphic point of view, to see if there is a dramatic change or not in the isotopic compositions between the Makganyene Formation and the over- and underlying formations.

| sample | $\delta^{13}C$ (PDB) | $\delta^{18}O$ (SMOW) | rock type | carbonate minerals |
|---|---|---|---|---|
| GA171-11 | -9‰ | 14.7‰ | diamictite | A |
| GA171-30 | -8.1‰ | 17.2‰ | BIF | A+S |
| GA171-14 | -9.7‰ | 16.3‰ | BIF | A |
| GA171-15 | -8.4‰ | 16.4‰ | BIF | A |
| GA171-25 | -9.7‰ | 15.7‰ | diamictite | A |

T. 3. Isotopic compositions of the Makganyene Formation. A=ankerite; S=siderite.

III.2.3.3.3. Interpretation of the isotopic compositions

According to Hoefs (1980), Faure (1986), Schoch (1989), Kauffman et al. (1991), oxygen occurs in the form of three natural isotopes, $^{16}O$, $^{17}O$, $^{18}O$, where currently over 99.75% of the oxygen is in the form of $^{16}O$, and a little over 0.2% is in the form of $^{18}O$. The $^{18}O/^{16}O$ reflects changes in temperatures, but according to Matthews (1984) and Schoch (1989), the global ice volume influences this ratio and this might be the primary determinant of the global $^{18}O/^{16}O$ ratio observed in sediments at any one time. Simplistically, as explained by Matthews (1984) and Schoch (1986), the proposed mechanism is that when water evaporates from the ocean, it is relatively enriched in $^{16}O$ relative to $^{18}O$ (simply because $^{16}O$ is lighter than $^{18}O$ and so water containing it will enter into a gaseous state more readily), and thus the $^{18}O/^{16}O$ ratio of the ocean water increases if the evaporated water is not returned to the oceans. Likewise, as water travels in a gaseous state, any precipitation will tend initially to favour water that might contain $^{18}O$. This effect will ensure that water carried far inland will be characterised by low $^{18}O/^{16}O$ ratios. When the glacial ice volumes increase due to the active growth of polar and continental glaciers, the water bound up in the ice does not return to the oceans and the $^{18}O/^{16}O$ ratios will vary. Because the ice is $^{16}O$-enriched, the $^{18}O/^{16}O$ ratio of the oceans increases. During deglaciation, water that was bound up in glaciers melted and returned to the oceans, the $^{18}O/^{16}O$ ratio of the oceans will decrease. Consequently, changes in $^{18}O/^{16}O$ ratios of the world's oceans apparently reflect fluctuations in the volume of ice bound up in continental glaciers and also sea level and position of the shore lines. It has been suggested by Faure (1986), Schoch (1989) that the mixing time of the oceans may be of the order of a thousand years, so that any global changes in isotopic ratios of ocean water will be geologically instantaneous. Thus these mechanisms of $^{18}O/^{16}O$

ratio variations must be contemporaneous throughout various parts of the world.

According to Schoch (1989) and Faure (1986), there are two stable isotopes of carbon, $^{12}C$ with an abundance of about 98.9% and $^{13}C$ with an abundance of approximately 1.1% (the radioactive $^{14}C$ occurs in trace amounts). $^{13}C/^{12}C$ ratios have been calculated for carbonates found in marine stratigraphic sections and exhibit systematic variations with time that have been used in correlations. Various factors can influence the $^{13}C$ content of ocean water. Organic materials, for instance, tend to be relatively low in $^{13}C$; and organic-rich waters may tend to be characterised by low $^{13}C/^{12}C$ ratios. Deep ocean water masses with a long residence time near the bottom may be relatively depleted in $^{13}C$. Organic matter, characterised by low $^{13}C/^{12}C$ ratios, that sinks from the surface to such deep waters will be oxidised and the carbon depleted in $^{13}C$ trapped in these water masses. If, due to sudden (on the scale of the geological time) changes in oceanic circulation patterns, there is upwelling of such deep waters, then $^{13}C/^{12}C$ ratios may be depressed in surface waters (Schoch, 1989).

As seen on the $\delta^{18}O$ curve displayed in figure 26, the $\delta^{18}O$ of the Campbellrand dolomites (21-22‰) (base of the Ghaap Group) is as heavy as the Mooidraai carbonates (top of the Postmasburg Group). The $\delta^{18}O$ of the Asbesheuwels Subgroup (close to 20‰) is steadily lighter than the $\delta^{18}O$ of the carbonate rocks, and is very similar to the $\delta^{18}O$ of the iron-formations from the Hotazel Formation. The lightest values are for the Makganyene Formation (average 15.2‰ for the diamictite and 15.6‰ for the iron-formation) which is the centre of symmetry of the succession carbonate-iron formations-diamictite-iron formations-carbonate. The figure 26 emphasises :

* symmetrical succession of rock types through the Transvaal Supergroup (carbonate-iron formation-diamictite-iron formation-carbonate);
* symmetrical isotopic variation of a smooth $\delta^{18}O$ curve where the values for the Makganyene Formation are lower than all the other formations throughout the Transvaal sedimentary sequence.

This $\delta^{18}O$ curve does not reflect primary $^{18}O/^{16}O$ ratios of the ocean, but the complex history of the different formations from the Transvaal Supergroup (diagenesis, metamorphism and alteration). The Makganyene Formation has a strong glacial influence (due to the presence of dropstones in iron-formations, striated and faceted pebbles) and the primary $^{18}O/^{16}O$ ratio should have been heavier due to the fractionation of the oxygen isotopes related to continental and polar glacier growths.

In the case of the $\delta^{13}C$, the values are all depleted, but this depletion is enhanced in the Makganyene Formation. According to Baur et al. (1985) and Kaufman et al. (1990), the consistent depletion of $^{13}C$ in Paleoproterozoic banded iron-formation carbonates indicates that these represent a mixture of oceanic carbonate ($^{13}C \approx 0$), with material formed by oxidation of isotopically light organic material of biological origin. It has been suggested by Baur et al. (1985) that banded iron-formation should be expected to contain isotopically light carbonate resulting from postdepositional oxidation of sedimentary organic carbon by ferric ions : a mixture of organic matter and ferric oxides is thermodynamically unstable at only slightly elevated temperatures, and in principle, production of light carbonate by this mechanism might not require extensive metamorphism. The most deeply buried, and presumably most strongly heated have the lightest carbonates (Baur et al., 1985). However the Makganyene Formation shows a very low grade of metamorphism (green-schist facies) and was not the most deeply buried formation. Therefore metamorphic effect is not the main cause of the $^{13}C$ depletion. For these reasons, and according to Baur et al. (1985), the main source of isotopically light carbon in iron formations was an early to late diagenetic oxidation of biologically fixed organic carbon. It is suggested by Beukes et al. (1990) that the siderites (but not optically differentiated from ankerite in this study) were deposited in an environment where oxidation of organic matter occurred, and if at all, by denitrification. The oxidation of organic matter by ferric iron is known to precede sulfate reduction and to follow denitrification in the diagenetic environment (Beukes et al., 1990), and all of these diagenetic processes, with additional contribution of low grade metamorphism, produced the isotopic composition of the samples analysed in this study. The values of the Makganyene diamictite should follow the same processes because diamictite and iron-formations analysed for stable isotopes come from the base of the Makganyene Formation where both rock types are intimately interbedded. Diagenetic processes should not have been dramatically different.

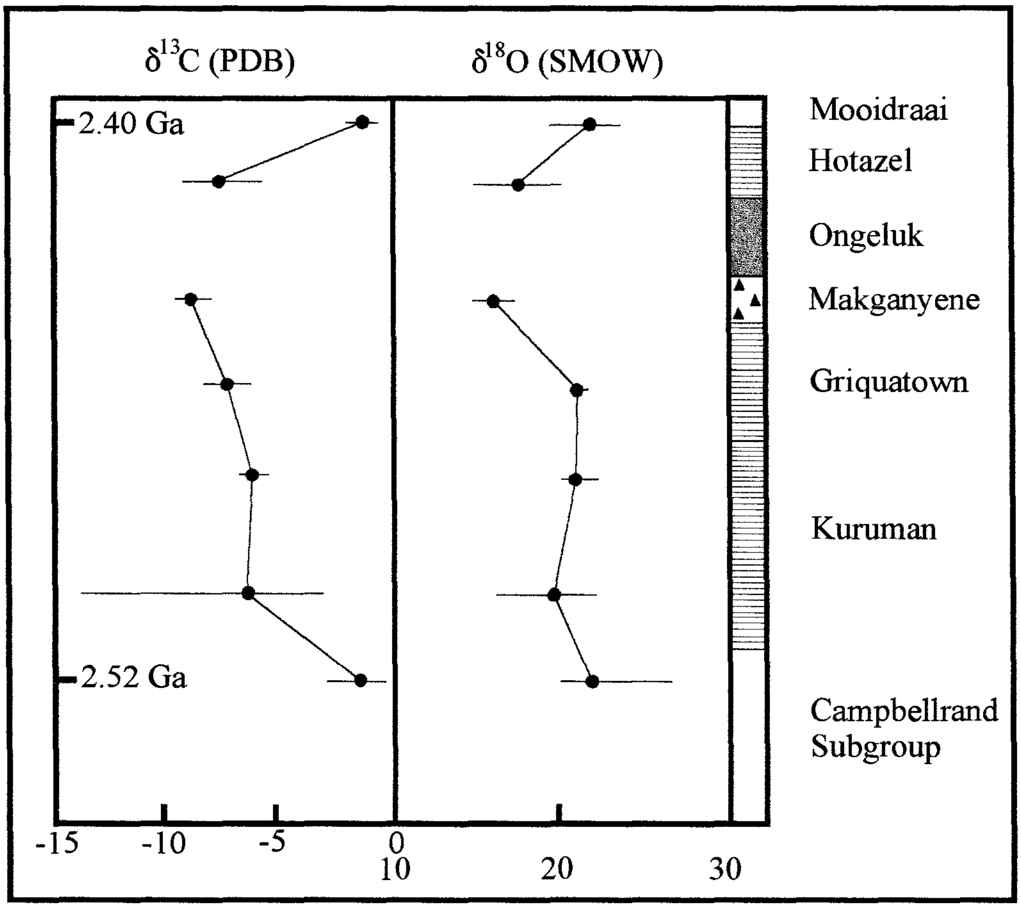


F. 26. Isotopic profile of the $\delta^{18}O$(SMOW) and $\delta^{13}C$(PDB) along the Transvaal Supergroup. Values for the Campbellrand Subgroup from Klein and Beukes, 1989 , values from Kuruman and Griquatown Formation are from Beukes and Klein, 1990 , and values from Voëlwater from Tsikos (personal communication).Diagram from Tsikos (personal communication).

# IV DISCUSSIONS

## IV Precambrian geological environments

### IV.1. Introduction

It is observed that the Makganyene Formation contains iron formations interbedded within glacigenic clastic sediments. A study of this paleo-position relative to the poles has been made by Evans et al. (1997) and the conclusion is that the Makganyene Formation was deposited only a few degrees from the equator by ice-sheets at sea level.

Therefore this chapter reviews the different environments of the Precambrian Earth, using geological evidences. Its content will be used in the paragraph IV.4.2. in an attempt to explain the unusual features of Precambrian rocks, particularly in the Makganyene Formation, taking account of the data obtained during the present study.

The geological model for the deposition of the Makganyene Formation will be discussed at the end of this present chapter.

### IV.2. Chemistry of Precambrian atmosphere and oceans

#### IV.2.1. Chemistry of the Precambrian atmosphere

The Precambrian atmospheric composition was different from its composition today. This statement is made to overcome the paradox associated with the increasing luminosity of the Sun with time (Newman and Rood, 1977; Kiehl and Dickinson, 1987; Kasting, 1987, 1991; Schmidt and Williams, 1995; Rye et al., 1995; Eriksson et al., 1998).

The luminosity of the Sun has increased by 30% since the formation of the Earth 4.5 Ga ago (Newman and Rood, 1977; Kiehl and Dickinson, 1987; Rye and al., 1995). During the Early Proterozoic times, this luminosity should have been roughly 10% less than it is today. With the same composition of the atmosphere as today, and because of the weaker luminosity of the Sun, the surface temperatures should have remained, according to Eriksson et al. (1998), below freezing until about 2 Ga. The presence of sedimentary rocks from 4-3.8 to 2 Ga suggests the presence of running water and unfrozen oceans.

The only solution yet proposed to the faint young Sun paradox is that the early atmosphere contained a much larger quantity of greenhouse gases than it does today (Newman and Rood, 1977;

Kiehl and Dickinson, 1987; Rye and al., 1995). The main greenhouse gases are $CO_2$ and $CH_4$, and thus are responsible to keep the thermal balance on the early Earth's surface.

The implications of a greater $CO_2$ content in the early atmosphere should have enhanced chemical weathering and thus decreased this $CO_2$ content. Another factor to remove the $CO_2$ from the atmosphere is the deposition of shallow marine carbonates within cratonic basins (Chuniespoort/Ghaap Group on the Kaapvaal Craton and the Hamersley Group on the Pilbara Craton). Thus a decrease of $CO_2$ from the atmosphere might have triggered (Marshall et al., 1988; Raymo, 1991; Young, 1991; Eriksson et al., 1998) the low latitude glaciations which occurred during the Precambrian. But, as suggested by Williams (1975, 1993, 1998), the length of a day in the Early Proterozoic was close to 14 hours. This implies a faster rotation rate of the Earth which would have reduced poleward transport of heat, causing warmer low latitudes and colder high latitudes (Kuhn et al., 1989). The paradoxical Proterozoic glacial climate challenges conventional views on the nature of the geomagnetic field, climatic zonation and Earth's orbital dynamics (Eriksson et al., 1998).

Besides the greenhouses gases and climate processes responsible for low-latitude glaciation at sea level, oxygen is another important factor in the Precambrian atmosphere. Kasting (1987, 1991) proposed a 3-stages box model and this is shown in figure 27.

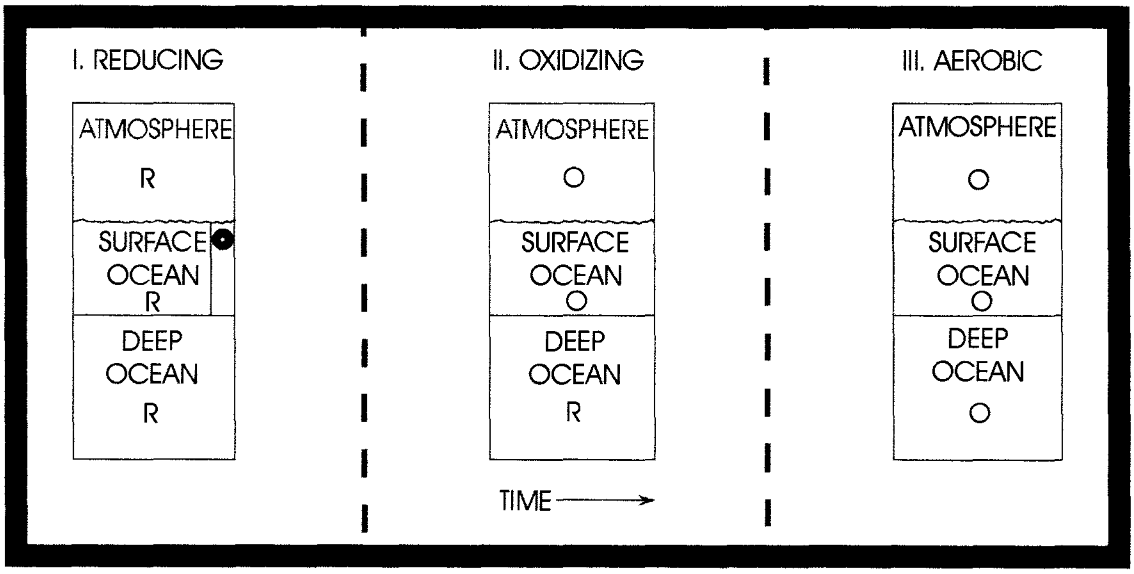


F. 27. 3D-box model showing the different stages of redox conditions of the atmosphere, surface ocean and deep ocean. O: oxidising environment, R: reducing environment (from Kasting (1987, 1991).

The main problem in this model is the timing of the different stages : Stage II has a duration of 150 to 700 million years, and it is not widely accepted that Stage II actually occurred. Following is a brief description of the three different stages (from Kasting, 1987, 1991) :

* Stage I is the reducing stage, anaerobic. As shown in figure 27, oxygen may have been present in low quantities in surface water.

* Stage II is the oxidising stage. The presence or absence of this stage is controversial, as well as its total duration. The oxygen concentration should have raised gradually due to the probability of a wetter atmosphere than today. Solar ultraviolet radiations would have broken down water molecules by protolysis, producing $H_2$ which escapes, and hence a parallel build-up of atmospheric $O_2$. This process was active during Stage I, and produced enough oxygen to oxidise and destroy uraninite .

* Stage III is the aerobic stage, where the atmosphere and deep water ocean are oxygenated. Biotic growth must have followed the trend of oxygen content. This stage is characterised by the oxidation of the last ferrous iron from the deep ocean. Downwelling of dissolved oxygen would then have ceased to be an immediate sink for oxygen, and $pO_2$ could have begun to climb to its present value. This raise in oxygen must have been high enough to provide the screen against solar ultraviolet radiation.

As reviewed in this section, the Precambrian atmosphere played an important role in controlling surface temperatures and hence climates, influencing the composition of oceans, and appearance of Precambrian life in the oceans. The climatic problems present in the Precambrian geological record will be presented in paragraph IV.2.3., with the different theories trying to explain one of the Precambrian paradox : the occurrence of glacial deposition at sea level at low latitudes.

### IV.2.2. Chemistry of Precambrian oceans

According to Holland et al. (1986), early studies in the 1960's proposed an equilibrium model for the chemistry of oceans, in which all the major compositional parameters of sea water were controlled by thermodynamic equilibrium between dissolved species in sea water and mineral phases in marine sediments. The implications of these models were profound, showing that the chemical composition of sea water would have been essentially locked into its present state during much of

Earth's history, for the past 3.5 Ga (Holland, 1972). The model did not survive. A careful look at the mechanisms of the removal of $SO_4^{2-}$ from the oceans showed that processes such as bioturbation, $SO_4^{2-}$ diffusion into sediments, and evaporitic basin development rather than thermodynamics, control the output of this ionic complex from the oceans. The nature and intensity of the processes that have determined the kinetics of the dominant removal processes of this and other ionic complexes have probably varied significantly during Earth's history (Holland et al., 1986). As pointed out by Holland et al. (1986), fluid inclusions from evaporite sequences do not show significant variations in the composition of the trapped sea water over the last 900 My, but that does not mean that this composition was the same before 900 My.

The atmospheric evolution controlled, in part, the concentration of volatile elements in sea water and the geological history of oceans (Holland et al., 1986; Eriksson et al., 1998). A widely accepted origin for the oceans is that they probably originated from condensation of the atmospheric water early in Earth history. According to Eriksson et al. (1998), it is likely that oceans and atmosphere have had a parallel growth rate, perhaps with a slight delay reflecting the time necessary for a steam atmosphere to cool and condense. A large fraction of the oceans probably formed during the late stages of planetary accretion, such that by 4.0 Ga most of the current volume of seawater (>90%) was in place on the Earth's surface (Eriksson et al., 1998).

Because the $p_{CO2}$ in the early atmosphere was considerably higher than it is today (Holland et al., 1986; Eriksson et al., 1998), the first seawater to condense must have had a low pH (<7). This acidity was induced by the high $CO_2$ content of the early atmosphere and other acidic components such as $H_2S$ and HCl. According to Eriksson et al. (1998), this situation was probably short-lived, because recycling through ocean ridges would have introduced large amounts of Na, Ca and Fe. A pH between 8 and 9 and a neutral or negative Eh were thus rapidly attained during the early evolution of the oceans and would have been maintained thereafter by silicate-seawater buffering reactions and recycling at ocean ridges.

Although it is commonly assumed that the composition of seawater has not changed appreciably with time, some observational and theorical data challenge this assumption (Eriksson et al., 1998). Grotzinger and Reed (1983) show the existence of primary precipitation of aragonite in the Lower Proterozoic (1.9 Ga) Rocknest Formation, northwest Canada. According to Grotzinger and Kasting (1993), Archean carbonate sedimentation featured prolific precipitation of aragonite as giant botryoids up to 1 m in radius and magnesian calcite as stratigraphic sheets up to several metres thick and extending for over 100 km. By comparison, the Lower Proterozoic, in general, was marked by less spectacular occurrences of massively precipitated aragonite and calcite, although sedimentation by precipitation of cement matrix occurred. In contrast, Meso-to Neo-Proterozoic carbonate sedimentation saw a progressive decline in precipitation of massive carbonate cement (Burdett et al., 1990, Grotzinger and Kasting, 1993). Today, it is significant that despite the oversaturation of modern surface seawater with respect to calcium carbonate, precipitation of massive seafloor cement is unknown (Grotzinger and Kasting, 1993).

During the evaporation of seawater today, the precipitation of a small amount of $CaCO_3$ with/without $CaMg(CO_3)_2$ is followed by the precipitation of large quantities of $CaSO_4$ with/without $CaSO_4$-$2H_2O$ (Holland et al., 1986). Halite begins to precipitate when ~90% of the initial amount of water has been lost by evaporation (Holland et al, 1986). By comparison, according to Grotzinger and Kasting (1993), evidence for halite is present throughout the geological record and for the earlier Precambrian, is developed where gypsum is absent, such as in the Late Archean of the Fortescue basin, Western Australia (2.7 Ga), the Rocknest Formation (1,9 Ga) of western Canada, and the Perthei Group (1.88 Ga) in the East Great Slave Lake, Canada. In these three locations, halite occurs on top of carbonates without the presence of gypsum or anhydrite. This might indicate a lack of calcium sulphate precipitation during the Early Proterozoic. This could be due to a low concentration of sulphates in the Early Proterozoic oceans prior to 1.9 Ga (Grotzinger and Kasting, 1993). Cameron (1982), Klein and Beukes,(1989), Grotzinger and Kasting (1993) and Walker (1985) established that sulphate was a minor constituent of seawater (concentration of 0.001 mol/l) until ~2.35 Ga and then increased to its present value. Grotzinger and Kasting (1993) proposed another possibility for the absence of calcium sulphate in the Early Proterozoic evaporitic sequences : that calcium would have been exhausted before the gypsum field was reached during evaporation due to a bicarbonate/sodium ratio which was sufficiently high.

Klein and Beukes (1989) recorded a negative Ce anomaly in the Kuruman Iron Formation of the Transvaal Supergroup. Such anomalies are ascribed to fractionation of Ce from sea water into deep-sea manganese nodules. By using the modern ocean as a model, this would imply that manganese nodules may have formed on the Early Proterozoic ocean floor, a process which has not been documented by any geologic occurrences (Klein and Beukes, 1989).

One important point to note is the influence of atmospheric oxygen concentration on the Proterozoic ocean. According to Holland (1992), free $O_2$ was probably present in the atmosphere in the Early Proterozoic times, but at extremely low concentrations (see figure 27 from Kasting, 1987, 1991).

The development of the second stage (appearance of oxygen in the atmosphere and surface water), according to Kasting (1987, 1991), is believed to have occurred possibly between 2.4 Ga and 1.7 Ga. This is consistent with geological evidence such as the disappearance of uraninite and the appearance of banded iron-formations and red beds. The Makganyene Formation would therefore be situated in the stage II of Kasting (1987, 1991) corresponding to a stratified ocean with deep waters being anaerobic and surface waters being oxic.

The idea of stratified ocean is in accord with current models regarding iron-formation genesis. According to Klein and Beukes (1992), the deep ocean, being reduced, acted as a reservoir of soluble ions such as iron, manganese and silica (supplied by hydrothermal activity). The surface waters were oxidising and therefore, at the mixing level of the two different water layers, iron and silica precipitated alternatively in bands. A single cycle of bands have been interpreted by William (1993) as varves representing the strong climatic cycles of a Early Precambrian year, going from cold to warm temperatures. In the paragraph IV.5., the case of manganese precipitation will be discussed with its possible relation with the Makganyene Formation.

In summary, the Precambrian oceans (mainly anoxic, stratified with aerobic surface waters) were slightly different compared to the modern ocean sedimentary deposits. These differences in the chemistry of the seawater imply that care must be taken in modelling chemical sedimentary processes which occurred only in the Precambrian.

IV.2.3. Precambrian climatic paradox : low latitude glaciations

Recent research on the paleomagnetism of Precambrian glacigenic successions in the world concludes that past glaciation near sea level was circumequatorial (Williams, 1998). These paleomagnetic studies have mainly been undertaken on several Neoproterozoic sequences. However these studies are extending to the Early Proterozoic with :

- a paleolatitude of 11±5° for the Ongeluk Lava, conformably overlying the Makganyene Formation (Evans et al., 1997);
- near-equatorial paleolatitude of 2.8±3.4° and 2.8±3° for the Coleman and Lorrain Formations respectively which belong to the Huronian sequence from North America (Williams and Schmidt, 1997);
- near paleoequator position for the Hamersley Basin (Schmidt and Clark, 1994) at ~2.2 Ga when the glacigenic Meteorite Bore Member (Trendall, 1976) was deposited.

Apparently, as a rule, Precambrian glacigenic rocks have been accumulated close to the equator.

Land covered by ice down to sea level at equatorial latitudes is difficult to explain. Crowley and Baum (1993) tried to produce a model where land is covered by ice at low latitude. The first conclusion they drew was that the configuration of the continents is important. In their model, they used one single supercontinent. The most favourable position for this continent is perpendicular to the equator, and it must extent to both mid-latitudes. They indeed produced a totally frozen continent where equatorial temperatures would be -25° to -45°C. But to obtain this result, Crowley and Baum (1993) used very low values ($CO2$=120ppm, and a decreased solar luminosity by roughly 22%, instead of the 6% modelised by previous workers).

By taking a solar luminosity decreased by 6%, Crowley and Baum (1993) were just able to produce, in their computer modelling, ice covering the land, but the snow line would not extend in a band between 25°N and 25°S.

Today, tropical glaciers exist, but none actually extend to sea level. They are all located between 4000 to 5500 m (Thompson et al., 1984), which negates the theory that these low-latitude glaciations occurred by uplift due to rifting because, according to Williams (1998), maximum crustal uplift is in the range of 0.1-1.5 km. Furthermore, the Neoproterozoic Marinoan glaciation in South

Australia, which saw permafrost develop near sea level on the cratonic Stuart Shelf, was unrelated to mountain building.

There are currently four hypotheses explaining low-latitude glaciations :

- The "snowball Earth" (Kirschvink, 1992) which implies a pole-to-pole glaciation;
- An equatorial ice-ring system that shielded low latitudes from solar radiations and induced low latitude glaciations (Schwarzbach, 1963);
- Non-axial geomagnetic field, invalidating all the paleomagnetic studies (Williams, 1993);
- Large obliquity of the Earth : $\epsilon > 54°$(William's theory since 1975).

IV.2.3.1. The snowball Earth

To explain low-latitude glacigenic deposits occurring during the Neoproterozoic and Paleoproterozoic along the equator, Kirschvink (1992) proposed the snowball Earth theory. In this case the whole Earth is frozen from pole to pole. The mechanism proposed here is that almost all the continents are located in equatorial positions. Most of the solar energy absorbed by the Earth today is trapped in the tropical oceans (in contrast to the continents which are relatively good reflectors) and in high-latitude oceans which often have fog or other cloud cover. Furthermore if extensive areas of shallow, epicontinental seas were within the tropics, a slight drop in sea level would convert large areas of energy-absorbing oceanic surface to highly reflective land surface, perhaps, according to Kirschvink (1992), enhancing glacial tendencies.

An ice-covered Earth, with higher albedo (ability to reflect solar radiation), may be immune to deglaciation even at luminosity values higher than the present. Escape from the "ice house" would presumably be through the gradual buildup of the greenhouse gases, such as $CO_2$, contributed to the air by volcanic emissions. An additional mechanism is the geothermal heating of deep waters which could raise the entire column of ocean water to 20°C in 400,000 years (Crowley and Baum, 1993). Both of these mechanisms would imply that, if complete ice-covered conditions were to occur, they may not be permanent.

IV.2.3.2. Ice-ring system

Ives (1940) in Schwarzbach (1963) explained this theory. In this theory, the focus is to explain the decrease in intensity of solar radiations outside the Earth's atmosphere. Some tiny satellites orbited around the Earth and formed a ring of the type that now forms Saturn's rings. The shadow of this ring was sharply focussed on the equatorial area, and could have given rise to the circumequatorial Precambrian glaciations.

IV.2.3.3. Non-axial geomagnetic field

According to Embleton and Williams (1986), the validity of the axial geocentric dipole model could be questioned. If this model does not apply for the Precambrian times, all the paleomagnetic interpretations must be revised. Any deviation from this model during the Precambrian, according to Embleton and Williams (1986), could not have been short-lived event, as the poles they found for the Elatina Formation fall within the group of poles for the quasi-static interval 700-560 m.y.. Invalidation of the axial geocentric dipole model for such a major interval of time would call into questions other Precambrian paleomagnetic data for which unequivocal support from paleoclimatic evidence was lacking.

IV.2.3.4. Large obliquity of the Earth : $\epsilon > 54°$

Williams (1975, 1993, 1998); Embleton and Williams (1986); Schmidt and Williams (1995) proposed an alternative solution to explain Precambrian low-latitude glaciations. Substantial increase in obliquity would result in important changes in global climates (see figure 28.(A) from Williams, 1993).

The amount of radiation received annually at either pole compared to that received at the equator would be increased (see figure 28.(A) from Williams, 1993). When the obliquity exceeded 54°, low latitudes would receive less insulation annually and hence would be preferentially glaciated. Figure 28.(B) (from Williams, 1993) shows that minimum insolation occurs at ±30° latitude for $\epsilon$ = 60°, and at the equator for $\epsilon > 60°$. Williams (1975, 1993, 1998) obtained the critical obliquity of 54°, at which the climatic zonation reverses.

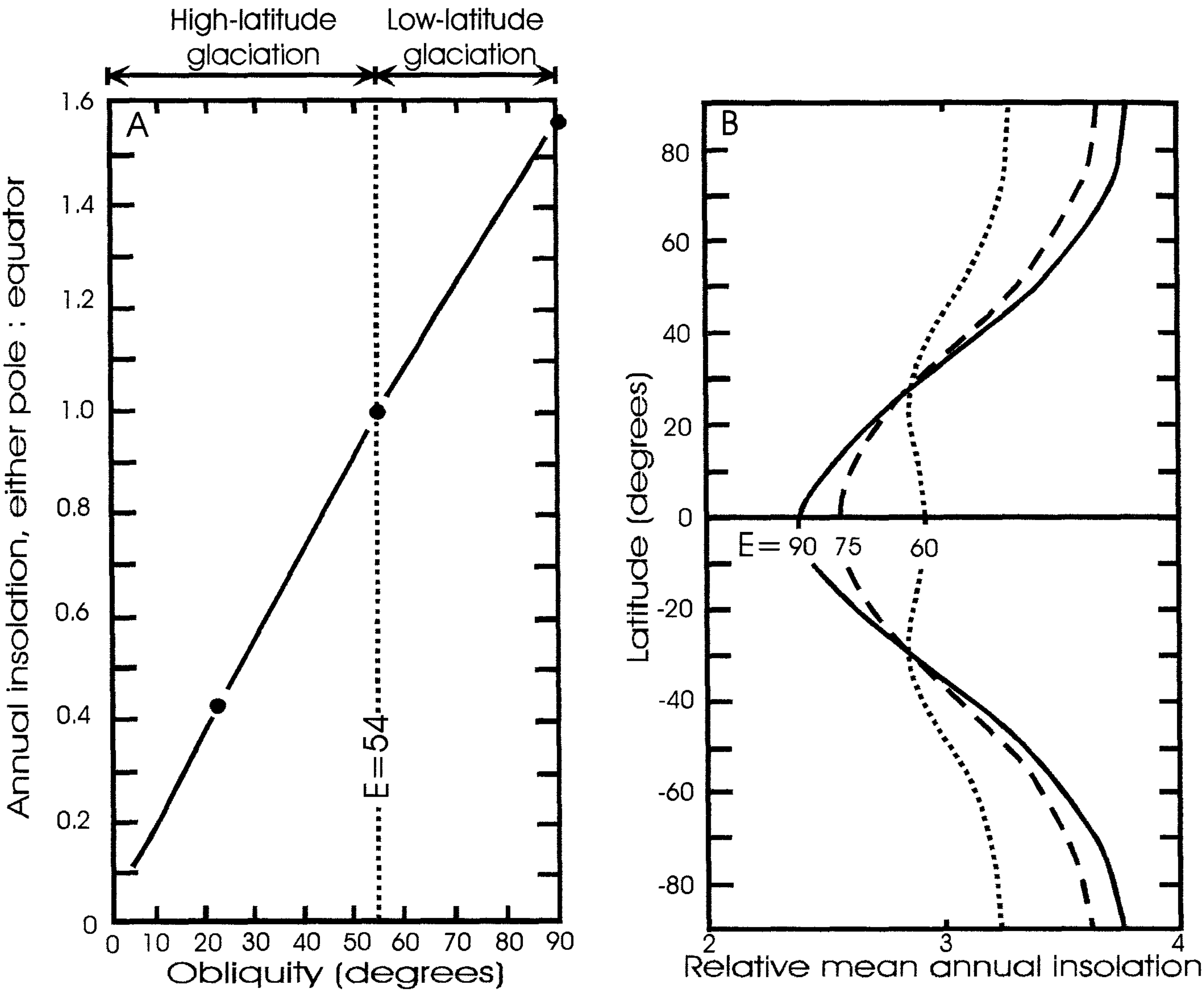


F. 28.(A) Relation between the obliquity of the ecliptic $\epsilon$ and the ration of annual insolation at either pole to that at the equator (solid line); the dashed line at $\epsilon = 54°$ separates the fields of potential low-latitude and high-latitude glaciation.
(B) Latitudinal variation of relative mean annual insolation of a planet for various values of obliquity (degrees); solid line for $\epsilon = 90°$, long-dashed line for $\epsilon = 75°$, short-dashed line for $\epsilon$=60 °. The plots in (A) and (B) together illustrate that for $\epsilon > 54°$, glaciation would occur preferentially in low to equatorial latitudes (from Williams, 1993).

According to Williams (1993), if an Earth with $\epsilon > 54°$ were to enter a glacial interval through some independent causes such as a decline in atmospheric $CO_2$ partial pressures or moderate decrease in solar luminosity (a large obliquity is not a direct cause of glaciation), low-to-equatorial latitudes ($\leq 30°$) would be glaciated preferentially. At high latitudes, the cold, arid winter atmosphere would allow only limited snowfall which would melt entirely during the very hot summers. Permanent ice could however form at low-latitudes. That zone, as well as receiving minimal solar radiation annually, would experience the additional cooling effect of frigid winds during each solstice and no extreme summer temperatures. The increased albedo resulting from snow cover in low to equatorial latitudes would further reduce effective insulation in that zone and allow the accumulation of permanent ice (Williams, 1993).

Seasonality would be greatly intensified, thus causing significant seasonal changes of temperature to extend into low latitudes. With an obliquity of 60°, for example, the tropics would be at 60°latitude and the polar circles at 30° latitude. The area between latitudes 30-60° thus would be within both the tropics and the polar circle (Williams, 1993)! This strong seasonal contrast would likely be too stressful for all but relatively primitive organisms.

Climatic zonation would be weakened. As local climates would be delicately balanced, any Milankovitch-type fluctuations in insulation arising from short-term ($10^4$ to $10^6$ years) changes in orbital parameters might cause large or exaggerated changes of climate over wide areas. These changes could result in the close association of tillites with warm-climate indicators such as red beds and primary dolostones, which is in fact a puzzling feature of the Precambrian glacigenic sequences (Fairchild and Hambrey, 1984; Fairchild et al., 1989)

The direction of zonal surface winds such as the tropical easterlies and mid-latitude westerlies would reverse for $\epsilon > 54°$ as the circulation in "Hadley cells" reversed direction. Westerly zonal surface winds would occur in low latitudes, which would receive much less precipitation than present-day low latitudes, and easterly zonal winds in mid-latitudes (Williams, 1993).

IV.2.3.5. Criticisms of the different theories

The snowball Earth implies that all the surface water present on Earth is frozen. This model of global glaciation is inconsistent with numerous observations (Embleton and Williams, 1986). The first point is that the frozen Earth would not have a strong seasonal regime as observed in Precambrian glacigenic successions (see Fairchild and Hambrey, 1984; Fairchild et al., 1989), and such very low temperatures would inhibit precipitation and sublimation (Schmidt and Williams, 1995). The creation of a frozen Earth would imply that solar radiation was anomalously low. The snowball Earth state would imply a major global regression which has not been observed during the

Neoproterozoic (Williams, 1998), and glacial evidence must be present on all high-latitude continents. According to Williams (1993), the North China Block was located in high latitudes during the Neoproterozoic and it does not show any evidence of a glacial event while the Yangtsi Block experienced glaciation in low latitudes. Furthermore, in a frozen Earth, the oceans would not be able to supply the water vapour needed to sustain the snowfall rates needed for the further advance of the snow cover over land.

To unfreeze such an Earth, the solar luminosity required, which is ~35% above its present value, would exceed the total increase in luminosity experienced by the Sun since its formation. Crowley and Baum (1993) proposed brines which would warm the water column up to 25° in 400,000 years, providing enough heat to melt the ice.

The ice-ring system also encounters major difficulties. The ice-rings can not exist so close to the Sun (Williams, 1993), even with a young Sun with slightly lower luminosity. Comparing with Saturn (obliquity of 26.7° and ice-ring present), the solar gradient from pole to pole is modified for the latitudes below 45° but not inverted, and insolation at the equator is not inverted (Williams, 1993). Therefore an Earth with ice-ring system would be glaciated preferentially at high latitudes.

By comparing the geomagnetic field with other planets (i.e. Uranus, Neptune) some conclusions can be drawn regarding a non-axial geomagnetic field. According to Williams (1993), the magnetic field of both Uranus and Neptune are tilted at large angles (58.6° and 46.9°, respectively) to the spin and that quadrupole moments are comparable to dipole. The observation that the magnetic fields of the two planets are of such configuration virtually rules out the possibility that they are undergoing transient excursions or reversals, and indicates that non-axial dipole-quadrupole planetary magnetic fields are indeed impossible (Williams, 1993). According to Williams (1993), the Precambrian paleomagnetic inclinations are also in accord with a geocentric dipole model.

Hence, global magnetic data and the wide spread of glacigenic sediments during the Neoproterozoic and apparently during the Paleoproterozoic, together argue against a non-axial, non-dipole geomagnetic field during the Proterozoic.

In contrast with all the above hypotheses, Williams's theory seems to overcome most of the problems. By increasing the Earth's obliquity, low-latitude glaciations would be preferred. The only unclear part of this theory is how the obliquity can vary between such large values. Williams (1975, 1993, 1998) explains all the geological evidence with his theory. According to Williams (1993), the origin of the large value of the Earth's obliquity ($\epsilon > 54°$) is induced by collision with a single giant impactor that was responsible for the formation of the Moon 4.5 Ga ago. This induced obliquity would have been up to 70° depending on the impact parameters. From then, this value would have decreased constantly to acquire a value of 60° just before the Cambrian lower boundary (see figure 29 from Williams, 1993). The curve of the values of the ecliptic versus time shows a sudden drop with a characteristic S-shape, to its present values, implying the "new" normal climatic zoning observed today. This sudden drop in the value of the ecliptic could be explained by some special and unique conditions at the core-mantle boundary which caused a significant increase in dissipative core-mantle torques at that time (Williams, 1993), but this can be coupled with the Earth's rotation, and other dynamic effects.

This postulated flip-over of climatic zonation at about 610 Ma ($\epsilon = 54°$) coincides with the widespread appearance of the Ediacaran metazoans at about 620-590 Ma, and the period of most rapid reduction of obliquity and seasonality at about 550 Ma with the "Cambrian explosion" of biota at 550±20 Ma (Williams, 1993, 1998).

This theory is regarded here as the most likely to have occurred, since variation of the obliquity has been explained. Low-latitude glacigenic sediment accumulation did occur due to the large obliquity of the Precambrian Earth.

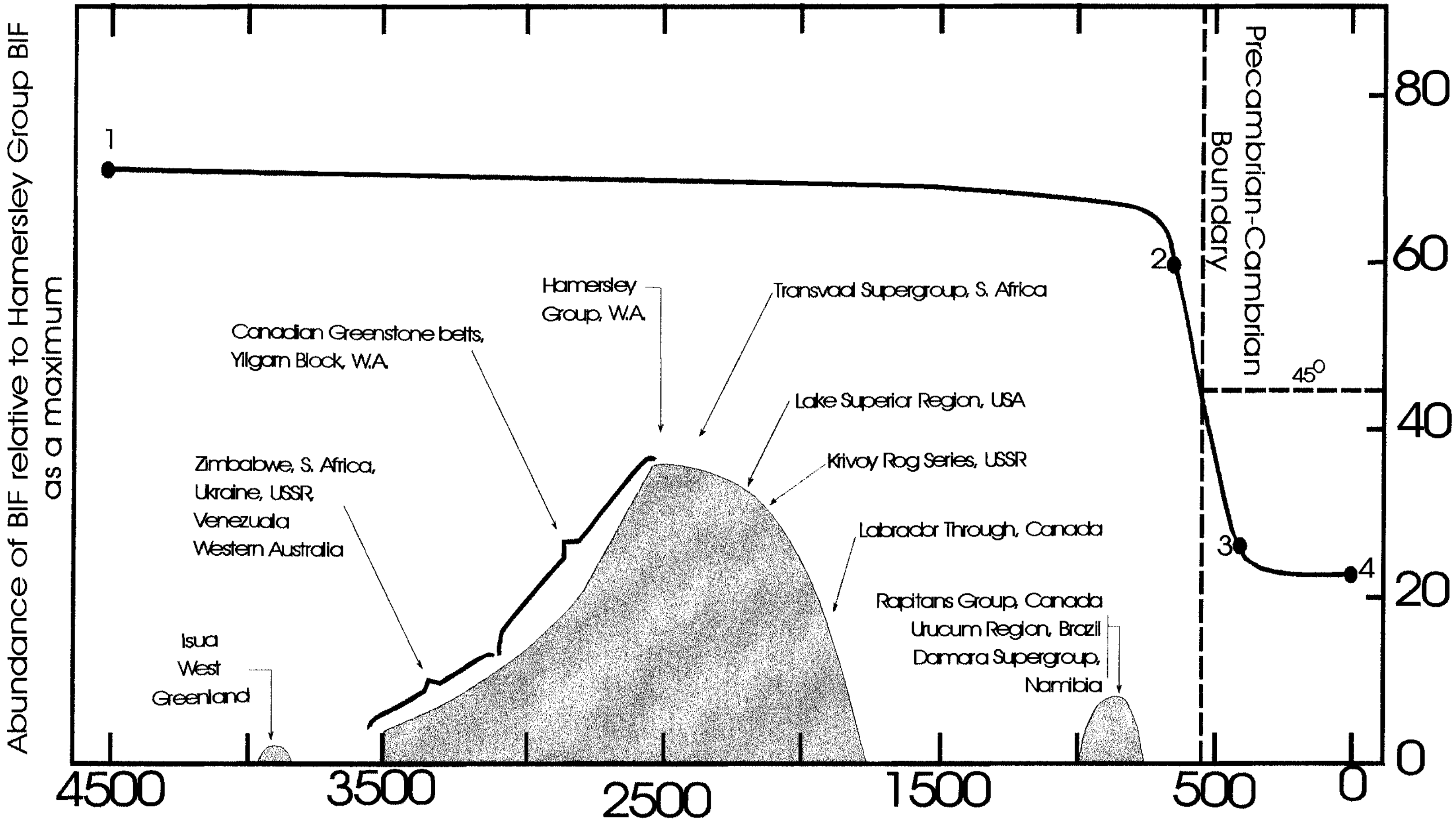


F. 29. Proposed curve of mean obliquity of the ecliptic against time, consistent with the single giant impactor hypothesis for the Moon's origin and interpretation of the geological record.

| | | | |
|---|---|---|---|
| Control point | 1 | corresponds to mean obliquity 70 | at 4500 Ga |
| | 2 | 60 | 650 |
| | 3 | 26 | 430 |
| | 4 | 23 | o. |

Highly schematic diagram associated showind the relative abundance of Precambrian banded iron-formations versus time, with several of the major iron-formations (and/or regions) identified. Estimated abundance values are relative to the Hamersley Group banded iron-formation volume taken as a maximum. The distribution of Phanerozoic iron-stones is not shown (after Klein and Beukes 1992, 1993; Williams, 1993).

## IV.3. Correlations using sequence stratigraphy

Sequence stratigraphy is widely used for stratigraphic correlations for the Phanerozoic cratons and passive margins. More recently, this powerful method has been used to correlate older sequences, from 1.4 to 3.1 Ga, and provides stratigraphic correlations from closely spaced basins within the same Proterozoic craton to distant cratons. Cheney (1996) gives three reasons for a more wider use of sequence stratigraphy for correlations throughout Proterozoic sequences :

- in rocks of all ages, sequence stratigraphy not only correlates the stratigraphic units, it allows comparisons of the tectonic or other events marked by unconformities.
- cover sequences commonly have a greater geographic extent than individual igneous and metamorphic belts, or commonly overlie more than one such belt. Thus cover sequences define and identify a particular geological province better than most of igneous and metamorphic belts, especially if the province is subsequently dismembered.
- the last reason for correlating Proterozoic sequences using sequence stratigraphy is due to their complex geological and thermal histories and the lack of paleontological evidence.

So far, the Kaapvaal craton has been correlated to the Pilbara craton in Western Australia by Beukes (1984), Cheney (1996), Martin et al. (1998) and Wingate (1998) by similarities in stratigraphic succession, tectonic setting, age, magmatism, metamorphism and metallogeny. Therefore, according to Cheney (1996) and Wingate (1998), these two cratons where in close proximity to each other, forming parts of the Vaalbara, a Precambrian supercontinent, from approximately 3.1 until 1.5 Ga (Wingate, 1998). According to Cheney (1996), another probable fragment of Vaalbara is the Grunehogna Province in Dronning Maud Land of East Antarctica. This possible fragment of Vaalbara rifted from the Kaapvaal Province during the break-up of Gondwana (Jacobs et al., 1993; Cheney, 1996). Unfortunately, the sedimentary succession on the crystalline basement of this province is not well known, and direct comparisons are not possible.

### IV.3.1. Review of the stratigraphic correlations within the Kaapvaal Craton

Within the Kaapvaal craton, the Transvaal basin and the Northern Cape basin have been correlated by a few authors (Cheney and Winter, 1995; Cheney, 1996; Martin et al., 1998) by the use of sequence stratigraphy. A review of these different correlations in South Africa is shown in table

4 (after Cheney and Winter, 1995; Eriksson et al., 1995 and Martin et al., 1998), this does not take into account the results from the present study. The correlation of the upper parts of the Ghaap Group with the Duitsland Formation (Martin et al.,1998) is questionable. The Duitsland Formation contains diamictite and no banded iron-formation whereas the banded iron-formations of the Koegas is conformable on the Penge-equivalent banded iron-formation of the Asbesheuwels Subgroup (Cheney and Winter, 1995). According to Cheney and Winter (1995), no lithological equivalent of the Duitsland Formation is preserved in the Northern Cape province, and no lithological equivalent of the Koegas occurs above the Penge Formation in the Transvaal Supergroup. To make them correlative, a major change in facies would be required and an unconformity which passes westward into a conformity (Cheney and Winter, 1995).

Correlation of the Makganyene Formation and the Rooihoogte, Timeball Hill and Boshoek Formations is made by Eriksson et al. (1993, 1995) and Eriksson and Reczko (1995) on the assumption that these formations are corresponding to a variation of facies, from glacial, fluvioglacial and glacimarine deposits (Visser, 1971) in the Makganyene Formation, to glaciofluvial in the Boshoek Formation (Schreiber, 1991), glaciolacustrine deposits in the Timeball Hill Formation and that the diamictite of Boshoek Formation represents more proximal glacial ablation deposits (Visser, 1971; Eriksson et al., 1993) in the basal parts of the Pretoria Group.

| Northern Cape basin | | | Transvaal basin | |
|---|---|---|---|---|
| Postmasburg Group | | Mooidraai and Hotazel Formations **(2066)** | Magaliesberg Formation | Pretoria Group |
| | | | Silverton Formation | |
| | | | Daspoort Formation | |
| | | | Strubenkop Formation | |
| | | | Dwaalheuwel/Droogedal Formations | |
| | | Ongeluk Formation **(2238)** | **(2224)** Hekpoort Formation | |
| | | **Makganyene Formation** | **Boshoek Formation** | |
| | | | **(2350) Timeball Hill Formation** | |
| | | | **Rooihoogte Formation /Duitsland Formation** | |
| conformable westwards | | | **unconformity estimated of 150 Ma** | |
| Ghaap Group | | **Koegas Subgroup** | **(2432) Penge Iron-Formation** | Chuniespoort Group |
| | Asbesheuwels Subgroup | Griquatown Formation **(2432)** | | |
| | | Kuruman Formation **(2465)** | | |
| | | Campbellrand Subgroup **(2521T, 2557B)** | **(2557 or 2552)** Malmani Formation | |
| | Schimdsdrift Subgroup | Lokommo Formation | ——— | |
| | | Boomplaas Formation | ——— | |
| | | Vryburg Formation **(2642)** | **(2642)** Black Reef Formation | |

T.4. Correlations of Northern Cape basin and Transvaal basin in South Africa (after Cheney and Winter, 1995; Eriksson et al., 1993, 1995; Cheney, 1996, and Martin et al., 1998). Formations in grey cell and thick characters are of glacial to peri-glacial environment. Formations in cell filled with diagonal lines are supposed to be of peri-glacial environment, as suggested by the stratigraphic correlations.

## IV.3.2. Possible new stratigraphic correlations within the Kaapvaal Craton

The "new" stratigraphic correlations within the Kaapvaal Craton are possible due to some remaining problems in the "old" stratigraphic correlations which are as follows:

The unconformity at the base of the Rooihoogte Formation is estimated to be about150 millions years by radiometric ages due to the karstic surface developed in the carbonates at the top of the Duitsland Formation (Eriksson et al., 1993). This unconformity would pass westward into a conformity if the Makganyene Formation is the correlative. Another major angular unconformity is present at the base of the Duitsland Formation. It preserves the underlying Penge Iron Formation erratically (Button, 1986). The Duitsland Formation rests in places directly on the dolomites of the Malmani Formation indicating an erosion of up to 2 kilometres of the Penge Formation (Button, 1986).

The ages, from the Vryburg Formation to the Mooidraai and Hotazel Formation, represent a time span of 600 million years of continuous sedimentary deposition, without any major unconformity (assuming that the Makganyene Formation is conformable with the underlying formations southwesternly). This would imply a very long tectonic stability of the Kaapvaal Craton during the Early Proterozoic times which is also unlikely to have occurred due to the high mobility of the cratons during these times.

Correlation between the Ongeluk volcanics (2.222 Ga, Pb-Pb isochron age) from the Northern Cape Basin and the Hekpoort Formation (2.184 Ga, Rb-Sr isochron age; Cornell et al., 1996) from the Transvaal Basin is based on similarities on lithologies and radiochronologic ages. As pointed out by Cheney (1996), the ages which are used to correlate the two volcanic formations of both basins might not be true due to a metamorphic reset. The Ongeluk Formation must be closer to 2432±31 Ma than to 2222 Ma (Cheney, 1996). This discrepancy in age between the Ongeluk Formation and the Hekpoort Formation implies new correlations within the Kaapvaal Craton. New ages on the Moodraai carbonates, top-most part of the Transvaal Supergroup in the Northern Cape, yielded 2394 +26 Ma (Pb-Pb isochron age; Romer and Bau, 1998). This indicate that the Ongeluk Formation is significantly older than previously believed of almost 200 Ma.

In the Transvaal Basin, 13 different formations (see table 5) are currently correlated to the only 4 formations present in the Northern Cape Basin.

In the stratigraphic column, the Duitsland Formation described by Martini (1979) and Taussig and Maiden (1986) might be a lateral equivalent of the Postmasburg Group. It shows a similar succession of lithologies as the Postmasburg Group : diamictite at the base, central andesitic, and carbonates on top. But there is still debate if the Duitsland Formation belongs to the Chuniespoort or Pretoria Group. In the proposed correlations, the Duitsland Formation is a lateral equivalent of the Rooihoogte Formation.

The proposed correlations are shown in table 5, in comparison with the current correlations.

| NORTHERN CAPE BASIN (CURRENT CORRELATION) | | TRANSVAAL BASIN (CURRENT STRATIGRAPHY) | | | NORTHERN CAPE BASIN (NEW CORRELATION) | |
|---|---|---|---|---|---|---|
| POSTMASBURG GROUP | MOOIDRAAI.HOTAZEL | PRETORIA GROUP | WOODLANDS/RAYTON | PRETORIA GROUP | | |
| | | | MAGALIESBERG | | | |
| | | | SILVERTON | | | |
| | | | DASPOORT | | | |
| | | | STRUBENKOP | | | |
| | | | DWAALHEUWEL/DROOGEDAL | | | |
| | ONGELUK (2.222 Ga) | | HEKPOORT (2.224 Ga) | | | |
| | MAKGANYENE | | BOSHOEK | | | |
| | | | TIMEBALL HILL | | | |
| | | | ROOIHOOGTE/DUITSCHLAND | | | |
| | | | | | MOOIDRAAI (2.395 Ga) | POSTMASBURG GROUP |
| | | | | | HOTAZEL | |
| | | | | | ONGELUK | |
| | | | | | MAKGANYENE | |
| GHAAP GROUP | KOEGAS SUBGROUP | | | | KOEGAS SUBGROUP | |
| | ASBESHEUWELS SUBGROUP TOP : 2.432 Ga BASE : 2.465 Ga | CHUNIESPOORT GROUP | PENGE | CHUNIESPOORT GROUP | ASBESHEUWELS SUBGROUP | GHAAP GROUP |
| | TOP : 2.521 Ga CAMPBELLRAND SUBGROUP (2.557 Ga) | | MALMANI (2.552Ga) | | CAMPBELLRAND SUBGROUP | |
| | SCHMIDTSDRIF SUBGROUP (2.642 Ga) | | BLACK REEF | | SCHMIDTSDRIF SUBGROUP | |

T.5. Current and proposed correlations between the Transvaal Supergroup in the Northern Cape and in the Tranvaal Basins (after Cheney and Winter, 1995; Eriksson et al., 1993, 1995; Cheney, 1996, Romer and Bau, 1998; Martin et al., 1998). Grey areas represent unconformities.

The Koegas Subgroup, lying on top of the Asbesheuwels Subgroup, equivalent of the Penge Iron-Formation, is now part of the Postmasburg Group. The Koegas Subgroup is only present in the Postmasburg area. The latter is considered to be a distal basal facies due to its intimate interbedding with the Makganyene Formation, and due to similar isotopic signature between the iron-formations from the base of the Makganyene Formation and the Koegas Subgroup. According to Moore et al. (in prep), the Makganyene Formation rests on the Asbesheuwels Subgroup (i.e. Kuruman and Griquatown Iron-Formations) further north in the Sishen area. The latter is considered as a proximal facies due to facies lithological, sedimentological, and geochemical studies.

The Postmasburg Group has therefore no lateral equivalent in the Transvaal Basin, resting broadly on the Ghaap Group conformably. The absence of the Postmasburg Group in the Transvaal Basin should be related to the pre-Pretoria erosional cycle. The top of the Postmasburg Group in the Northern Cape is terminated by a major unconformity of the Olifantshoek Supergroup.

The implications for these correlations within the Transvaal Supergroup involve major changes in current theories reaching far more than only stratigraphy. The Transvaal Supergroup in the Northern Cape represents a climatic variation with a cold-peak at the Makganyene Formation. Compare to the Pretoria Group, which does not be part of the Transvaal Supergroup, the succession is truncated before the major glacial peak.

This implies that there was at least two ice-ages occurring in the Transvaal Sea, the older corresponding with the Makganyene Formation, and a younger event corresponding with the Rooihoogte/Duitsland, Timeball Hill and Boshoek Formations. The Huronian glacial event which occurred in Canada has three glacial events (Symons, 1975; Young and Nesbitt, 1985; Miall, 1985; Mustard and Donaldson, 1987; Aspler and Chiarenzelli, 1997), and the Meteorite Bore Member from the Turee Creek Formation in Australia has only one (Trendall, 1976). Assuming that these continents were forming Vaalbara Supercontinent in the Early Proterozoic during Huronian times (Beukes, 1984; Cheney, 1996; Martin et al. 1998; and Wingate,1998), correlations of these three basins are very tempting.

IV.3.3. Vaalbara Supercontinent

By using sequence stratigraphy, correlations within the Kaapvaal craton are possible, but the possible existence of Vaalbara with the use of the same method can link the stratigraphy of the Kaapvaal craton of southern Africa and the Pilbara craton of Western Australia. These correlations are shown in table 6 (after Cheney, 1996). However, the existence of the Vaalbara Supercontinent is challenged by Nelson et al. (1999). Despite numerous similarities in geological development between the Kaapvaal and the Pilbara Cratons, discrepancies remains on the timing of volcanic eruptions, intrusion emplacements, and similar lithologies and major periods of erosion could be explained by global see level changes (Nelson et al., 1999). Therefore table 6 should be read with care and criticism.

| Pilbara Province | age (Ga) | Northern Cape Province | Transvaal Province | Typical lithology |
|---|---|---|---|---|
| absent | 2.1 | absent | Dullstroom volcanics to Loskop Formation | andesite, felsite and quartz arenite |
| Beaskley River Quartzite to Wooly Dolomite | 2.2 | absent | Pretoria Group | absent |
| Turee Creek Group | 2.4 | Postmasburg Group Koegas Subgroup | absent | limestone, lutite, volcanics and diamictite |
| Jeerinah Formation and Hamersley Group | 2.6 | Ghaap Group Schmidtsdrif Formation | Chuniespoort Group Black Reef Formation | dolomite, iron-formation and quartzite |

T. 6. Sequence stratigraphy of Vaalbara between 2.6 and 2.1 Ga (after Cheney, 1996).

Evidence of glaciation occurs on both cratons at almost the same age. Their paleo-latitude position have been :

- at 2772 Ma for the Pilbara craton (Wingate, 1998) at 34.3±6.4 (measured on the Mount Roe Basalt),
- at 2782 Ma for the Kaapvaal craton (Wingate, 1998) at 64.5±17.5 (measured on the Derdepoort Basalt).
- at about 2394 Ma for the Kaapvaal craton(Romer and Bau, 1998) at 11±5 (measured on the Ongeluk lava)(Evans et al., 1997).

The glacial events were therefore at low latitude, and this is the Precambrian climatic paradox.

## IV.4. Environmental deposition of the Makganyene Formation

### IV.4.1. Introduction

This depositional model for the Makganyene Formation is highly speculative, due mainly to the restricted area of study compared to its wide extent throughout the Postmasburg area, and because glaciogenic deposits are very complex in nature due to the multitude of different processes involved in the deposition of this type of sediment. This model has been established using descriptions of currently observed glacial processes and comparing the present-day observed facies with those of the Makganyene diamictite. Also, the shape of the western margin of the Kaapvaal craton must be of major importance, controlling the formation of ice-sheets or tide-water glaciers, and hence greatly influencing facies distribution along the zones of deposition. Therefore, existing paleogeographic models of the Transvaal continental shelf have been used, but they generally are very simplistic.

### IV.4.2. Depositional model of the Makganyene Formation

The Makganyene Formation was deposited on a passive continental margin, in fairly open ocean settings. High precipitation and annual mean temperature up to 1°C, would have supplied snow accumulation and glacial advance would have been very rapid.

The factors which control the distribution of glaciers are complex, but in general, glacial growth is favored by low temperatures and high precipitation. The most common glacier types present in high latitudes are ice shelf or tidal water glaciers. The type of glacimarine lithofacies are very dependent on glacial budget, temperature gradient through a glacier, and basal temperature because these three factor can control the type of glacial front (Powell and Molnia, 1989), rates of frontal advance and so type of glacier, debris budget, that is, rates and volumes of debris supplied to the sea (erosion and glacial flow or transportation rates), and melting rate, sediment load and discharges from meltwater streams. But due to the numerous limiting factors of ice-shelf formation, any embayment present would be a preferential site for ice-sheet growth, and elsewhere tidewater glaciers would form. Because the theory of the snowball Earth is very popular, and as soon as a glacial deposit is studied, ice shelves are involved in their depositional model (Visser, 1971; Young, 1976; De Villier and Visser, 1977; Klein and Beukes, 1993). A brief description of the limiting factors needed for the formation of ice shelves and tidewater glacier follows.

Most modern ice shelves exist in Antarctic, where they occupy about 47% of the coastline of permanent ice and 12% of the surface area of permanent ice, but contain <3% of the total volume of permanent ice (Alley et al., 1989). The small volume of ice shelves average between 475 and 670 m thick whereas grounded ice averages 2450 m. Their dimensions are huge and can be in the order of about 800 km length by 500 km wide (Ross Ice Shelf). According to Alley et al. (1989), an ice shelf is "a sheet of very thick ice, with a level or gently undulating surface, which is attached to the land along one side but most of which is afloat and bounded on the seaward side by a steep cliff". With very few exceptions the upglacier, end of an ice shelf, consists of snow and ice that accumulated on a grounded ice sheet and then flowed downglacier until it crossed the grounding line (Alley et al., 1989). According to Powell (1984), the grounding lines occur where a glacier begins to float, and the calving zone can be separated by perhaps hundreds of kilometres from its grounding line.

Within an ice shelf, ice streams are present. They are considered as the most dynamic part of an ice shelf (Anderson et al., 1984) and participate actively to the ice drainage in to the sea. They are longitudinal extensions of inland valley glaciers which join the ice sheet at sea level and keep their high flow speed compared to the rest of the ice shelf. An ice stream is a fast-moving ice flowing between regions of slow-moving ice.

If an ice shelf were composed of temperate ice, spreading would be very rapid and water filled surface crevasses would be able to join with basal crevasses and cause rapid calving (Alley et al., 1989). A huge ice shelf can form, like the Ross ice shelf of Antarctica, due to an embayment with local high spots in the bed and with cold temperatures (average midsummer temperature <10°C or mean annual temperature <-10°C). Sea ice, according to Styvinski (1989), forms when the air temperature falls below the freezing point of sea water (-1.8°C at salinity of 34‰). Freezing-up progresses from the shoreline, initially forming an icefoot, followed by a transition zone of tidal cracks and leads where the flow of ice contracts and expands with the tide, and mobile floating ice. This does not mean that temperate ice shelves cannot exist, but only that the requirements of lateral constraint and protection from bottom melting to sustain a temperate ice shelf are sufficiently severe that none exist today (Alley et al., 1989). Under sub-arctic conditions, or where the tidal energy is sufficiently strong, a complete ice cover will not form. The duration and thickness of the ice cover depends on a variety of meteorological and oceanographical conditions, but both increase generally with latitude.

The conditions required for maintaining large ice shelves are restrictive :
- sheltered bays are required to protect ice shelves from oceanic currents, tides, waves and winds that facilitate ice break-out;
- anchor points are required for protection against those forces mentioned;
- grounded-ice discharge must be high to counteract ablation processes of calving and basal (and occasionally top) melting;
- most of the upper surface of an ice shelf is an accumulation area to counteract ablation processes;
- ice shelves comprise of cold ice because ice pressure melting point has lower tensile strength and experiences easier fracture propagation.
- ice shelves are restricted to certain tectonic settings (early stage oceanic rift, passive margin embayments, aulacogens, pull-apart basins, back-arc basins, some fore-arc basins and remnant ocean basins).

If an ice shelf regime is suggested from an interpretation of ancient glacimarine sediment, then an automatic definition and restriction is placed on paleogeographic, paleoglacial and paleoclimatic conditions (Powell, 1984). A tidewater glacier interpretation does not have such restrictions. They exist today on open coasts under both polar and temperate climates and in enclosed bays such as fjords (Powell, 1984). If continental shelves were not as extensive during some periods of geologic time, then protection afforded to ice shelves would be lacking and tidewater fronts would be most common (Powell, 1984), the glacimarine deposits will only be preserved on continental shelves or other shallow siliclastic seas (e.g. epeiric seas) if they are not subsequently eroded by grounded ice.

At present, tidewater glaciers cover about 20% of the Gulf of Alaska coastal area (Powell and Molnia, 1989), and more than 100 valley glaciers end in the sea as grounded tidewater cliffs under the cool-temperate to mild sub-polar climatic conditions. Tidewater glaciers are more common today than ice shelves (Powell, 1984), and this may have been also true under full glacial climates, because of limiting conditions under which large ice shelves can form and maintain.

Tidewater glaciers in the South Shetland Islands and the Trinity Peninsula, northern Antarctic peninsula, are grounded at an average depth of 80 to 120 m (Griffith and Anderson, 1989). Griffith and Anderson (1989) describe the tidewater glacial surfaces which commonly rise steeply back from the ice front, indicating that they are grounded at the most landward pinning point available. The grounding lines of tidewater glaciers are where the glaciers end as a nearly vertical cliff (Powell, 1984), and hence the grounding lines of tidewater glaciers coincide with their calving zone.

According to Styvinski (1989), the terminal position of a tidewater valley glacier fluctuates seasonally, affected by the seaward flowing ice mass and the landward directed rates of iceberg calving and ice-front melting. Together, these processes combine to make ice margins very dynamic. According to Styvinski (1989), ice flows fastest in the central part of the glacier; thus, through the winter (when calving is of less importance) the front will assume a curved convex shape.

Icebergs may fall from near vertical ice walls (Styvinski, 1989), pop up from below the water line or simply launch out into the water. There are four styles of iceberg production from a tidewater glacier (Styvinski, 1989) :

- subaerial jointing of ice blocks;
- tidewater jointing of ice blocks around ice caves formed from submarine discharge or from along the tidewater indenture;
- subaqueous jointing as affected by buoyancy forces;
- detachments of large mega-icebergs along a transverse crevasse system, which commonly occur at basin constrictions.

Development of any floating glacial front is inhibited because of tensile weakness due to water films between ice crystals (Powell and Molnia, 1989). Most glacial advance into the sea are commonly slow because either a sediment threshold (morainal bank) needs to be constructed and/or sea level must fall in order to maintain a stable water depth at tidewater front. However, some glacier along the south-southeast Alaska coast are known to surge and some of them can move quickly in to the sea (Powell and Molnia, 1989).

Facies interpretation is dependant on the type of glacial front (ice shelf or tidewater glacier) and will be discriminated in the proposed model of this study. The type of glacier responsible for the deposition of the Makganyene Formation will give insights on the paleomorphology of the coastal region of the western margin of the Kaapvaal Craton.

In the proposed depositional model, the Makganyene Diamictite occurs as the centre of symmetry of the Transvaal Supergroup (carbonates-BIFs-Makganynene/Ongeluk-BIFs-carbonates). Following, is a description of each stage, designated by the letter corresponding to the figure 30.

A : The first stage is the deposition of the Campbellrand Subgroup in the Transvaal epeiric sea on the western edge of the Kaapvaal Craton. The depth of the water on the shelf was about 50 metres, allowing the photic zone to reach down the floor of the shelf. Cryptalgal limestone precipitated in this area. Benthic microbial mats, forming stromatolites in the carbonates, supplied large amounts of organic carbon to the deep waters below the photic zone (Klein and Beukes, 1989). This carbon was the source for carbonaceous shale to precipitate in the anoxic, deeper parts of the basin. The contact of oxygenated waters with deep anoxic waters is termed a "chemocline" and is a zone of mixing. The deep water is enriched in metallic ions in solution ($Fe^{2+}$ and $Mn^{2+}$ for example).

B : This stage represents the deposition of banded iron-formations due to a transgression. The photic zone does not reach the bottom of the shelf because of a deepening of the water column. This inhibited micro-algae from supplying organic carbon to the deep waters and to the chemocline. Oxygen was still available resulting in oxic conditions. Hematite- and magnetite-rich iron-formations have been precipitated because very little organic carbon was present to reduce the primary iron oxides into hydroxides (Klein and Beukes, 1989). When the oxygen was in short supply at the chemocline, and some carbon was available, $Fe^{2+}$ and $P_{CO_2}$ would have built up to saturation levels resulting in the primary precipitation of siderite-rich iron-formations (Klein and Beukes, 1989). The mechanism for ion supply ($Fe^{2+}$) was the upwelling of deep anoxic and ion-rich waters up to the chemocline where they are oxidised. $Mn^{2+}$ is left behind in solution because manganese is more soluble than iron, and it needs higher Eh to precipitate as $Mn^{3+}$. Thus while $Fe^{2+}$ is oxidised and deposited as oxides or hydroxides, $Mn^{2+}$ concentration started to buildup.

C : Early workers described the banded iron-formation series as becoming more cherty towards the top of the Koegas Subgroup. This change, according to Truter et al. (1938) is very gradual and almost imperceptible. This might be due to changes in sedimentation style and in ocean chemistry, probably induced by climatic changes over a significant period of time. Variation in climate was

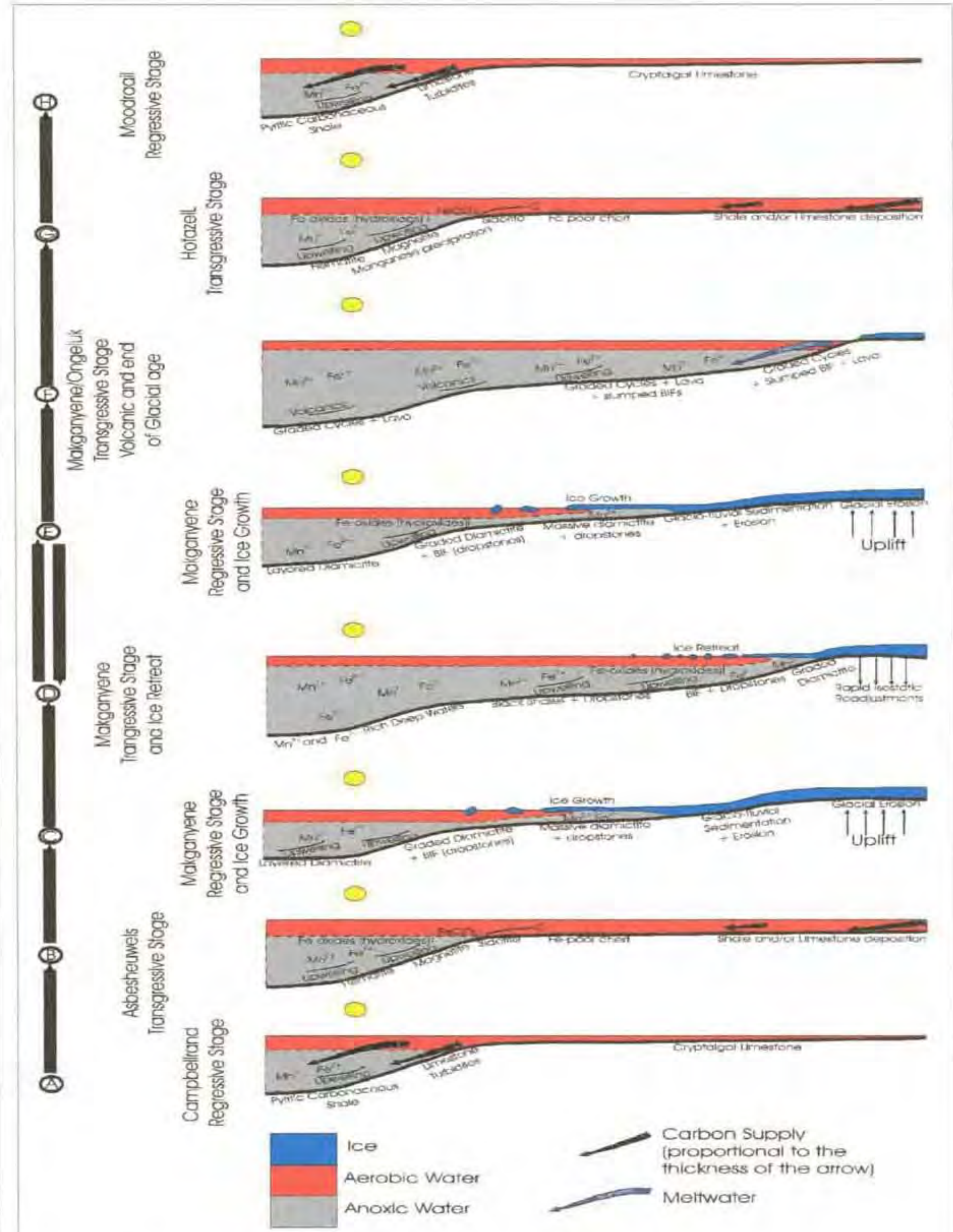


F. 30. Depositional model for the Transvaal Supergroup in the Northern Cape Province.

somehow smooth in the Transvaal Supergroup. This progressive climatic change is emphasised by the symmetry of the Transvaal Supergroup (Tsikos and Moore, 1997; and Tsikos, 1999) changing gradually from carbonate facies to iron-formation facies as shown in figure 26.

The development of large land continental ice sheets on the western margin of the Kaapvaal Craton produced global changes in sea level (glacio-eustatic) because large volumes of water were locked up as ice. In addition to glacio-eustatic changes, glacio-isostatic sea level changes were caused by ice-loading and unloading of the Earth's crust (Edwards, 1986; Eyles and Eyles, 1992). This results in elevation or depression of the sea floor and thus created relative changes in sea level and water depth local to the glaciated Northern Cape Basin. Variation in the magnitude of crustal loading across the glaciated Northern Cape Basin could have caused one part of the basin to experience a fall in relative sea level at the same time as water depths increased elsewhere in the basin. According to Eyles and Eyles (1992), the combination of these effects in glaciated basins makes assessment of the stratigraphic significance of individual unconformity surfaces extremely difficult.

As explained by Eyles and Eyles (1992), the position of ice margins which have moved onto continental shelves is controlled not much by climate, but by crustal downwarping below the ice sheet. This crustal downwarping induced a displacement of the mantle material beneath and immediately adjacent to the ice sheet, and was reflected by a peripheral forebulge. According to Eyles and Eyles (1992), the crust can be depressed by as much as 600 m below the ice sheet and for some distance beyond the ice margin. Such displacement far exceeds the magnitude of glacio-eustatic sea level drop (approximately 150 m) and so created the situation where high relative sea levels occurred around the ice margin at times of global glacio-eustatic sea level low stand. The forebulge migrated away from a growing ice sheet to a distance of several hundred kilometres from the ice margin, and collapsed as the ice sheet retreated. This gave rise to a very complex succession of sea level changes resulting from both glacio-eustatic and glacio-isostatic adjustments through-out the glacial cycles and across glaciated continental shelves of the western margin of the Kaapvaal Craton.

Subglacial deposition from a grounded glacier occurred during periods glacial advance on to the continental shelf of the Northern Cape Basin, and deposits may commonly be preserved at the base of a glacimarine sequence as interbedding of lodgement and melt-out till with sediment gravity flow and fluvial deposits (Powell, 1984). This type of sediments are present on top of local unconformities between the Makganyene Formation and the underlying iron-formations, and they have not been observed during the present study. Below the main thrust fault, a wide variety of sediments are interbedded (sandstone with planar laminations, siltstone, BIFs, diamictites) at the base of the cores GA171, GA129 (see figures 13 and 14) and could represent a distal expression the subglacial zone of deposition, i.e. in ice-proximal zone. In the field (Koodooskloof96 and Vaalwater 84), the contact is also represented by interbedding of diamictites with BIFs and red shales, representing a more evolved subglacial zone. Above the main thrust fault (farm Paauvlei 190), the contact is sharp and only a layer of clastic sandstone approximately 2 metres thick occurs between underlying banded iron-formation/red shale and the regularly layered diamictite. These immature sandstones were also described by De Villiers and Visser (1977), but due to the restricted area of field work, generalisation of the presence of this clastic sandstone at the base of the Makganyene Formation is difficult to make. They might represent the first clastic input into the basin at the snout of a submarine canyon. The subglacial zone represents the first increment of glacial sediments into the basin.

According to Powell (1984), the ice-proximal zone includes ice-contact grounding line facies which interfingers with more distal diamicton and/or mud.

Freezing-on of sea water at the grounding line of an ice shelf can prevent formation of a morainal bank because very little debris may be released from the ice (Powell, 1984)

When a grounded tidewater glacier is melting at its base near its grounding line, subglacial meltwater streams discharge. Subglacial streams at temperate valley glacier receive most of their water from supraglacial sources. However, in ice shelf regimes glacier ice is cold and supraglacial water cannot contribute to subglacial discharges which subsequently have only subglacial melting source (Powell, 1984). The Makganyene Formation displays a huge amount of clasts, with the majority of them being cherty in composition. These clast imbrications occur below the main thrust fault (Vaalwater 84), and therefore must be closer to the ice-capped continent. They occur in massive diamictite and correspond to the "massive diamictite + dropstones" zone of deposition in figure 30.(C). These imbrications of clasts suggest that the glaciers were wet-based and were certainly originating from subglacial stream discharge of a temperate valley glacier. Subglacial streams produce a situation unique from any other natural sedimentary environment by discharging and releasing their load at the base of a sea water column rather than at sea level. Sea water density stratification and ocean currents control the paths of water/sediment plumes from the efflux. According to Powell (1984), exact mechanisms of sediment transportation and release are unclear at present, but bedload is probably dumped at the efflux to form a mouth bar and fine-grained sand and mud forms interflow or overflow sediment plumes. Proximal deposits from turbid subglacial streams are coarse grained clast-supported gravels and sand that can comprise the core of a morainal bank, and this facies has been observed in one borehole (MTP4). More distant deposits comprise sand and silt laminae with dropstone diamicton or dropstone iron-formation within about 0.5 to 1 km of a grounding line (Powell, 1984; Mackiewicz et al., 1984). At the snout of a submarine canyon on the farm Paauvlei 190; the sediments are layered, and are represented by the regularly layered diamictites situated above the main thrust fault, these sediments were laid down deeper into the basin, corresponding to the "layered diamictite" zone of deposition in figure 30.(C). The sediments above the main thrust fault are deeper in the basin because deep facies have been thrusted over more proximal facies (boreholes from Sishen and Matsap, and farms Vaalwater 84 and Koodooskloof 96).

Figure 31. from Powell and Molnia (1989) shows very schematically the distribution of debris at the front of a glacier. The debris transported within the ice in this model might have been completely differently distributed for the Makganyene glaciers. The rock flour was washed out into the ocean and deposited and coarser clastic components were also transported at the base of the glacier, by glacio-fluvial processes and/or scratched against the pavement. These glacial sediments took the geochemical signature of the source rocks which were predominantly banded iron-formations. As suggested by Visser (1971), and shown during this study, the granitic basement was still covered up to the end of the glacial ages due to the quasi-absence (Visser, 1971) or total absence (this study) of plagioclase.

In summary, ice-proximal zone sediment overlies subglacial facies and comprises diamictons of melt-out till, dropped para-till, compound para-till and gravity flow deposits. Sorted and stratified facies are produced by iceberg dumping, fall sorting, water column and bottom winnowing, melt water stream interflows, interflows and overflows, and low density and low viscosity gravity flows.

D-E : Sea level changes non-related to glaciation in a glaciated basin can change radically the environment of deposition (Eyles and Eyles, 1992). The ice sheets are stable on the continental shelf when they are grounded. Therefore their maximal extension seawards is the top of the slope where the ice sheet begins to float. If a transgression occurs, the ice sheet would be disintegrated by extensive and active calving along the ice margin. This effect could, according to Eyles and Eyles (1992) , be sufficient to initiate deglaciation.

The banded iron-formation deposition is believed to be due to a transgression (Klein and Beukes, 1993) where any present ice-sheet would have undergone intense calving because of the limiting factors to maintain them. The clastic input was limited to icebergs (in the Matsap area) which released their load by melting, and chemical precipitation has proceed. As shown by geochemical analysis, the iron-formations within the Makganyene Formation do not show any terrigenous contamination. This similarity with the Rapitan Iron-Formation in Canada (Klein and Beukes, 1993) strongly suggest that the iron-formations from the Makganyene Formation were deposited in a clear water system, probably without any floating ice in the water column. Only the Matsap samples contain dropstones within the banded iron-formations suggesting deposition of iron-formation in glacigenic environment and that icebergs were present but localised since the Sishen samples contain no dropstones. This iceberg distribution is dependant on oceanic currents. Iron-formation deposition was far removed from the glacial influence. The clear water environment of deposition envisaged for the iron-formations for the Makganyene Formation and the Rapitan Formation strongly contrasts with the turbid environment of accumulation of siliclastics from suspension and dropping from icebergs. Klein and Beukes (1993) associated iron-formations from the Rapitan Formation as some kind of condensed interval deposited during an interval of very rapid rate of relative sea-level rise. This assumption was made due to the presence of sharp bottom contact of the iron-formations with the diamictite, which is also the case for the iron-formations of the Makganyene Formation. The presence of black shale units within the banded iron-formations, and even black shale matrix to diamictite, grading into more oxidised diamictite suggests that oceans were stratified with anoxic deep waters and could be interpreted as a slow rate of relative sea level change.

On the other hand, a regression would give rise to a growth of the ice basinwards, the ice progression would stop when conditions of equilibrium with the bedrock and buoyancy in sea water will cease. This regression would re-establish the depositional zones of the figure 30.(C).

The sea-level fluctuations were important, since banded-iron formations are interbedded with clastic rocks. These relative changes in sea level occurred several times during the Makganyene times, and are revealed by alterning clastic and chemical sedimentation.

F : During deglaciation towards the end of the Makganyene times, thawing of most of the ice would have released large volumes of water, causing widespread slumping observed as small-scale, fine-grained graded cycles. Chemical sedimentation was also re-established, but probably caused by tectonic instability due to the onset of volcanic activity (Ongeluk), slumped iron-formations are interbedded with the graded cycles,. These slumps would have been deposited in deeper water environment due to the post-glacial transgression.

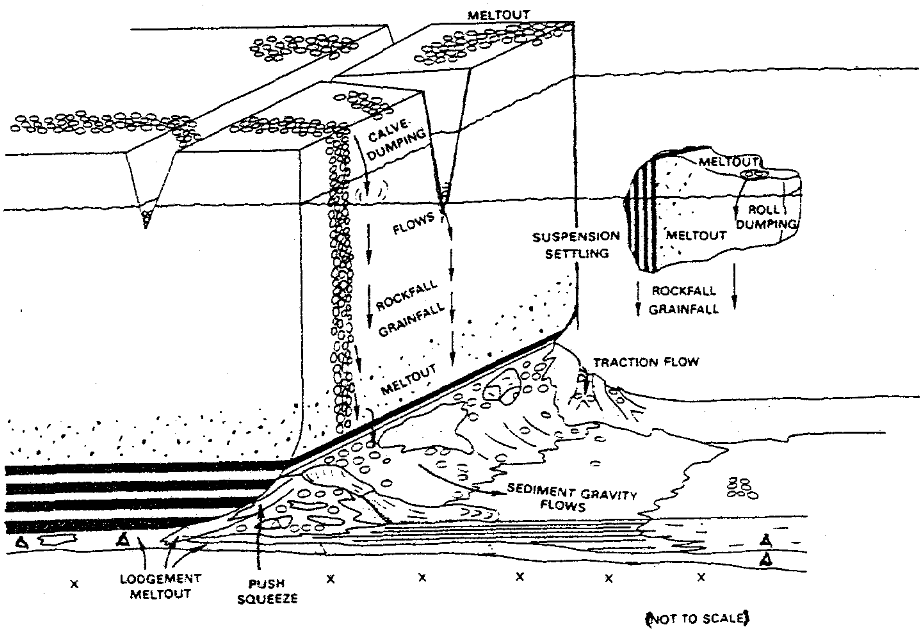


F. 31. Processes and lithofacies associations at tidewater fronts of temperate glaciers (from Powell and Molnia, 1989).

G : The settings have been re-established, similar to those of the figure 30.(B) where banded iron-formations from the Asbesheuwels Subgroup were laid down in the Transvaal Sea. Mn that accumulated in the oceans due to selective precipitation of Fe, precipitated once carbonate formation was re-established in the warming ocean. These processes are discussed in the next paragraph (see paragraph IV.5.3.).

H : Following Manganese deposition in restricted basins, a gradual regression occurred, and the Hotazel Formation grades into the carbonates of the Moodraai Formation with the settings of figure 30.(H). After this stage, a a major erosional and angular unconformity separates the Transvaal Supergroup and the Olifantshoek Sequence.

IV.4.3. Conclusions

Typical glacial depositional zones could not easily be discriminated, but a paleomorphologic reconstruction of the coast of the western margin of the Kaapvaal craton for the Makganyene Sea could be very useful for placing embayment, allowing an accurate distribution of tide water and ice sheet glaciers. Facies models would be more constraint. However, the rocks studied in the Rooinekke area must correspond to a tide water glacier setting, with a high production of ice rafted debris (presence of dropstones) and sub-aqueous debris flows laid layered diamictite deeper into the basin (like in Paauvlei 196 above the main thrust fault), but closer to the glacier snout, the diamictite is more massive and interbedded with chemical sediments.

Visser (1971) interpreted that the diamictite represents a partly reworked ground-moraine deposit, but due to the very scarce presence of striated pebbles, the author suggests that the diamictite derives mostly from rafted material due to the presence of dropstones, both within banded iron-formations and diamictite itself and from meltwater discharges at the snout of the glacier. These sediments can then be reworked by current or debris flow actions, slumping in a sub-aqueous environment, and become deposited deep in the basin in the form of layered diamictite, possibly graded on big scale (few metres).

Geochemical analyses show evidence that the granitic basement has not acted as a source for sediments, but also show that the carbonate content of the diamictite from the Sishen area is significantly higher than the diamictite from the Matsap area. The carbonate content in the diamictite come from the Campbellrand Subgroup which acted as a source. The Campbellrand Subgroup is stratigraphically older than the Asbesheuwels Subgroup (iron-formation). High reliefs were responsible for a deeper erosion on the centre of glaciation situated on the Vryburg rise (Visser, 1971; De Villier and Visser; 1977). The Sishen area was closer than the Matsap area to the centre of glaciation due to their carbonate content. This also implies that the centre of glaciation was localised and that the Matsap area was far from the centre of glaciation, or close to low lying reliefs.

## IV.5. Genetic models of the Kalahari Manganese Field

### IV.5.1. Introduction : the Kalahari Manganese Field

The Kalahari manganese field, situated some 60 km to the northwest of Kuruman in the Northern Cape Province in South Africa represents the world's largest manganese deposit with some 13500 Mt of Mn ore with a minimum of 20% Mn (Gutzmer and Beukes, 1996, 1997). The primary manganese ore is of sedimentary origin (Gutzmer and Beukes, 1996) and interbedded with iron-formation of the Hotazel Formation, part of the Voëlwater Subgroup top-most part of the Transvaal Supergroup which is best preserved as an erosional relict in the southernmost part of the Kalahari area. South of the Kalahari Manganese Field, the Voëlwater Subgroup consists of unmineralised chert and dolomite (Cornell and Schütte, 1995). Three manganese beds are present in the Hotazel Formation (see figure V.2.3.(1). from Tsikos and Moore, 1997). Most previous studies concentrated on the manganese ore beds and not on the associated iron-formations, but Tsikos (1994) and Tsikos and Moore (1997) present mineralogical and geochemical data on the host banded iron-formations.

According to Beukes (1983), Tsikos (1994), Tsikos and Moore (1997), the Hotazel Formation reflects evidences of cyclicity on all scales (see figure 35). The Hotazel megacycle is dominated by oxide-facies banded iron-formation at the base, then silicate facies banded iron-formation in the central portion, and carbonate-rich banded iron-formation at the top where it grades into the carbonates of the Mooidraai Formation (Tsikos and Moore, 1997). Three macro-cycles are also present, consisting of banded iron-formation-hematite lutite-Mn ore-hematite lutite-banded iron-formation (see figure 35).

### IV.5.2. Review of the genetic models for the Kalahari Manganese Field

Previous workers have proposed different genetic models for the Kalahari manganese ores. The first model is the volcanic-exhalative origin proposed by Beukes (1983), Nel et al. (1986) and Cornell and Schütte (1995). In the Cornell and Schütte model (1995), a major hydrothermal alteration in the underlying Ongeluk lava is supposed to have occurred in a submarine environment, very similar to the present day mid-ocean ridge manganese accumulation. In this model, hydrothermal circulation through the volcanics is the primary source to supply most of the chemical sediments in the Hotazel Formation, specifically the manganese and iron ores and chert (Cornell and Schütte, 1995). The most widely accepted exhalative model is the one proposed by Beukes (1983) and Nel et al. (1986) where the source for the silica and metallic ions is remote volcanogenic and/or fumarolic activity. The fractional precipitation of iron and manganese would be related to different Eh and pH conditions induced by transgression-regression cycles.

The second model, called the upwelling model (Klein and Beukes, 1989, 1993; Beukes and Klein, 1990; Schissel and Aro, 1992; Morris, 1993; Isley, 1995; Tsikos and Moore, 1997) envisages multiple incursions of $Fe^{2+}$ saturated bottom water into the oxygenated Si-saturated shelf environment where the metallic ions are oxidised and precipitated as banded iron-formations. In the case of the Hotazel Formation, $Mn^{2+}$ should have accompanied $Fe^{2+}$ ions. The figure 32 (from Schissel and Aro, 1992) shows on the Eh-pH diagram that if deep anoxic iron-silica-manganese-rich waters upwelled onto a continental shelf, iron carbonate and iron and iron silica oxides would precipitate first to form a banded iron-formation facies. Manganese carbonate and manganese oxide would eventually precipitate as the remaining solutions reached the more oxidised portion of the shelf. This model requires a stratified ocean with predominantly anoxic waters with only the upper portion freshly oxygenated by the newly evolving photosynthetic bacteria (Schissel and Aro, 1992). As pointed out by Force and Cannon (1988), both manganese and iron are strongly enriched in ocean water under anoxic and low pH conditions. This deep anoxic water saturated in metallic ions originated from a remote hydrothermal source (Klein and Beukes, 1989; Isley, 1995).

The third model is the transgression-regression model (Frakes and Bolton, 1984, 1992) is based on the mechanisms of formation of midwater oxygen-minimum zones in modern oceans and oxygen-density stratification in today's Black and Baltic Seas and their relation to manganese concentration (Roy, 1992). During a high sea-level stand, according to Roy (1992), warmer climates were implied, reducing the pole to equator thermal gradient and resulting in a diminished deep-sea circulation and a decrease in the rate of oxygen supply to the deeper ocean. Concomitantly, an increase in temperature led to decreases solubility of oxygen in sea water. The sea-level highstand resulted in a marine transgression on the cratonic shelf, overrunning areas of high biological productivity (Force and Cannon, 1988). The coincident episodes of oxygen consumption (by

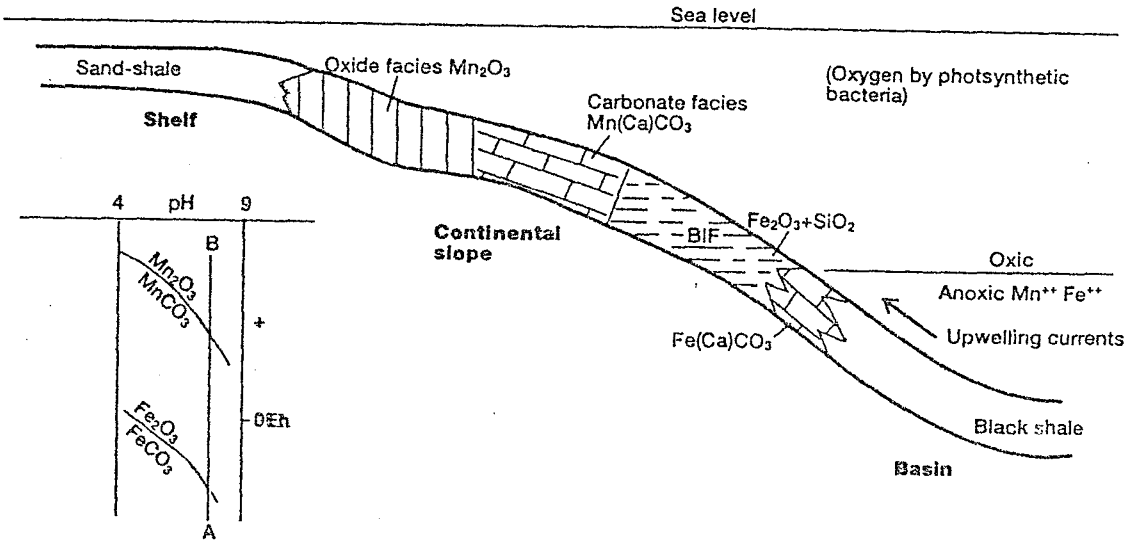


F. 32. Model for deposition of manganese and banded iron-formation from upwelling of anoxic waters (from Schissel and Aro, 1992).

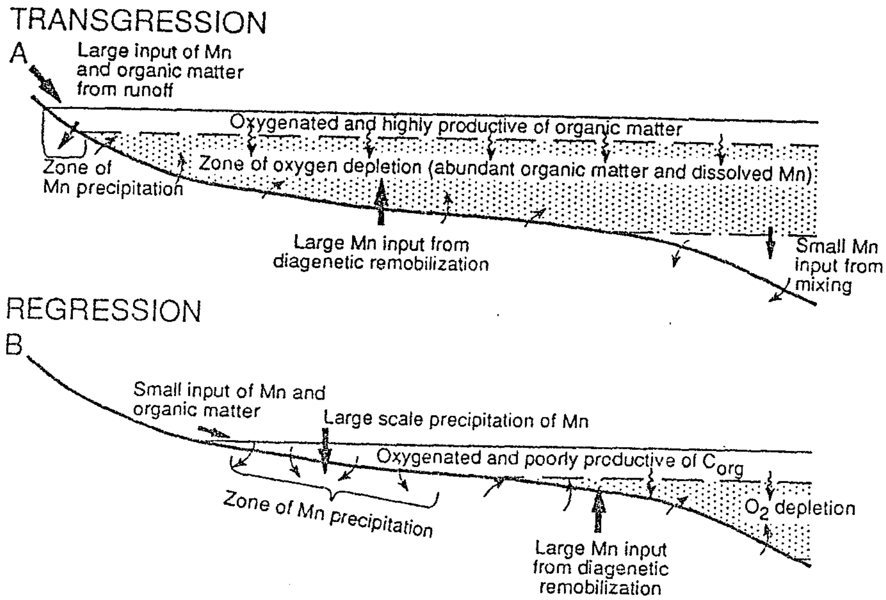


F. 33. A. Relationships at a basin margin during marine transgression, showing zone of depletion and dissolved manganese enrichment impinging on the bottom and inferred movements on Mn. B. Relationships during marine regression, showing abundant diagenetic remobilisation and precipitation of Mn in reducing and oxidising zones, respectively (from Frakes and Bolton, 1992).

degrading organic matter) and its nonrenewal led to anoxia through much of the water column with only a shallow layer oxygenated by atmospheric interaction at the surface (Roy, 1992). Inversally, a regression stage would extend the oxidised layer and allow large-scale manganese precipitation over the shelf (Frakes and Bolton, 1984, 1992). In this model, the manganese deposit occurs in coastal zones of open or intracratonic basins supplied by the weathering in the source area of rocks containing manganese at average crustal abundance.(see figure 33 from Frakes and Bolton, 1992).

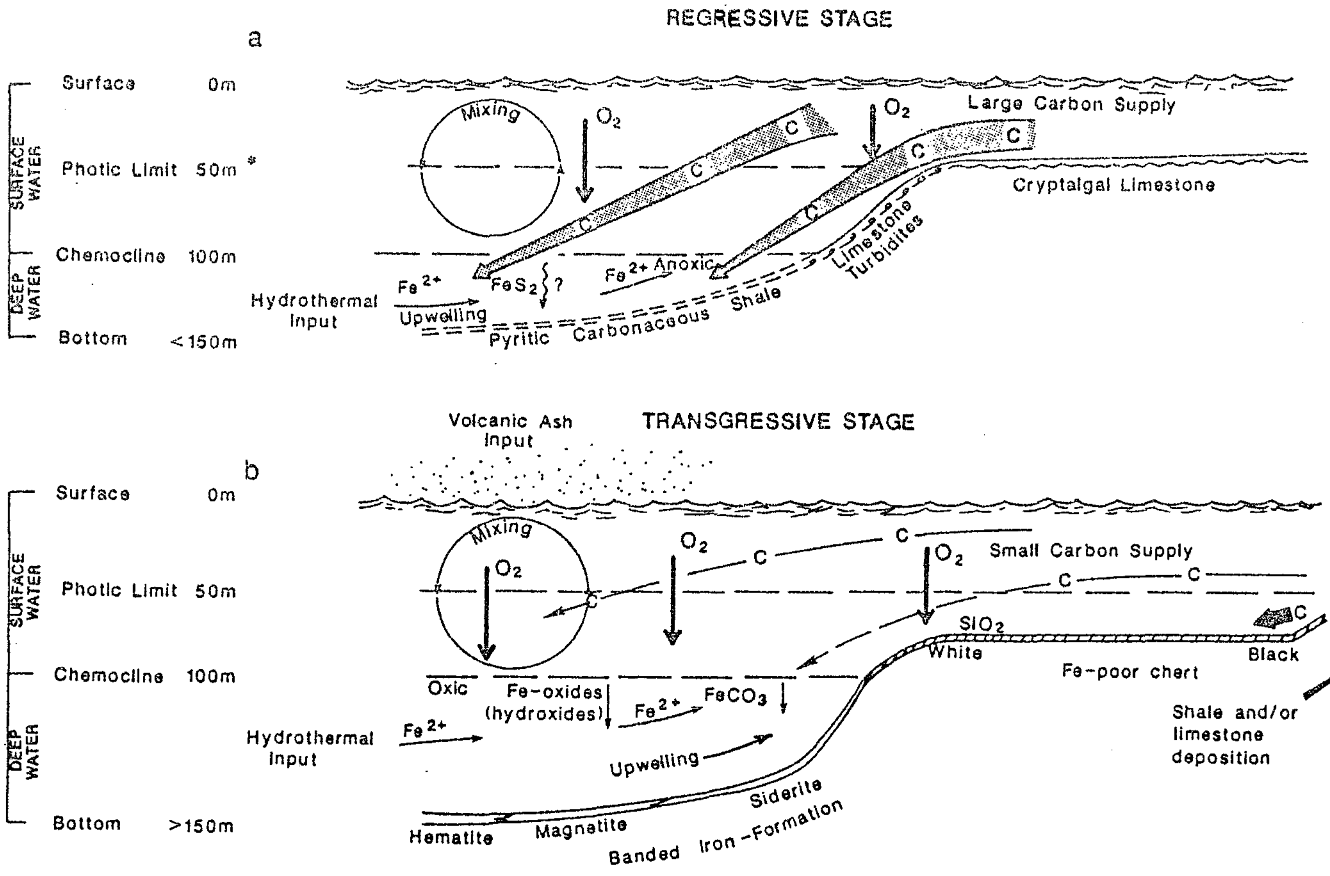


F. 34. Schematic depositional environment for iron-formation deposition and associated lithofacies in a marine system with a stratified water column in (a) a regressive stage, and (b) a transgressive stage. In (a) the photic zone reaches the floor of the deep shelf, allowing for cryptalgalaminated limestone deposition. In (b) the photic zone is considerably above the floor of the deep shelf, causing the deposition of various iron-formation facies and chert. The thick arrows labelled C (carbon) in (a) represent high carbon productivity and supply, and the narrow arrows in (b) represent much less carbon productivity and supply (from Klein and Beukes, 1989).

An alternative model is a compromise between the upwelling and the transgression-regression models (Klein and Beukes, 1989). In this model, the ocean is also stratified with deep anoxic and shallow oxygenated waters. During a regressive stage ( figure 34.(a.)), abundant supply of carbon to the zone of mixing above the chemocline occurs. Where the photic zone reaches down to the floor of the deep shelf, this is the region for precipitation of cryptalgal limestones (Klein and Beukes, 1989). In the deep-water zone, pyritic carbonaceous shales were deposited. In figure 34.(b), a transgressive stage is characterised by a small carbon supply, such that oxygen still available. Here the photic zone does not reach the bottom and input of siliclastic material is reduced. This would have resulted in oxic conditions and deposition of oxidised iron-formations.

On the other hand, when oxygen was in short supply at the water interface (chemocline), and some carbon was available, primary siderite-rich iron-formations would have precipitated (Klein and Beukes, 1989). Thus a transgressive stage (warmer climate) would have favoured the deposition of manganese oxides (Cornell and Schütte, 1995). The supply of metallic ions would have come from upwelling of saturated deep anoxic waters from remote hydrothermal input (Klein and Beukes, 1989; Isley, 1995). Upwelling-associated models require open basins and not restricted stagnant basins to allow these ocean circulations.

### IV.5.3. Discrimination between the different models

All these models tend to explain one geochemical, or sedimentological characteristic of the Hotazel Formation. For example, the Cornell and Schütte model (1995) tried just to explain the source for the manganese and iron. The other models explain the cyclic features of the Hotazel Formation by sea-level changes, but the processes of accumulation of manganese in solution, supposedly coming from a distal volcanic activity, is left aside.

The Cornell and Schütte model (1995) have been discarded by Beukes and Gutzmer (1996) and Tsikos and Moore (1997) due to obvious failures in explaining petrographic, geochemical and sedimentological features of the Hotazel Formation. According to Beukes and Gutzmer (1996), leaching of all the manganese present in the Ongeluk lava would lead to a manganese ore bed of only 1.3 metre thick at a manganese content of 31 wt%. As also pointed out by Tsikos and Moore (1997), Cornell and Schütte did not take into account the cyclic nature of the iron-formation and the manganese ore within the Hotazel Formation.

The upwelling model is challenged by Morris (1993). In this model, oxygen is limited to the superficial layer of a mainly anoxic ocean. If upwelling of deep water would occur, a counter current is the required, and this would result in the aeration of the deep waters if surface waters were significantly oxygenated, in turn preventing substantial transport of ferrous iron. But the oxygen levels present during the Early Proterozoic times were significantly low to allow very little oxygenation of the deep waters.

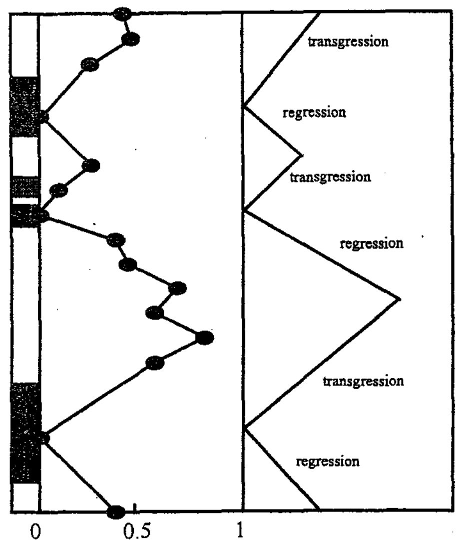


F. 35. Vertical variation in FeO/(FeO + Fe2O3) values 12 Hotazel banded iron-formation samples, and values for the three manganese beds are based on mineralogical data by Nel et al. (1986) (from Tsikos and Moore, 1997).

Transgression-regression (Frakes and Bolton, 1984, 1992) cycles can be seen in the cyclic nature of the Hotazel Formation (Tsikos and Moore, 1997). The vertical variation in $Fe^{2+}$ ($Fe^{2+}$ + $Fe^{3+}$) seen in figure V.2.3.(1) (from Tsikos and Moore, 1997) provides significant cyclic fluctuations in $Fe^{2+}$/ ($Fe^{2+}$ + $Fe^{3+}$) of the Hotazel iron-formations indicating relatively rapid changes in the paleoenvironment of deposition that essentially support a transgression-regression model, but where the cyclic deposition of the manganese beds are due to chemical sedimentation (Tsikos and Moore, 1997) rather than sea-level fluctuations in relation to submarine volcanism (Beukes, 1983).

As observed by Tsikos and Moore (1997, 1998), the Transvaal Supergroup displays a symmetry in the Northern Cape consisting of basal and uppermost platform carbonate associated with banded iron-formations and central diamictite and lava (see figure 36; from Tsikos and Moore, 1998). The time span for the deposition of the all sequence in the Northern Cape basin was approximately 100 My (see chapter IV.1) without any major unconformity at the base of the Makganyene Formation. This implies that the cyclicity of the Transvaal Supergroup represents episodic fluctuations in the paleodepositional environments and paleoclimatic conditions recorded continuously in the stratigraphy. The absence of significant time gap during the sedimentation of the Transvaal Supergroup coupled by its cyclicity represents regional paleoclimatic variations. In this regard, the Kalahari Manganese Field would be in direct relation with the glacigenic rocks of the Makganyene Formation. It is important to consider similar associations of glacigenic rocks-Fe-Mn deposits which occurred in the Neoproterozoic in different part of the world.

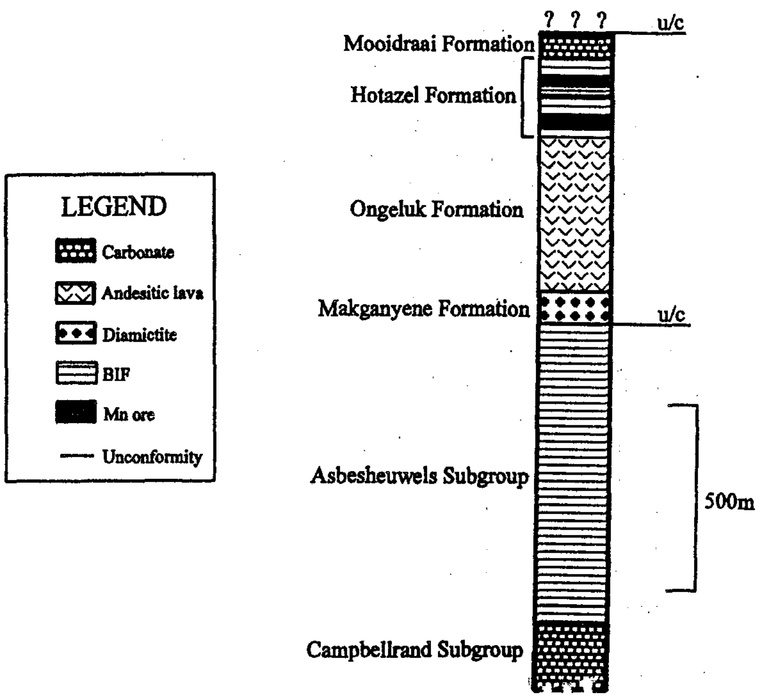


F. 36. Cyclic nature of the Transvaal Supergroup in the Northern Cape (after Tsikos and Moore, 1998).

The occurrence of manganese associated with banded iron-formations and glacial deposits occurs in several parts of the world, including Canada, Southern Africa, and Brazil (Bühn et al., 1992;Urban et al., 1992; Klein and Beukes, 1993) and in actual post-glacial sediments in the Gulf of Bothnia (Ingrid and Pontér, 1986). The glacial event recorded in the Rapitan Formation in Canada is responsible for the build up of Fe and Mn in the ocean (Klein and Beukes, 1993). They relate the occurrence of iron-formations with glacial events (see figure29, after Klein and Beukes, 1992, 1993; Williams 1993). But their glacial event is related to the snowball Earth (Kirschvink, 1992) where surface waters are frozen. No oxygen would be available to the anoxic deep-water of a stagnant ice-capped ocean, and build up of metallic ions such as $Mn^{2+}$ and $Fe^{2+}$ would develop. When transgression occurs, deglaciation immediately follows, re-establishing ocean circulation, mixing of surface and deep-waters, and selective precipitation of Fe and Mn takes place.

Actual similar processes occur ; distinct stratification of iron and manganese is observed in recent postglacial sediments. The stratification of the oxidised sediment layers appears to be predominantly the result of a solution-precipitation mechanism. Fe and Mn-oxyhydroxides tend to be solubilised under reducing conditions, thus creating concentration gradient observed in the pore waters to migrate upwards and precipitates as oxyhydroxides along favourable horizons (Ingrid and Pontér, 1986). A strong redox gradient develops, and as Fe precipitates at lower redox values than Mn together with a slower oxidation kinetics for Mn, the Fe-rich layers always occur below the Mn-rich horizons. Changes in pH are not of a major significance, whereas the redox gradient is of major significance and governs the composition of the oxidised zone in the sediments from the Gulf of Bothnia (Ingrid and Pontér, 1986). But the source of manganese in that case is continental, supplied by rivers.

The presence of manganese in the Northern Cape was described by Thatcher et al. (1993) in the Rooinekke Formation of the Koegas Subgroup where highly manganiferous iron-formations occur. Manganese precipitation stopped certainly due to changes both in physical and chemical conditions of the environment. Glacial influence was responsible for global ocean circulations. In glaciated areas, cold oxygenated surface-water downwelled into anoxic deep-water. The oxygen made available to the deep anoxic water was quickly used by oxidation processes (organic matter, oxidation of primary magnetite to hematite) so that the deep ocean stayed anoxic. In the case of the

Makganyene Formation, at least in the study area, wet-based tidewater glacier sediments were observed. Subglacial streams were important making the water turbid, inhibiting chemical precipitation and allowing the build up of metallic ions. Ice-cap development was certainly localised in restricted basins, such as the Kalahari Manganese Field Basin situated at about 200 km north from the study area. Each transgression (inter-glacial stage) is accompanied by precipitation of iron-formations in clear water conditions. $Mn^{2+}$ did not precipitate yet because of its absence in the iron-formations of the Makganyene Formation and so was left in solution. This is due to selective precipitation processes between $Mn^{2+}$ and $Fe^{2+}$: manganese needs a higher Eh than iron to precipitate. A post-glacial transgression allowed the deposition of the iron-formations of the Hotazel Formation. Manganese ore formed during regressions in restricted basins on submarine topographic highs where Eh conditions allowed manganese precipitation (Tsikos, personal communication) by upwelling of deep waters, supplying high nutrient levels in the continental shelf waters (Jacobs, 1989). The Makganyene ice-age was responsible for the build up over a significant time period of massive amount of manganese present in the ore of the Kalahari Manganese Field.

## IV.6. Further studies

This preliminary study of the Makganyene diamictite was restricted to the Rooinekke area for the field work, and Sishen and Matsap area for selected geochemical analyses, sedimentological, stratigraphical and facies studies; and clearly demonstrate the lack of stratigraphic constraints on successions and correlations between the different basins of the Transvaal Supergroup. The generally accepted unconformity at the base of the Makganyene Formation was described in the field as a rather gradational contact with interbedded iron-formations and diamictites. New stratigraphic correlations across the Transvaal Supergroup were drawn between the Griqualand West and Transvaal basins. The Pretoria Group does not have any lateral equivalent in the Northern Cape basin, and the position of the Postmasburg Group would be in the karstic unconformity overlying the Penge Iron-Formation in the Transvaal Basin. This would lead to a post-glacial position for the Hotazel Formation, host of the Kalahari Manganese Field.

Therefore the potential effects of the Makganyene Formation on the genesis of the Kalahari Manganese Field would have been the buildup of the concentration of Mn (and iron) in solution in restricted basins and precipitation during warmer periods.

To gain a better understanding of the effects of a glacial event on the metallogenesis of manganese ore, further studies on a more regional scale should be undertaken. New problems have been revealed and now requires a research project on the Makganyene Formation, with the following aims:

1) to establish a proper stratigraphic succession with possible lateral equivalents within the Griqualand West Basin (relation between the Koegas and Griquatown iron formations are not clear) by assessing the associations of the Makganyene Diamictite with the banded iron-formation above and beneath the main thrust fault and to assess the conformity or not of the Makganyene Formation throughout the Northern Cape.

2) sedimentological, petrological, geochemical attributes of the diamictite should be assessed on a regional scale to establish the variation in source composition with a view to establishing the paleodepositional setting pre-dating the manganese accumulation of the Kalahari field.

3) systematic petrography, sedimentology and geochemistry studies of the associated iron-formations should be undertaken to compare the depletion of certain elements in comparison with the Hotazel Formation and determine the chemical depositional environment.

4) available data (seismic profiles, bore-hole data) should be used to produce a 3D model of the shape of the western edge of the Kaapvaal Craton to locate the position of the restricted anoxic basins where Mn and Fe were concentrated, such as the Kalahari Mn field. This model will then be used to establish the depositional model of the Postmasburg Group, and for exploration purposes by determining where Mn could have accumulated.

## IV.7. Summary and conclusion

This thesis was supposed to answer certain questions : what is the stratigraphic position of the Makganyene Formation and its relationships with the under/overlying formations. The next question was to assess the geochemical signature of the diamictite to interpret the chemical index of alteration (CIA) and assess the source for provenance studies, and to compare the banded iron-formations interbedded with the other banded iron-formations from the Transvaal Supergroup. The last question was to propose a depositional model for the Makganyene Formation with emphasis on the genetic model for the Kalahari Manganese Field.

The study of the Makganyene Formation is important because of its central position within the Transvaal Supergroup in the Northern Cape. The observation and description of the basal contact was made and field evidence shows that the Makganyene Formation is broadly conformable and interbedded with the underlying formations. This contact was generally believed to be an unconformity. Only early workers such as Nel (1929) mentioned the conformability of this formation. It must be emphasised that these early workers spent most of their time in the field, and their descriptions of outcrops are very accurate, that even non-geologists could identify any formation. It was first De Villier who (1967) gave a wrong interpretation of the stratigraphy. The main thrust fault running north-south from Sishen iron ore mine to Rooinekke area was mapped as an unconformity, placing the Gamagara Formation as part of the Transvaal Supergroup, even though the former is younger than the latter. It was twenty years later that Beukes and Smit (1987) re-established the correct succession and the Gamagara Formation is not part of the Transvaal Supergroup anymore.

The significance of the conformability of the Makganyene Formation is very important. It means that the Transvaal Supergroup is conformable throughout the Griqualand West Basin, and therefore no significant time gap was present, but rather continuous sedimentation occurred in this basin 2.4 Ga ago. The Transvaal Supergroup is also present in the Transvaal Basin, and is generally correlated to the Transvaal Supergroup in the Northern Cape. After doing a literature review of the different possible correlations between the two basins, using field evidence that the Makganyene Formation is conformable, certain problems arose :

* the ages given by radiochronology on different formations from the Northern Cape give a deposition

time span of 600 Ma. This is supposed to be continuous due to the conformability of the Makganyene Formation, but this period of sedimentation required 600 Ma of tectonic stability in the Early Proterozoic, a period when the cratons were greatly mobile.

* the correlations between the different formations of the Postmasburg Group (Northern Cape) and Pretoria Group (Transvaal Basin) are mainly based on similarities in age and composition of the Ongeluk and Hekpoort lavas. Their similar age is around 2.2 Ga (Cheney, 1996; Walvaren et al., 1990), but the Voëlwater Subgroup yield ages of around 2.4 (Romer and Bau, ). The last age of 2.4 Ga places the Ongeluk lava at least 200 Ma younger. Therefore correlations between Ongeluk and Hekpoort lavas are not possible.

* an unconformity is present at the base of the Pretoria Group in the Transvaal Basin, estimated to be 150 Ma due to karstic weathering (radiometric ages, Eriksson et al., 1993). On the other side, the Makganyene Formation is conformable. The major unconformity at the base of the Pretoria Group cannot be the correlative of the conformable contact situated at the base of the Postmasburg Group.

* only four formations are present in the Postmasburg Group in the Griqualand West Basin. The sediments above the Ongeluk lava are typically chemical with manganese ore intimately interbedded with banded iron-formations and with carbonates. On the other hand, thirteen formations from the Pretoria Group are present in the Transvaal Basin with several disconformities/unconformities.

This leads to proposals for new correlations between the two basins. The Postmasburg Group is not correlable at all with the Pretoria Group. The Pretoria Group, younger than the Postmasburg Group of 200 Ma, and having at least one major unconformity at its base, should not be part of the Transvaal Supergroup. Implications for these new correlations can be far more important than thought, not just touching the field of stratigraphy, but also manganese metallogenesis.

Correlation with other continents is possible, but is still highly speculative. Early Proterozoic glacigenic rocks of certain glacial origin (see figure 1, after Hambrey and Harland, 1981; Marko and Ojokangas, 1984; Strand and Laajoki, 1993) are present in few parts of the world : in North America, Australia, and here in South Africa. These deposits are situated on cratons which might have formed the Vaalbara supercontinent (Cheney, 1996).

Stable isotopes studies (C and O) were undertaken from the Makganyene Formation and the results were plotted in a curve with other values from the Transvaal Supergroup in the Griqualand West Basin. This curve displays a progressive relative depletion in isotope compositions with the values being most depleted for the Makganyene Formation, placing these glacigenic rocks in the centre of a gradual evolutionary trend.

Bulk rock analyses were also made of selected samples of diamictite. These rocks are supposed to be of glacial origin, thus by using the chemical index of alteration (CIA), one is able to tell the dominant weathering process : mechanical or chemical. Low values are for mechanical weathering (between 50-70%), and values close to 100% are for highly leached sediments. The values for the Makganyene Formation are very high, implying that it did not have mechanical weathering as a dominant process, but rather humid and heavily leached conditions. The presence of dropstones in banded iron-formations within the Makganyene Formation and presence of faceted striated pebbles are for a glacial origin. But the bulk composition of the diamictite of the diamictite is that of an iron-formation. The CIA is made to calculate the efficiency of the leaching of soluble elements (Al, Ca, K, Na) assuming the source rock to be of an igneous origin. So the CIA was not a good indicator for the weathering processes because the source rocks for the Makganyene Formation were mainly iron-formations.

A source rock diagram was constructed to estimate the potential role played by different rock types as source rocks. This ternary diagram, having poles for iron-formations, carbonate, and granite, shows clearly the dominance of iron-formations as a source. The amount of carbonate influence increased towards the north at Sishen, and the granitic influence is always minimised and only accounts for the presence of aluminium and potassium.

Other ternary diagrams (A-F-K; A-CN-K; A-FM-CNK) were also constructed and these discriminate between fine-grained diamictite (more Al-rich) coarse-grained diamictite (more Fe-rich).These three ternary diagrams emphasise the sorting processes which induced differences in bulk composition.

For the interbedded banded iron-formations in the Makganyene Formation, they are very similar in major element composition to all the Transvaal Supergroup banded iron-formations.

An important problem is that these glacial clastic sediments from the Precambrian, as a rule, were apparently deposited at sea level a few degrees from the equator. This is the Precambrian climatic paradox. The fact that an ice sheet formed at sea level in the vicinity of the equator is difficult to explain. Computer modelling by Crowley and Baum (1993) indicated that the configuration of the continents plays a major role, and a supercontinent is preferable for the onset of a global glaciation. In their model, they produced ice sheets at sea level, but they used very low $CO_2$ values (120ppm) and a solar luminosity 22% lower than today. There are currently four models which try to explain this unusual feature of Precambrian glaciations :

* the "snowball Earth", proposed by Kirschvink (1992);
* equatorial ice-ring system that shielded low-latitudes from solar radiation and induced low-latitude glaciations;
* a non-axial geomagnetic field invalidating all previous paleomagnetic studies;
* a large obliquity of the Earth : $\epsilon > 54°$.

The snowball Earth, or pole-to-pole glaciation, is proposed to explain low-latitude glaciations in the Precambrian. In this model, escape from this ice house would presumably be through the gradual build up of the greenhouse gases such as $CO_2$, contributed to the air by volcanic emissions. But numerous observations discredit this theory. The first is that the low temperatures would inhibit precipitations and sublimations. The second is that this snowball Earth would have implied a major regression which have not been observed during the Neoproterozoic (Williams, 1998). The third is that a frozen Earth would not be able to sustain the snowfall rates needed for further advance of snow cover over land. The last is that some deposits situated in paleo-high-latitudes did not experience glaciation. Furthermore this model implies a rapid freezing of the oceans, which contradicts the gradual curve of the isotope values from the Transvaal Supergroup that suggest that this event was gradational (shown as well by the symmetry in the Transvaal Supergroup in Northern Cape).

The ice-ring system does not need to be discussed because an ice-ring could not exist so close from the Sun. The non-dipolarity of the geomagnetic field can also be discarded. This is due to comparisons with the other planets of the Solar System that indicate that non-axial dipole-quadrupole planetary magnetic fields are impossible (Williams, 1998).

The last theory is Williams theory (1975, 1993, 1998) which argues that the obliquity of the Earth varied from the Precambrian to the present values, starting at 4.5 Ga ago with possibility of 70°

and that these values decreased with time to the present value. This variation in obliquity was caused by the impact of a meteorite with the Earth which caused the formation of the Moon 4.4 Ga ago. The Earth was then tilted to around 70°. When the obliquity of the earth is above the critical value of 54°, glaciations preferentially take place at low-latitudes, and below this value the present climatic zonation is observed. The postulated flip-over of the climatic zonations induced by this high obliquity is supposed to have just at the end of the Precambrian, 610 Ma ago. This change in obliquity value is postulated to come from in increase in dissipative core-mantle torques, and established the present climatic zonations. The stratigraphic succession of the Transvaal Supergroup in the Northern Cape shows gradual climatic variations which support the model of the large obliquity of the Earth. The clastic sediments of the Makganyene Formation are typical of a wet-based glacier. Subglacial water was present and discharged large volumes of sediments into the basin, following similar to that of present day glaciations. The observations made during this study support the large obliquity theory and totally reject the snowball Earth theory.

To provide a depositional model for the Makganyene Formation, a review of actual glacial processes was made. These glacial environments are intensely studied nowadays to understand older glacigenic deposits in view of their significance in petroleum exploration. Due to the inhospitable environment, certain models are available, but still only as initial working hypotheses. Sea-level changes induced by glaciation are important, due to ice-loading, isostatic readjustments, regression due to mobilisation of water into ice. In general, these sea-level changes can be very local, and in some places where regression occurs, some other undergo relative transgression due to these crustal adjustments. A glacio-eustatic sea-level drop is estimated to be 150 metres, but deepening from crustal warping could be up to 600 metres.

The Makganyene Formation has a glacigenic origin, possibly deposited under an ice sheet. But the ice sheet formation requires specific favourable conditions : embayments protecting the ice growth from destructive waves and tides, and therefore tide-water glaciers are more likely to form. Many processes are involved in glacial sedimentation regimes, from transport of the sediments by ice and streams, or by remobilisation (currents, slumping, debris flows). These processes are interacting with each other, making the glacial environment one of the most difficult to study. And when these models are available, they are still very simplistic and reflect just part of reality.

The Makganyene Formation depositional model is also presented in this study, in relation with the Transvaal Supergroup in the Griqualand West Basin. Due to the scarcity of clastic deposits in the Transvaal Sea, an epicontinental sea covering land-masses is envisaged in this particular model. Sea-level changes allowed deposition of carbonate (low sea-level) or banded iron-formations (higher sea-level). The model presented starts with the deposition of the Campbellrand dolomites, which were deposited in a shallow epicontinental sea. After this event, the Asbesheuwels and Koegas Subgroup were accumulated because of a relative transgression. Glacial eustatic sea-level drop caused the onset of the Makganyene glaciation by emersion of the continental-masses allowing ice growth. Interbedding of iron-formations and clastic glacial sediments was caused by slumping of the clastic sediments to a distal part in the basin.

The development of large land continental ice sheets on the Vryburg rise produced a global drop in sea level (glacio-eustatic) because large volumes of water were locked up as ice. A wide variety of clastic glacial sediments are interbedded with iron-formations at the base of the Makganyene Formation and could represent a distal expression the subglacial zone of deposition, i.e. in ice-proximal zone. This interbedding was certainly enhanced by glacial advance and retreat, resulting in important isostatic readjustments. In one location (Paauvlei 190), no interbedding is present, but instead a two metre thick clastic sandstone layer might represent the first distal clastic input into the basin at the snout of a submarine canyon. The most common type of glacier was a wet-based tide-water glacier similar to most of the present day mid-latitudes glaciers where the influence of water by subglacial stream discharges is important and causes turbid water conditions. In these conditions, ice shelves could have developed, but in small sheltered bays/basins.

Over-deepening of the basin during transgression was also responsible for black shale accumulation; strong evidence for anoxic deep-waters penetrating the continental shelf zone. Each transgression was responsible for a glacial retreat due to shift landward of the grounding-line causing important calving. Clear water conditions were established allowing chemical precipitation (banded iron-formations) during these interglacial stages. Cycles of glacial advance and retreat occurred several times during the deposition of the Makganyene Formation.

Towards the end of the glacial period, volcanism started and lava overrode the continental shelf, as well as significant thawing of the remnant ice. All the debris was finally released into the basin, and numerous small scale slumping took place. These slumps which include graded cycles are interbedded with lava. Instability of the continental shelf caused the slumping. The end of the Makganyene times is characterised by a transgression, re-establishing clear water conditions allowing deposition of banded iron-formations as well as manganese. The top of the Transvaal Supergroup in the Northern Cape is characterised by a regression and carbonate deposition took place.

Highly manganiferous iron-formations from the Rooinekke Formation were precipitated just before the Makganyene Formation, showing clearly that manganese already was present in the ocean in large quantities to precipitate when conditions were favourable. Glacial influence stopped the precipitation of manganese. In glaciated areas, cold oxygenated surface-water downwelled into anoxic deep-water. In the case of the Makganyene Formation, at least in the study area, wet-based tidewater glacier sediments were observed. Subglacial streams were important making the water turbid, inhibiting chemical precipitation allowing the build up of metallic ions. Ice-cap development was certainly localised in restricted basins, such as the Kalahari Manganese Field Basin situated at about 200 km north from the study area. Each transgression (inter-glacial stage) is accompanied by precipitation of iron-formations in clear water conditions. $Mn^{2+}$ did not precipitate yet because of its absence in the iron-formations of the Makganyene Formation and was left in solution. This is due to selective precipitation processes between $Mn^{2+}$ and $Fe^{2+}$: manganese needs a higher Eh than iron to precipitate. A post-glacial transgression allowed the deposition of the iron-formations of the Hotazel Formation. Manganese ore deposition took place during regressions in restricted basins on submarine topographic highs where Eh conditions allowed precipitation of manganese (Tsikos, personal communication) by upwelling of deep waters, supplying high nutrient levels in the continental shelf waters (Jacobs, 1989). The Makganyene ice period was responsible for the build up over a significant time period of massive amount of manganese present in the ore of the Kalahari Manganese Field.

For this theory to be verified, further studies are necessary. The definition of the morphology of the western margin of the Kaapvaal Craton is vital in understanding the ice-growth and possible areas of manganese precipitation which would accumulate in restricted basins. Also the stratigraphic succession of the Transvaal Supergroup in the Northern Cape should be re-assessed to provide inter-relations between formations, facies variations, possibly from chemical to clastic. Regional sedimentological, petrological, and geochemical studies of the Makganyene Formation should be undertaken to assess the variation in composition of the source. Geochemical, petrological and sedimentological studies of the associated banded iron-formations underneath the Kalahari Manganese Field should also be undertaken to assess the chemical conditions in the restricted basins.

To finally conclude, this thesis was a preliminary study of the Makganyene Formation, and provided valuable insights on the stratigraphy of the Transvaal Supergroup and metallogenesis of the Kalahari Manganese Field.

V. References

Alley R.B., Blankenship D.D., Rooney S.T. and Bentley C.R. (1989) -Sedimentation Beneath Ice Shelves - The View from Ice Stream B- Marine Geology (85), 101-120.

Altermann W. and Hälbich I.W. (1990) -Thrusting, Folding and Stratigraphy of the Ghaap Group Along the Southwestern Margin of the Kaapvaal Craton- S.Afr.J.Geol. (93), 553-566.

Altermann W. and Hälbich I.W. (1991) -Structural History of the Southwestern Corner of the Kaapvaal Craton and the Adjacent Namaqua Real : New Observations and a Reappraisal- Precambrian Research (52), 133-166.

Anderson J.B., Brake C.F. and Myers N.C. (1984) -Sedimentation on the Ross Sea Continental Shelf, Antarctica- Marine Geology (57), 295-333.

Andrews J.E., Brimblecombe P., Jickells T.D. and Liss P.S. (1996) -An Introduction to Environmental Chemistry- Blackwell Science, 209pp.

Aspler L.B. and Chiarenzelly J.R. (1997) -Initiation of ~ 2.45-2.1 Ga Intravratonic Basin Sedimentation of the Hurwitz Group, Keewatin Hinterlan, Northwest Territories, Canada- Precambrian Research (81), 265-297.

Barbola J.M., Raynaud D., Korotkevich Y.C. and Lorius C. (1987) -Vostok Ice Core Provides 160,000-Year of Atmospheric $CO_2$- Nature (329), 408-414.

Beukes N.J. (1980) -Lithofacies and Stratigraphy of Kuruman and Griquatown Iron-Formations- Trans. Geol. S. Afr (83), 69-86.

Bathia M.R. and Crook K.A.W (1986) -Trace Element Characteristics of Graywackes and Tectonic Setting Discrimination of Sedimentary Basins- Contribution Mineralogy Petrology (92), 181-193.

Baur M.E., Hayes J.M., Studley S.A., Walter M.R. (1985) -Millimeter-Scale Variations of Stable Isotope Abundances in the Hamersley Basin of Western Australia- Economic Geology (80), 270-282.

Beukes N.J. (1983) -Paleoenvironmental Settings of Iron-Formations in the Depositional Basin of the Transvaal Supergroup- 131-209, In : Trendall A.F. and Morris S.C., Eds, Iron-formations, Facts and Problems, Elsevier, Amsterdam, 558pp.

Beukes N.J. (1984) -Sedimentology of the Kuruman and Griquatown Iron Formations, Transvaal Supergroup, Griqualand West, South Africa - Precambrian Research (24), 47-84.

Beukes N.J. and Smit C.A. (1987) -New Evidence for Thrust Faulting in Griqualand West, South Africa : Implications for Stratigraphy and the Age of Red Beds- Trans. Geol. S. Afr. (90), 378-394.

Beukes N.J. and Klein C. (1990) -Geochemistry and Sedimentology of a Facies Transition -from Microbanded to Granular Iron-Formation- in The Early Proterozoic Transvaal Supergroup, South Africa- Precambrian research (47), 99-139.

Beukes N.J., Klein C., Kaufman A.J., Hayes J.M. (1990) -Carbonate Petrography, Kerogen Distribution, and Carbon and Oxygen Isotope Variations in an Early Proterozoic Transition from Limestone to Iron-Formation Deposition, Transvaal Supergroup, South Africa- Economic Geology (85), 663-690.

Beukes N.J., Burger A.M. and Gutzmer J. (1995) - Fault-Controlled Hydrothermal Alteration of the Paleoproterozoic Manganese Ore in Wessels Mine, Kalahari Manganese Field - S. Afr. J. Geol (4), 430-451.

Beukes N.J. and Gutzmer J. (1996) -A Volcanic-Exhalative Origin for the World's Largest (Kalahari) Manganese Field, a Discussion of the Paper by D.H. Cornell and S.S. Schütte- Mineral Deposita (31), 242-245.

Bolton B. And Frakes L. (1985) -Geology and Genesis of Manganese Oolite, Chiatura, Geogia, U.S.S.R.- Geological Society of America Bulletin (96), 1398-1406.

Bühn B., Stanistreet I.G. and Okrush M. (1992) -Late Proterozoic Outer Shelf Manganese and Iron Deposits at Otjosondu (Namibia) Related to the Damaran Oceanic Opening- Economic Geology (87), 1393-1411.

Burdett J.W., Grotzinger J.P., Arthur M.A. (1990) -Did Major Changes in Stable-Isotope Composition of Proterozoic Seawater Occur?- Geology (18), 227-230.

Cameron E.M. (1982) -Sulphate and Sulphate Reduction in Early Precambrian Oceans- Nature (296), 145-148.

Cheney E.S. and Winter H. De la R. (1995) -The Late Archaean to Mesoproterozoic Major Unconformity-Bounded Units of the Kaapvaal Province of Southern Africa- Precambrian Research (74), 203-223.

Cheney E.S. (1996) -Sequence Stratigraphy and Plate Tectonic Significance of the Transvaal Succession of Southern Africa and its Equivalent in Western Australia- Precamvrian Research, (79), 3-24.

Clendenin W. (1989) -Tectonic Influence on the Evolution of the Early Proterozoic Transvaal Sea, Southern Africa- PhD thesis, University of the Witwatersrand, Johannesburg.

Clemmey H. and Badham N. (1982) -Oxygen in the Precambrian Atmosphere : an Evaluation of the Geological Evidence- Geology (10), 141-146.

Condie K.C. (1986) -Geochemistry and Tectonic Setting of Early Proterozoic Supracrustal Rocks in the Southwestern United States- Journal of Geology (94), 845-864.

Condie K.C. and Wronkiewicz D.J. (1990) -The Cr/Th Ratio in Precambrian Pelites From the Kaapvaal Craton as an Index of Craton Evolution- Earth and Planetary Science Letters (97), 256-267.

Cornell D.H. and Schütte S.S. (1995) -A Volcanic-Exhalative Origin for the World's Largest (Kalahari) Manganese Field- Mineral Deposita (30), 146-151.

Crowley T.J and Baum S.K. (1993) -Effect of Decreased Solar Luminosity on Late Precambrian Ice Extent- Journal of Physical Research (98), 16723-16732.

De Villiers J.E. (1983) - The Manganese Deposits of Griqualand West, South Africa : Some Mineralogic Aspects - Economic Geology (78), 1108-1118.

De Villier P.R. (1967) -New Stratigraphic Correlation and Interpretation of the Geological Structure of the Postmasburg-Sishen Area- Ann. Geol Surv. S. Afr. (6), 39-42.

De Villier P.R. and Visser J.N.J (1977) -The Glacial Beds of the Griqualand West Supergroup as Revealed by Four Deep Boreholes Between Postmasburg and Sishen- Trans. Geol. S. Afr. (80), 1-8.

Dixon R.D. (1985) - Sigilite and Associated Minerals from Wessels Mine, Kalahari Manganese Field - Trans. Geol. Soc. S. Afr. (88), 11-17.

Dunn P.J., Brummer J.J. and Belsky H. (1980) - Sigilite, a Second Occurrence : Wessels Mine, Kalahari Manganese Field, Republic of South Africa - Canadian Mineralogist (18), 37-39.

Dymek R.F. and Klein C. (1988) -Chemistry, Petrology and Origin of Banded Iron-Formation Lithologies from the 3800 Ma Isua Supracrustal Belt, West Greenland- Precambrian Research (39), 247-302.

Edwards M. (1986) -Glacial Environments- *In* Sedimentary Environments and Facies, Reading H.G. editor, Blackwell Scientific Publications, 445-470.

Embleton J.J. and Williams G.E. (1986) -Low Paleolatitude of Deposition for the Late Precambrian Varvites in South Australia : Implications for Paleoclimatology- Earth and Planetary Science Letters (79), 419-430.

Eriksson P.G. and Cheney E.S (1992) -Evidence for the Transition to an Oxigen-Rich Atmosphere During the Evolution of Red Beds in the Lower Proterozoic Sequences of Southern Africa- Precambrian Research (54), 257-269.

Eriksson P.G., Schweitzer J.K., Bosch P.J.A., Schereiber U.M., Van Deventer J.L. and Hatton C.J. (1993) -The Transvaal Sequence : an Overview- Journal of African Earth Sciences (16), 25-51.

Eriksson P.G. and Reczko B.F.F. (1995) -The Sedimentary and Tectonic Setting of the Transvaal Supergroup Floor Rocks to the Bushveld Complex- Journal of African Earth Sciences (21), 487-504.

Eriksson P.G., Hattingh P.J. and Altermann W. (1995) -An Overview of the Geology of the Transvaal Sequence and Bushveld Complex, South Africa- Mineralium Deposita (30), 98-111.

Eriksson P.G., Condie K.C., Tirsgaard H., Mueller W.U., Altermann W., Miall A.D., Aspler L.B., Catuneanu O., Chiarenzelli J.R. (1998) -Precambriam Clastic Sedimentation Systems- Sedimentary Geology (120), 5-53.

Evans D.A., Beukes N.J., Kischink J.J. (1997) -Low-Latitude Glaciation in the Paleoproterozoic Era- Nature (386), 262-266.

Eyles N. and Eyles C.H. (1992) -Glacial Depositional Systems- *In* Facies Models Response to Sea Level Change, Walker R.G. and James N.P editors, Geological Association of Canada, 73-100.

Fairchild I.J. and Hambrey M.J. (1984) -The Vendian Succession on Northestern Spitsbergen : Petrogenesis of a Dolomite-Tillite Association- Precambrian Research (26), 111,167.

Fairchild I.J., Hambrey M.J., Spiro B. and Jefferson T.H. (1989) -Late Proterozoic Glacial Carbonates in Northeast Spitsbergen : New Insights Into the Carbonate-Tillite Association- Geological Magazine (126), 469-490.

Faure G. (1986) -Principles of Isotope Geology- John Wiley & Sons Editors, 589pp.

Fedo C.M., Eriksson K.A., and Krogstad E.J. (1996) -Geochemistry of the Shales From the Archean (~3.0 Ga) Buhwa Greenstone Belt, Zimbabwe : Implications for Provenance and Source-Area Weathering- Geochimica et Cosmochimica Acta (60), 1751-1763.

Fedo C.M, Young G.M. and Nesbitt H.W (1997) -Paleoclimatic Control on the Composition of the Paleoproterozoic Serpent Formation, Huronian Supergroup, Canada : a Greenhouse to Icehouse Transition- Precambrian Research (86), 201-223.

Feng R. And Kerrich R. (1990) -Geochemistry of Fine-Grained Clastic Sediments in the Archean Abitibi Greenstone Belt, Canada : Implications for Provenance and Tectonic Setting- Geochimica et Cosmochimica Acta (54), 1061-1081.

Force E.R. and Cannon W.F. (1988) -Depositional Model for Shallow-Marine Manganese Deposits Around Black Shale Basins- Economic Geology (83), 93-117.

Frakes L. And Bolton B. (1984) -Origin of Manganese Giants : Sea-Level Change and Anoxic-Oxic History- Geology (12), 83-86.

Frakes L. And Bolton B. (1992) -Effects of Ocean Chemistry, Sea Level, and Climate on the Formation of Primary Sedimentary Manganese Ore Deposits- Economic Geology (87), 1207-1217.

Gair J.E. (1981) -Lower Proterozoic Glacial Deposit of Northern Michigan, U.S.A.- in Hambrey and Harland ediors, *Earth's Pre-Pleistocene Glacial Record :* Cambridge, England, Cambridge University Press, 803-806.

Genthon C., Barnola J.M., Raynaud D., Lorius C., Jouzel J., Barkov N.I., Korotkevich Y.S. and Kotlyakov V.M. (1987) -Vostok Ice Core : Climatic Response to $CO_2$ and Orbital Forcing Changes Over the Last Climatic Cycle- Nature (329), 414-418.

Griffith T.W. and Anderson J.B. (1989) -Climatic Control of Sedimentation in Bays and Fjords of the Northern Antarctic Peninsula- Marine Geology (85), 181-204.

Grobbelaar W.S., Burger M.A., Pretorius A.I., Marais W., Van Nierkerk I.J.M. (1995) -Stratigraphy and Structural Setting of the Griqualand West and the Olifantshoek Sequences at Black Rock, Beeshoek and Rooinekke Mines, Griqualand West, South Africa- Mineralum Deposita, (30), 152-161.

Grobler N.J. and Botha B.J.V. (1976) -Pillow-Lavas and Hyaloclastite in the Ongeluk Andesite Formation in a Road-Cutting West of Griquatown, South Africa- Trans. Geol. S. Afr. (76), 53-57.

Grotzinger J.P. and Reed J.F. (1983) -Evidence for Primary Aragonite Precipitation, Lower Proterozoic (1.9 Ga) Rocknest Dolomite, Wopmay Orogen, Northwest Canada- Geology (11), 710-713.

Grotzinger J.P. and Kasting J.F. (1993) -New Constraints on Precambrian Ocean Composition- The Journal of Geology (101), 235-243.

Gutzmer J. And Beukes N.J. (1995) - Fault-Controlled Metasomatic Alteration of Early Proterozoic Sedimentary Manganese Ores in the Kalahari Manganese Field, South Africa - Economic Geology

(90), 823-844.

Gutzmer J. and Beukes N.J. (1996) - Mineral Paragenesis of the Kalahari Manganese Field, South Africa - Ore Geology Review (11), 405-428.

Gutzmer J. and Beukes N.J. (1997) - Effects of Mass Transfer, Compaction and Secondary Porosity on Hydrothermal Upgrading of Paleoproterozoic Sedimentary Manganese Ore in the Kalahari Manganese Field, South Africa - Mineralum Deposita (32), 250-256.

Gutzmer J., Beukes N.J. and Yeh H.-W. (1997) - Fault-Controlled Metasomatic Alteration of Early Proterozoic Sedimentary Manganese Ore at Mamatwan Mine, Kalahari Manganese Field, South Africa - S. Afr. J. Geol. (100-1), 53-71.

Harland M.J. and Hambrey W.B. (1981) -Earth's Pre-Pleistocene Glacial Record- Cambridge, England, Cambridge University Press, 1004pp.

Hoefs J. (1980) -Stable Isotope Geochemistry- Springer-Verlag Editors, 3rd edition, 241pp.

Holland H.D. (1972) -The Geologic History of Sea Water-an Attempt to Solve the Problem- Geochimica et Cosmochimica Acta (36), 637-651.

Holland H.D., Lazar B., McCaffrey M., (1986) -Evolution of the Atmosphere and Oceans- Nature (320), 27-33.

Holland H.D. (1992) -Chemistry and Evolution of Proterozoic Ocean- in *The Proterpzoic Biosphere, a Multidisciplinary Study*, Schopf & Klein editors, Cambridge, England, Cambridge University Press, 169-172.

Houston R.S., Lanthier L.R., Karlstrom K.K, and Sylvester G.G. (1981) -Early Proterozoic

Diamictite of Southern Wyoming- in Hambrey and Harland ediors, *Earth's Pre-Pleistocene Glacial Record :* Cambridge, England, Cambridge University Press, 795-799.

Ingrid J. And Pontér C. (1986) -Iron and Manganese Layering in Recent Sediments in the Gulf of Bothnia- Chemical Geology (56), 105-116.

Isley A.E. (1995) -Hydrothermal Plumes and the Delivery of Iron to Banded Iron Formation- Journal of Geology (103), 169-185.

Jacobs J., Thomas R.J., and Weber K. (1993) -Accretion and Indentation Tectonics at the Southern Edge of the Kaapvaal Craton During the Kibaran (Grenville) Orogeny- Geology (21), 203-206.

Jacobs S.S. (1989) -Marine Control on Modern Sedimentation on the Antarctic Continental Shelf- Marine Geology (85), 121-153.

James H.L. (1969) -Comparison Between Red Sea Deposits and Older Ironstone and Iron-Formation- In : Hot Brines and Recent Heavy Metal Deposits in the Red Sea, Degens E.T. and Ross D.A. editors, Springer-Verlag, Berlin, 525-532.

Johnsson M.J., Stallard R.F., Meade R.H. (1988) -First-Cycle Quartz Arenites in the Orinoco River Basin, Venezuela and Colombia- Journal Geology (96), 263-277.

Kasting J.F. (1987) -Theorical Constraints on Oxygen and Carbon Dioxide Concentrations in the Precambran Atmosphere- Precambrian Research (34), 205-229.

Kasting J.F. (1991) -Box Model for the Evolution of the Atmospheric Oxygen : an Update- Paleogeography, Paleoclimatology, Paleoecology (Global and Planetary Change Section) (97), 125-131.

Kasting J.F., Eggler D.H. and Raeburn S.P. (1993) -Mantle Redox Evolution and the Oxidation State of the Archean Atmosphere- Journal of Geology (101), 245-257.

Kaufman A.J., Hayes J.M., Klein C. (1990) -Primary and Diagenetic Controls of Isotopic Compositions of Iron-Formation Carbonates- Geochimica Cosmochimica Acta (54), 3461-3473.

Kauffiman E.G., Elder W.P., Sageman B.B. (1991) -High-Resolution Correlation : a New Tool in Chronostratigraphy- In : Cyclesand Events in Stratigraphy, Einsele G., Ricken W.and Seilacher A. Editors, 795-819.

Kiehl J.T. and Dickinson R.E. (1987) -A Study of the Radiative Effects of Enhanced Atmospheric $CO_2$ and $CH_4$ on Early Earth Surface Temperatures- Journal of Geophysical Research (92, NoD3), 2991-2998.

Kirschvink J.L. (1992) -Late Proterozoic Late-Latitude Global Glaciation : The Snowball Earth- In The Proterozoic Biosphere : a Multidisciplinary Study, Schopf J.W and Klein C. edtrs., Cambridge, Cambridge University Press, 51-52.

Klein C. And Beukes N.J. (1989) -Geochemistry and Sedimentology of a Facies Transition from Limestone to Iron-Formation Deposition in the Early Proterozoic Transvaal Supergroup, South Africa- Economic Geology (84), 1733-1774.

Klein C. and Beukes N.J. (1992) -Models for Iron-Formation Deposition- *In* The Proterozoic Biosphere, a Multidisciplinary Study, Schopf J.W. and Klein C., Cambridge University Press, 147-152.

Klein C. and Beukes N.J. (1993) -Sedimentology and Geochemistry of the Glaciogenic Late Proterozoic Rapitan Iron-Formation in Canada- Economic Geology (88), 542-565.

Kleyenstüber A.S.E. (1984) - The Mineralogy of the Manganese-Bearing Hotazel Formation of the

Proterozoic Transvaal Sequence in Griqualand West, South Africa - Geological Society of South Africa Transactions (87), 257-272.

Kuhn W.R., Walker J.C.G. and Marshall H.G. (1989) -The effect on Earth's Surface Temperature from Variations in Rotation Rate, Continent Formation, Solar Luminosity, and Carbon Dioxide- Journal of Geophysical Research (94), 11129-11136.

Kurtz D.D. (1981) -Early Proterozoic Diamictites of the Black Hills, South Dakota- in Hambrey and Harland ediors, *Earth's Pre-Pleistocene Glacial Record :* Cambridge, England, Cambridge University Press, 800-802.

Marmo J.S. and Ojakangas R.W. (1984) -Lower Proterozoic Glaciogenic Deposits, Eastern Finland- Geological Society of America Bulletin (95), 1055-1062.

Marshall H.G., Walker J.C.G. and Kuhn W.R. (1988) -Long-Term Climatic Change and the Geochemical Cycle of Carbon- Journal of Geophysical Research (93), 791-801.

Martin D.McB., Clendenin C.W., Krapez B. and McNaughton N.J. (1998) -Tectonic and Geochronological Constraints on Late Archaean and Paleoproterozoic Stratigraphic Correlation Within and Between the Kaapvaal and Pilbara Cratons- Journal of the Geological Society, London (155), 311-322.

Martini J.E.J (1979) -A Copper-Bearing Bed in the Pretoria Group in Northeastern Transvaal- Geocongress 77 : Geol.Soc.S.Afr.Spec.Publ (6), 65-72.

Marthur S.M. (1981) -The Middle Precambrian Gangau Tillite, Bijawar Group, Central India- in Hambrey and Harland ediors, *Earth's Pre-Pleistocene Glacial Record :* Cambridge, England, Cambridge University Press, 428-430.

Matthews R.K. (1984) -Dynamic Stratigraphy : an Introduction to Sedimentation and Stratigraphy, 2nd Edition, Prentice-Hall, Englewood Cliffs, New Jersey.

McLennan S.M. and Taylor S.R. (1985) - The Continental Crust : Its Composition and Evolution- Oxford, Blackwell, 312pp.

McLennan S.M. and Taylor S.R. (1991) -Sedimentary Rocks and Crustal Evolution : Tectonic Setting and Secular Trends- Journal of Geology (99), 1-21.

McLennan S.M., Hemming S.R., Taylor S.R., and Eriksson K.A. (1995) -Early Proterozoic Crustal Evolution : Geochemical and Nd-Pb Isotopic Evidence From Metasedimentary Rocks, Southwestern North America- Geochimica et Cosmochimica Acta (59), 1153-1177.

Miall A.D. (1985) -Sedimentation on an Early Proterozoic Continental Margin Under Glacial Influence : the Gowgonda Formation (Huronian), Elliot Lake Area, Ontario, Canada- Sedimentology (32), 763-788.

Miyano T. And Beukes N.J. (1987) - Physicochemical Environments for the Formation of Quartz-Free Manganese Oxide Ores from the Early Proterozoic Hotazel Formation, Kalahari Manganese Field, South Africa - Economic Geology (82), 706-718.

Morris R.C. (1993) -Genetic Modelling for Banded Iron-Formation of the Hamersley Group, Pilbara Craton, Western Australia- Precambrian Research (60), 243-286.

Mustard P.S. and Donaldson J.A. (1987) -Early Proterozoic Ice-Proximal Glaciomarine Deposition : the Lower Gowgonda Formation at Cobalt, Ontario, Canada- Geol.Soc.Ame.Bull (98), 337-387.

Nel C.J., Beukes N.J. and De Villiers J.P.R. (1986) -The Mamatwan Manganese Mine of the Kalahari Manganese Field- In Anhaeuser C.R. and Maske S. Eds, Mineral deposits of Southern Africa :

Johannesburg, Geological Society of South Africa, 963-978.

Nel L.T. (1929) -The Geology of the Postmasburg Manganese Deposits and the Surrounding Country- Geological Survey of South Africa, an explanation of the geological map, 109pp.

Nelson D.R., Trendall A.F., and Altermann W. (1999) -Chronological Correlations Between the Pilbara and Kaapvaal Cratons- Precambrian Research (97), 165-189.

Nesbitt H.W., Young G.M., McLennan S.M., Keays R.R. (1996)-Effects of Chemical Weathering and Sorting on the Petrogenesis of Siliclastic Sediments, With Implications For Provenance Studies- Journal Geology (104), 525-542.

Nesbitt H.W., Fedo C.M. and Young G.M. (1997) -Quartz and Feldspar Stability, Steady-State Weathering and Petrogenesis of Siliclastic Sands and Muds- Journal Geology (105),173-191.
Plehwe E. von and Klemm D.D. (1995) - Geology and Ore Genesis of the Manganese Ore Deposits of the Postmasburg Manganese-Field, South Africa - Mineralum Deposita (30), 257-267.

Newman M.J. and Rood R.T. (1977) -Implications of Solar Evolution for the Earth's Early Atmosphere- Science (198), 1035-1037.

Norrish K. And Hutton J.T. (1969) -An Accurate X-Ray Spectrography Method For the Analysis of a Wide Range of Geological Samples- Geoch.Cosm.Acte (33),431-453.

Powell R.D. (1984) -Glacimarine Processes and Inductive Lithofacies Modelling of Ice Shelf and Tidewater Glacier Sediments Based on Quaternary Examples- Marine Geology (57), 1-52.

Powell R.D. and Molnia B.F. (1989) -Glacimarine Sedimentary Processes, Facies and Morphology of the South-Southeast Alaska Shelf and Fjords- Marine Geology (85), 359-390.

Raymo M.E. (1991) -Geochemical Evidence Supporting T.C. Chamberlin's Theory of Glaciation- Geology (19), 344-347.

Rollinson H. (1993) -Using Geochemical Data : Evaluation, Presentation, Interpretation- Geochemistry Series

Romer and Bau (1998), Chenese Science Bulletin Supplement (43), 109.

Rosenbaum J. And Sheppard S.M.F. (1986) -An Isotopic Study of Siderites, Dolomites and Ankerites at High Temperatures- Geochim. Cosmochim. Acta (50), 1147-1150.

Roy S. (1992) -Environments and Processes of Manganese Deposition- Economic Geology (87), 1218-1236.

Rye R., Kuo P.H. and Holland H.D. (1995) -Atmospheric Carbon Dioxide Concentrations Before 2.2 Billion Years Ago- Nature (378), 603-605.

SACS (1980) -Stratigraphy of South Africa- Part 1 (Comp. L.E.Kent). Lithostratigraphy of the Republic of South Africa, South West Africa/Namibia and the Republic of Bophuthatswana, Transkei and Venda. Handbook Geol. Surv. S. Afr. (8), 690pp.

Sandrock J., Studley S.A., Hayes J.M. (1985) -Isotopic Analyses Based on the Mass Spectrum of Carbon Dioxide- Anal. Chem. (57), 1444-1448.

Schissel D. and Aro P. (1992) -The Major Early Proterozoic Sedimentary Iron and Manganese Deposits and their Tectonic Setting- Economic Geology (87), 1367-1374.

Schlegel G.C.J. (1988) -Contribution to the Metamorphic and Structural Evolution of the Kheis Tectonic Province, Northern Cape, South Africa- S.Afr.J.Geol. (91), 27-37.

Schmidt P.W. and Williams G.E. (1995) -The Neoproterozoic Climatic Paradox : Equatorial Paleolatitude for Marinoan Glaciation Near Sea Level in South Australia- Earth and Planetary Science Letters (134), 107-124.

Schoch R.M. (1989) -Stratigraphy : Principles and Methods- Van Nostrand Reinhold Editors, 375pp.

Schreiber U.M. (1991) -A Paleoenvironmental Study of the Pretoria Group in the Eastern Transvaal- PhD thesis (unpubl.), University of Pretoria, Pretoria, South Africa.

Schwellnus J.S.I, Engelbrecht L.N.J., Coertze F.J., Russel H.D., Malherbe S.J., van Rooyen D.P. and Cooke R. (1962) -The Geology of the Olifants River Area, Transvaal- Explanation of Sheets 2429B (Chuniespoort) and 2430A (Wolkberg), Geol.Surv.S.Afr, 87pp.

Sellwood B.W. (1986) -Shallow-Marine Carbonate Environments- In Sedimentary Environments and Facies, Reading H.G. Editor, Blackwell Scientific Publications, 283-342.

Stowe C.W. (1986) -Synthesis and Interpretation of Structures Along the North-Eastern Boundary of the Namaqua Tectonic Province, South Africa- Trans.Geol.SOc.S.Afr. (89), 185-198.

Strand K.O. and Laajoki K. (1993) -Paleoproterozoic Glaciomarine Sedimentation in an Extensional Setting : the Honkala Formation, Finland- Precambrian Research (64), 253-271.

Schwarzbach M. (1963) -Climates of the Past : an Introduction to Paleoclimatology- Fairbridge R.W. edtr, The University Series in Geology, D. Van Nostrand Company, Ltd, 328pp.

Symons D.T.A. (1975) -Huronian Glaciation and Polar Wander From the Gowganda Formation, Ontario- Geology (3), 303-305.

Syvitski J.P.M. (1989) -On the Deposition of Sediment Within Glacier-Influenced Fjords :

Oceanographic Controls- Marine Geology (85), 301-329.

Tatcher E.C. and Associates (1993) -Photogeology and Landsat-TM Interpretation Sishen-Postmasburg-Wolhaarkop-Rooinekke Area, Northern Cape Province- Associated Manganese Mines of South Africa LTD, 128pp.

Taussig D. and Maiden K. (1986) -Stratabound Copper Mineralisation in the Duitsland Formation, Transvaal Basin- Geocongress'86 (Johannesburh, South Africa), Abstracts, 545-547.

Taylor S.R. and McLennan S.M. (1985) -The Continental Crust : Its Composition and Evolution, An Examination of the Geochemical Record Preserved in Sedimentary Rocks- Blackwell Scientific Publications, Geoscience texts.

Thompson L.G., Mosley-Thompson E., Grootes P.M., Pourchet M. and Hastenrath S. (1984) -Tropical Glaciers : Potential for Ice Core Paleoclimatic Reconstructions- Journal of Geophysical Research (89), 4638-4646.

Trendall A.F. (1976) -Striated and Faceted Boulders From Turee Creek Formation - Evidence for a Possible Huronian Glaciation on the Australian Continent- Western Australia Geological Survey Annual Report 1975, 88-92.

Tsikos H. (1994) - - (unpl. M.Sc. thesis), Rhodes University, Grahamstown, South Africa

Tsikos H. and Moore J.M.M. (1997) - Petrography and Geochemistry of the Paleoproterozoic Hotazel Iron-Formation, Kalahari Manganese Field, South Africa : Implications for Precambrien Manganese Metallogenesis - Economic Geology (92), 87-97.

Tsikos H. And Moore J.M. (1998) -The Kalahari Manganese Field : and Enigmatic Association of Iron and Manganese- South African Journal Geology (101), 287-290.

Tsikos H. (1999) - -Phd thesis (unpubl.), Rhodes University, Grahamstown, South Africa.

Trendall A.F. (1976) -Striated and Faceted Boulders from Turee Creek Formation - Evidence for a Possible Huronian Glaciation on the Australian Continent- Western Australia Geol.Surv.Ann.Rep (1975), 88-92.

Trendall A.F. (1981) -The Lower Proterozoic Meteorite Bore Member, Hamersley Basin, Western Australia- in Hambrey and Harland ediors, *Earth's Pre-Pleistocene Glacial Record :* Cambridge, England, Cambridge University Press, 555-559.

Truter F.C., Wasserstein B., Botha P.R, Visser D.J.L, Boardman L.G., Paver G.L. (1938) - The Geology and Mineral Deposits of the Oliphants Hoek Area- Geological Survey of South Africa, Explanation sheet No173, 144pp.

Urban H., Stribrny B. And Lippolt H.J. (1992) -Iron and Manganese Deposits of the Urucum District, Matto Grosso Do Sul, Brazil- Economic Geology (87), 1375-1392.

Visser D.J.L (1944) -Stratigraphic Features and Tectonics of Portions of Bechuanaland and Griqualand West- Trans. Geol. Sth. Afr. (47), 197-

Visser D.J.L (1958) -The Geology and Mineral Deposits of the Griquatown Area, Cape Province- Geological Survey of South Africa, Explanation Sheet No175, 72pp.

Visser J.N.J (1971) -The Deposition of the Griquatown Glacial Member in the Transvaal Supergroup- Trans. Geol. S. Afr. (), 187-199.

Walker J.C.G. (1985) -Iron and Sulfur in the Pre-Biologic Ocean- Precambrian Research (28), 205-222.

Wiggering H. and Beukes N.J. (1990) -Petrography and Geochemistery of a 2000-2200-Ma-Old Hematitc Paleo-Alteration Profile on Ongeluk Basalt of the Transvaal Supergroup, Griqualand West, South Africa- Precambrien Research (46), 241-258.

Williams G.E. (1975) -Late Precambrian Glacial Climate and the Earth's Obliquity- Geological Magazine (112), 441-465.

Williams G.E. (1993) -History of Earth's Obliquity- Earth-Science Reviews (34), 1-45.

Williams G.E. and Schmidt P.W. (1997) -Paleomagnetism of the Paleoproterozoic Gowganda and Lorrain Formations, Ontario : Low Paleolatitude for Huronian Glaciation- Earth and Planetary Science Letters (153), 157-169.

Williams G.E. (1998) -Precambrian Tidal and Glacial Clastic Deposits : Implication for Precambrian Earth-Moon Dynamics and Paleoclimate- Sedimentary Geology (120), 55-74.

Schmidt P.W. and Clark D.A. (1994) -Paleomagnetism and Magnetic Anisotropy of Proterozoic Banded-Iron Formations and Iron Ores of the Hamersley Basin, Western Australia- Precambrian Research (69), 133-155.

Wingate M.T.D. (1998) -A Paleomagnetic Test of the Kaapvaal - Pilbara (Vaalbara) Connection at 2.78 Ga- S.Afr.J.Geol. (101), 257-274.

Wronkiewicz D.J. and Condie K.C. (1987) -Geochemistry of Archean Shales from the Witwatersrand Supergroup, South Africa : Source-Area Weathering and Provenace- Geochimica et Cosmochimica Acta (51), 2401-2416.

Wronkiewicz D.J. and Condie K.C. (1989) -Geochemistry and Provenance of Sediments from the Pongola Supergroup, South Africa : Evidence for a 3.0-Ga-Old Continental Craton- Geochimica et Cosmochimica Acta (53), 1537-1549.

Young G.M. and McLennan S.M. (1981) -Early Proterozoic Padlei Formation, Northwest Territories, Cananda- in Hambrey and Harland ediors, *Earth's Pre-Pleistocene Glacial Record :* Cambridge, England, Cambridge University Press, 790-794.

Young G.M. and Nesbitt H.W. (1985) -The Gowganda Formation in the Southern Part of the Huronian Outcrop Belt, Ontario, Canada : Stratigraphy, Depositional Environments and Regional Tectonic Significance- Precambrian Research (29), 265-301.

Young G.M. (1991) -The Geological Record of Glaciation : Relevance to the Climatic History of Earth- Geoscience Canada (18), 100-108.

A1 Boreholes locations

Ga129 : X coordinate : 73686.53
Y coordinate : -46070.67
Z coordinate : 1191.77

Ga171 : X coordinate : 72224.29
Y coordinate : -46068.66
Z coordinate : 1190.11

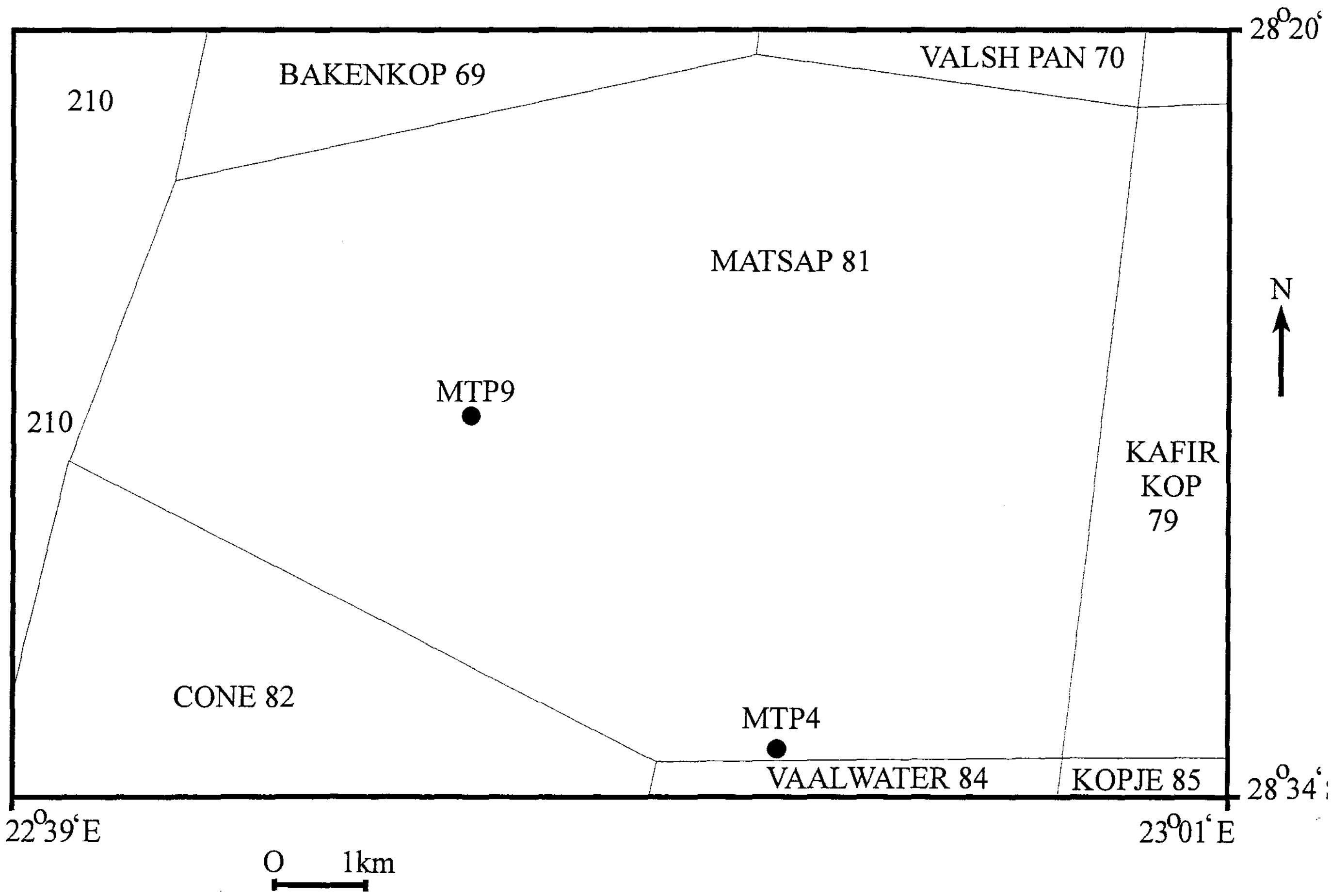

| SAMPLE | GA171-5 | GA129-3 | GA129-5 | GA129.9 | MTP4-10 | MTP4-P1 | GA129-16 | GA129-40 | GA129-20 | MTP4-E1 | MTP4-8A" | MTP4-7A" | GA171-11 | MTP4-M2 | MTP4-P15" |
|---|---|---|---|---|---|---|---|---|---|---|---|---|---|---|---|
| SiO2 | 48.907 | 44.22 | 50.518 | 43.022 | 70.16 | 70.89 | 51.012 | 64.581 | 62.892 | 59.947 | 49.166 | 52.883 | 40.407 | 67.526 | 76.645 |
| TiO2 | 0.4 | 0.207 | 0.0185 | 0.133 | 0.213 | 0.287 | 0.15 | 0.339 | 0.378 | 0.358 | 0.204 | 0.265 | 0.13 | 0.163 | 0.339 |
| Al2O3 | 6.477 | 4.047 | 4.297 | 3.222 | 6.24 | 8.322 | 3.847 | 9.095 | 9.863 | 9.005 | 5.281 | 5.612 | 3.065 | 4.971 | 9.786 |
| Fe2O3 | 16.026 | 17.413 | 19.926 | 24.75 | 15.441 | 11.061 | 21.893 | 13.206 | 11.908 | 17.897 | 26.693 | 24.878 | 16.155 | 16.507 | 6.188 |
| Fe0 | 0 | 0 | 0 | 0 | 0 | 0 | 0 | 0 | 0 | 0 | 0 | 0 | 0 | 0 | 0 |
| MnO | 0.302 | 0.54 | 0.335 | 0.398 | 0.974 | 0.509 | 0.418 | 0.107 | 0.161 | 1.348 | 2.555 | 2.559 | 0.267 | 1.721 | 0.049 |
| MgO | 7.316 | 5.896 | 3.949 | 5.208 | 1.724 | 2.013 | 4.014 | 2.61 | 2.56 | 2.982 | 2.634 | 2.615 | 3.067 | 1.532 | 1.213 |
| CaO | 7.129 | 10.534 | 7.609 | 6.9 | 0.081 | 0.747 | 6.175 | 2.063 | 2.071 | 0.175 | 0.247 | 0.158 | 4.505 | 0.251 | 0.095 |
| Na2O | 0 | 0.15 | 0.1 | 0.091 | 0.011 | 0.143 | 0.203 | 0.007 | 0 | 0.053 | 0.001 | 0.002 | 0.2 | 0.012 | 0.229 |
| K2O | 0.024 | 0.346 | 0.244 | 0.292 | 0.338 | 1.267 | 0.451 | 2.692 | 2.781 | 0.967 | 0.024 | 0.027 | 0.322 | 0.372 | 2.357 |
| P2O5 | 0.088 | 0.07 | 0.072 | 0.063 | 0.011 | 0.064 | 0.071 | .0.88 | 0.09 | 0.027 | 0.012 | 0.01 | 0.054 | 0.01 | 0.033 |
| Cr2O3 | 0 | 0 | 0 | 0 | 0 | 0 | 0 | 0 | 0 | 0 | 0 | 0 | 0 | 0 | 0 |
| NiO | 0 | 0 | 0 | 0 | 0 | 0 | 0 | 0 | 0 | 0 | 0 | 0 | 0 | 0 | 0 |
| LOI | 11.79 | 14.616 | 11.19 | 14.69 | 4.284 | 3.707 | 11.483 | 4.782 | 7.236 | 6.952 | 12.41 | 11.12 | 31.813 | 7.468 | 1.945 |
| H2O | 0.971 | 1.52 | 1.476 | 1.395 | 0.731 | 0.306 | 0.397 | 0.254 | 0.493 | 0.009 | 0.353 | 0.113 | 0.426 | 0.058 | 0.375 |
| Sc | 8.5 | 6 | 6 | 5.7 | 4.3 | 7.7 | 5.3 | 9.4 | 10.6 | 9.4 | 7.4 | 8 | 5.4 | 4.3 | 8.4 |
| V | 60.4 | 35.1 | 33.9 | 26.3 | 29.1 | 54.1 | 31.3 | 58.1 | 67 | 66.3 | 50.4 | 54.6 | 28.9 | 24.7 | 40.9 |
| Cr | 98.5 | 58.3 | 45.4 | 35.2 | 51.9 | 77.8 | 43.9 | 85.7 | 93.3 | 99.6 | 66.2 | 71.7 | 42.8 | 43.9 | 93.5 |
| Co | 25.8 | 6.8 | 5.8 | 3 | 17.5 | 25 | 5 | 12.3 | 12.1 | 22.2 | 14.1 | 15.7 | 4.3 | 12.2 | 19.7 |
| Ni | 62.2 | 33.1 | 27.9 | 26.1 | 34.4 | 39.4 | 44.7 | 39.8 | 45.2 | 50.7 | 46.3 | 43.9 | 25.3 | 32.1 | 79.9 |
| Cu | 39.8 | 29.1 | 22.4 | 15.9 | 13.2 | 270.8 | 23.8 | 32.9 | 14.2 | 93.8 | 24.5 | 38.6 | 19.7 | 13.6 | 12 |
| Zn | 48.5 | 27.5 | 30.1 | 27.9 | 51.5 | 65.4 | 25.7 | 52.5 | 36 | 53 | 51.2 | 56.7 | 22 | 39.1 | 30.4 |
| Rb | 2.02 | 26.33 | 19.89 | 32.23 | 8.39 | 40.15 | 34.23 | 69.5 | 94.88 | 30.66 | 2.04 | **LLD** | 26.78 | 9.47 | 71.25 |
| Sr | 22.71 | 27.71 | 31.99 | 22.3 | 10.07 | 11.76 | 16.45 | 24.44 | 5.16 | 20.76 | 8.64 | 11.43 | 22.86 | 6.96 | 30.73 |
| Y | 16.04 | 11.77 | 13.47 | 12.64 | 16.36 | 18.3 | 12.77 | 17.92 | 18.84 | 20.06 | 16.6 | 14.76 | 13.09 | 12.06 | 19.94 |
| Zr | 112.6 | 61.15 | 67.18 | 47.06 | 118.65 | 108.55 | 56.54 | 120.42 | 127.19 | 119.01 | 73.33 | 74.1 | 59.92 | 120.33 | 128.19 |
| Nb | 10.68 | 4.37 | 4.07 | **LLD** | 5.3 | 7.03 | 3.8 | 7.63 | 9.6 | 8.65 | 6.31 | 5.75 | 3.42 | 4.13 | 9.58 |
| Ba | 4.4 | 85.9 | 45 | 60.2 | 12.9 | 79.2 | 25.2 | 262.6 | 31.8 | 34.2 | 9.8 | 10.9 | 247.4 | 11.8 | 226.2 |
| La | 19.14 | 16.85 | 14.25 | 12.29 | 29.32 | 25.65 | 14.72 | 26.03 | 28.35 | 44.03 | 18.75 | 21.14 | 16.81 | 23.26 | 47.96 |
| Ce | 38.84 | 35.84 | 30.42 | 30.18 | 55.82 | 46.05 | 28.9 | 50.38 | 56.35 | 79.24 | 42.84 | 37.06 | 31.61 | 40.57 | 85 |
| Nd | 16.35 | 14.39 | 13.46 | 11.62 | 19.1 | 15.71 | 11.37 | 20.41 | 22.24 | 29.04 | 21.48 | 11.45 | 12.48 | 15.99 | 32.17 |
| Pb | 23.22 | 4.83 | 6.02 | 8.55 | 4.39 | **LLD** | 4.52 | 13.96 | 3.5 | 4.95 | 5.33 | 3.53 | 5.58 | 3.11 | 129.11 |
| Th | 10.89 | 5.82 | 6.91 | 6.27 | 8.4 | 9.01 | 5.69 | 10.94 | 13.69 | 13.48 | 8.62 | 7.32 | 5.52 | 6.71 | 74.26 |

A2 Geochemical results for clastic sediments

# A3 Geochemical results for banded iron-formations

| | GA171-13 | GA171-23 | GA129-24 | GA171-21 | GA171-30 | GA129-29 | GA129-27 | GA171-14 | GA171-15" |
|---|---|---|---|---|---|---|---|---|---|
| SiO2 | 41.962 | 44.322 | 58.98 | 55.003 | 53.569 | 60.433 | 52.396 | 52.13 | 46.543 |
| TiO2 | 0.139 | 0.069 | 0.066 | 0.029 | 0.028 | 0.028 | 0.028 | 0.028 | 0.024 |
| Al2O3 | 3.035 | 1.74 | 1.321 | 0.376 | 0.318 | 0.559 | 0.482 | 0.454 | 0.312 |
| Fe2O3 | 28.892 | 22.311 | 10.082 | 31.218 | 31.215 | 19.43 | 28.396 | 34.996 | 45.887 |
| Fe0 | 0 | 0 | 0 | 0 | 0 | 0 | 0 | 0 | 0 |
| MnO | 0.406 | 0.968 | 0.803 | 0.211 | 0.421 | 0.208 | 0.175 | 0.165 | 0.127 |
| MgO | 4.792 | 3.807 | 2.041 | 1.539 | 1.879 | 2.393 | 2.489 | 1.475 | 1.021 |
| CaO | 4.038 | 7.704 | 11.371 | 4.618 | 4.503 | 7.566 | 6.687 | 4.706 | 2.756 |
| Na2O | 0.083 | 0 | 0 | 0 | 0 | 0.052 | 0.044 | 0.017 | 0.005 |
| K2O | 0.115 | 0.109 | 0.129 | 0.113 | 0.012 | 0.118 | 0.183 | 0.053 | 0.108 |
| P2O5 | 0.048 | 0.046 | 0.055 | 0.037 | 0.047 | 0.05 | 0.04 | 0.106 | 0.04 |
| Cr2O3 | 0 | 0 | 0 | 0 | 0 | 0 | 0 | 0 | 0 |
| NiO | 0 | 0 | 0 | 0 | 0 | 0 | 0 | 0 | 0 |
| LOI | 15.498 | 18.453 | 13.457 | 6.58 | 7.481 | 9.161 | 8.969 | 5.316 | 2.03 |
| H2O | 0.325 | 0.22 | 0.229 | 0.089 | 0.329 | 0.12 | 0.214 | 0.24 | 0.562 |
| Sc | 8.9 | 3.3 | 3.1 | 3.3 | 2.9 | 2.5 | 2.5 | 3.1 | 2.5 |
| V | 39.8 | 17.8 | 14.8 | 12.1 | 9.8 | 8.3 | 8.6 | 11.9 | 12.1 |
| Cr | 50.1 | 23.5 | 20.3 | 24.2 | 20.1 | 17.2 | 14.9 | 24.2 | 20.5 |
| Co | 6 | 6.7 | 3.9 | **LLD** | **LLD** | **LLD** | **LLD** | **LLD** | **LLD** |
| Ni | 29.3 | 19.1 | 14.6 | 16.6 | 23.5 | 15.9 | 20.8 | 27 | 41.3 |
| Cu | 15.4 | 61.5 | 13.3 | 17.9 | 19.3 | 17.5 | 17.2 | 26 | 28.5 |
| Zn | 19.8 | 19.1 | 20.3 | 16.7 | 12.1 | 14.3 | 13.5 | 10 | 14.1 |
| Rb | 13.05 | **LLD** | **LLD** | **LLD** | **LLD** | 7.12 | 11.72 | 2.58 | **LLD** |
| Sr | 16.56 | 22.69 | 37.39 | 12.47 | 9.18 | 38.61 | 41.42 | 22.85 | 9.92 |
| Y | 15.22 | 11.58 | 19.88 | 6.01 | 11.73 | 23.05 | 13.33 | 14.43 | 7.84 |
| Zr | 35.15 | 17.38 | 17.11 | 4.88 | 5.2 | 7.21 | 9.06 | 6.43 | 7.61 |
| Nb | 2.85 | **LLD** | **LLD** | **LLD** | **LLD** | **LLD** | **LLD** | **LLD** | **LLD** |
| Ba | 208.3 | **LLD** | **LLD** | 2.7 | 4.5 | 9.6 | 6.6 | 27.2 | 20.1 |
| La | 11.59 | 4.97 | 11.58 | 3.16 | **LLD** | 4.48 | 6.93 | 5.71 | **LLD** |
| Ce | 30.6 | 20.38 | 19.53 | 15.76 | 9.51 | 16.74 | 20.5 | 22.39 | 18.42 |
| Nd | 10.68 | 8.16 | 8.2 | 6.92 | **LLD** | 7.18 | 8.39 | 7.89 | 8.88 |
| Pb | 19.81 | 3.67 | 15.88 | **LLD** | 2.96 | 2.53 | **LLD** | 4.56 | 4.42 |
| Th | 5.65 | 3.57 | 2.36 | **LLD** | **LLD** | 2.13 | 2.54 | 3.53 | 6.22 |

## A4 Sample description for boreholes MTP4 and MTP9

| MTP4 | depth | type | | P1-P7 | 451.37 | Graded cycle fining upwards : siltstone to SS |
|---|---|---|---|---|---|---|
| A1-A3 | 368.20 | IS breccia | | P8-P16 | 451.99 | Fine diamictites |
| B1-B2 | 369.28 | Hematised lava | | Q1-Q8 | 454.06 | Hematised diamictite |
| C1-C6 | 375.17 | Lava | | Q9-Q10 | 454.44 | Sandstone |
| D1 | 377.33 | lava | | Q11-Q12 | 454.68 | IS breccia |
| 1A-1C | 382.68 | Graded cycles + BIF breccia | | Q13-Q22 | 454.76 | Sandstone |
| 1D | 382.78 | IS | | R1-R6 | 457.55 | sandstone hematised |
| 1E | 382.90 | Graded cycle | | D10A | 458.64 | Siltstone |
| 1F-1H | 382.95 | Shale sulphide rich | | D10B | | siltstone _ IS breccia |
| 1I-1J | 383.01 | IS breccia | | D10C | | siltstone |
| 1K | 383.18 | Graded cycle | | D10E | | siltstone + IS breccia |
| 1L-1M | 383.20 | IS breccia | | E10A-E10C | 465.31 | Diamictites |
| 2A-2E | 383.66 | Very fine siltsone (mudstone) | | S1 | 469.05 | diamictite |
| 2F-2ZE | 384.04 | Graded cycles fining upwards | | T1-T8 | 471.43 | diamictites, with patchs hematised |
| 3A-3D | 386.79 | IS breccia | | 11A-11F | 472.34 | Mudstone with big clasts at the bottom |
| 3E-3I | 387.05 | Hematised siltstone | | 12A-12K | 472.65 | Hematised mudstone |
| E1-E2 | 387.38 | Graded cycles | | 13A-13I | 473.28 | Hematised diamictites |
| 4A-4F | 387.80 | Graded cycles fining upwards | | 14A-14D | 747.70 | Hematised diamictites |
| 5A-5D | 388.65 | Graded cycles | | 15A | 483.08 | Hematised diamictite |
| 6A-6D | 388.82 | IS breccia | | 16A | 484.41 | Hematised diamictite |
| F1-F5 | 389 | graded cycles, hematised | | | | |
| G1-G4 | 391.35 | Hematised siltstone + mudstone + sulphides | | | | |
| H1-H2 | 393.20 | Hematised diamictite | | | | |
| I1-I2 | 394.25 | Diamictite | | MTP9 | | |
| J1-J8 | 399.99 | diamictites | | A1-A4 | 228.84 | Lava |
| 7A-7B | 407.37 | diamictites | | B1-B10 | 230.03 | Mudstone |
| 8A | 413.15 | diamictites | | C1-C2 | 231.20 | Graded cycles |
| K1-K3 | 415.34 | diamictites | | D1-D10 | 231.58 | Graded cycles |
| 9A-9H | 416.91 | diamictites + big clasts : mattrix poor at the bottom | | E1-E2 | 234.16 | Mudstone |
| 10A-10B | 417.10 | Clast suported diamictite | | E3-E5 | 234.33 | Dark IS |
| 10C-10F | 417.33 | Graded cycles | | E6-E7 | 234.54 | Graded diamictite : fine to coars |
| 10G-10O | 417.80 | Diamictites | | F1 | 236.33 | Diamictite |
| L1-L15 | 418.75 | Sandstone (L1) + clast supported diamicites + FSS | | G1 | 238.58 | diamictite |
| M1-M11 | 421.59 | Siltstone | | H1-H3 | 239.51 | diamictite |
| M12-M19 | 422.82 | Fine diamictite | | I1-I5 | 241.05 | diamictite, dropstone in IS (I2) |
| N1-N4 | 428.13 | Diamictite | | J1-J2 | 244.98 | Diamictite |
| O1-O3 | 441.01 | Siltstone + lenses of fine sandstone | | K1-K9 | 246.42 | dark IS (K1-K2) + diamictite with dark IS |
| B10A-B10B | 442.15 | IS | | | | |

# A5 Sample description for boreholes GA171 and GA129

| GA 129 | depth | type |
|---|---|---|
| 1 | 153.51 | lava or dyke |
| 2 | 179.59 | lava or dyke |
| 3 | 197.3 | diam |
| 4 A-B | 209.3 | fine diam |
| 5 | 216 | diam |
| 6 | 217.33 | diam |
| 7 | 229.16 | diam |
| 8 | 232.41 | diam |
| 9 | 238.35 | diam |
| 10 A-B | 256.61 | diam |
| 11 A-B | 269.6 | diam |
| 12 | 294.76 | diam |
| 13 A-B | 298.5 | diam |
| 14 A-B | 307.9 | diam |
| 15 | 315.8 | fine diam |
| 16 | 316.6 | fine diam |
| 17 | 329.91 | diam |
| 18 | 338.08 | diam |
| 19 | 342.74 | diam |
| 30 | 346.7 | dyke |
| 31 | 347.4 | dyke |
| 32 | 347.55 | dyke |
| 33 | 365.3 | dyke |
| 29 | 373.2 | IS WM |
| 28 A-B | 373.7 | IS SM |
| 27 | 377 | IS SM |
| 26 | 377.3 | IS SM, WM at bottom |
| 25 | 379.4 | IS PL |
| 24 A-B | 380.1 | IS PL |
| 23 | 387.43 | fine diam |
| 40 | 391.04 | fine diam |
| 22 | 398.7 | dyke |
| 21 | 399.25 | dyke |
| 20 | 400.6 | fine diam |
| 19 | 401.65 | sandstone |
| 38 | 408.1 | shaly sandstone |

| GA 171 | depth | type |
|---|---|---|
| 1 A-B | 238.7 | graded cycles |
| 2 | 240.5 | lava |
| 3 | 245 | lava |
| 4 | 254.8 | siltstone |
| 5 | 259.9 | diam |
| 6 | 264.7 | siltstone |
| 7 A-B | 273.5 | fine diam |
| 8 | 282.6 | diam |
| 8 A-B | 289.6 | fine diam |
| 9 | 300.7 | diam |
| 10 | 312 | diam |
| 11 | 317.4 | diam |
| 12 | 329 | black shale |
| 30 | 338 | IS WM |
| 31 | 339.5 | black shale |
| 32 | 341 | black shale |
| 13 A-B | 347.6 | black shale + IS WM at bottom |
| 14 | 348.5 | IS SM |
| 15 | 351.1 | IS SM |
| 16 | 357.1 | IS PL |
| 17 | 359 | IS PL |
| 18 | 372.5 | fine diam |
| 19 | 375.3 | fine diam |
| 20 | 383.3 | diam |
| 1 A-B-C-D-E | 383.9 | IS / diam / IS |
| 22 | 391 | IS WM |
| 23 | 395.2 | IS PL |
| 24 | 398.4 | graded cycle |
| 25 | 399 | graded cycles |

diam : diamictite
IS : iron stone
WM : weakly magnetic
SM : strongly magnetic
PL : pillow lutite

A6 MTP4 vertical profile of major elements

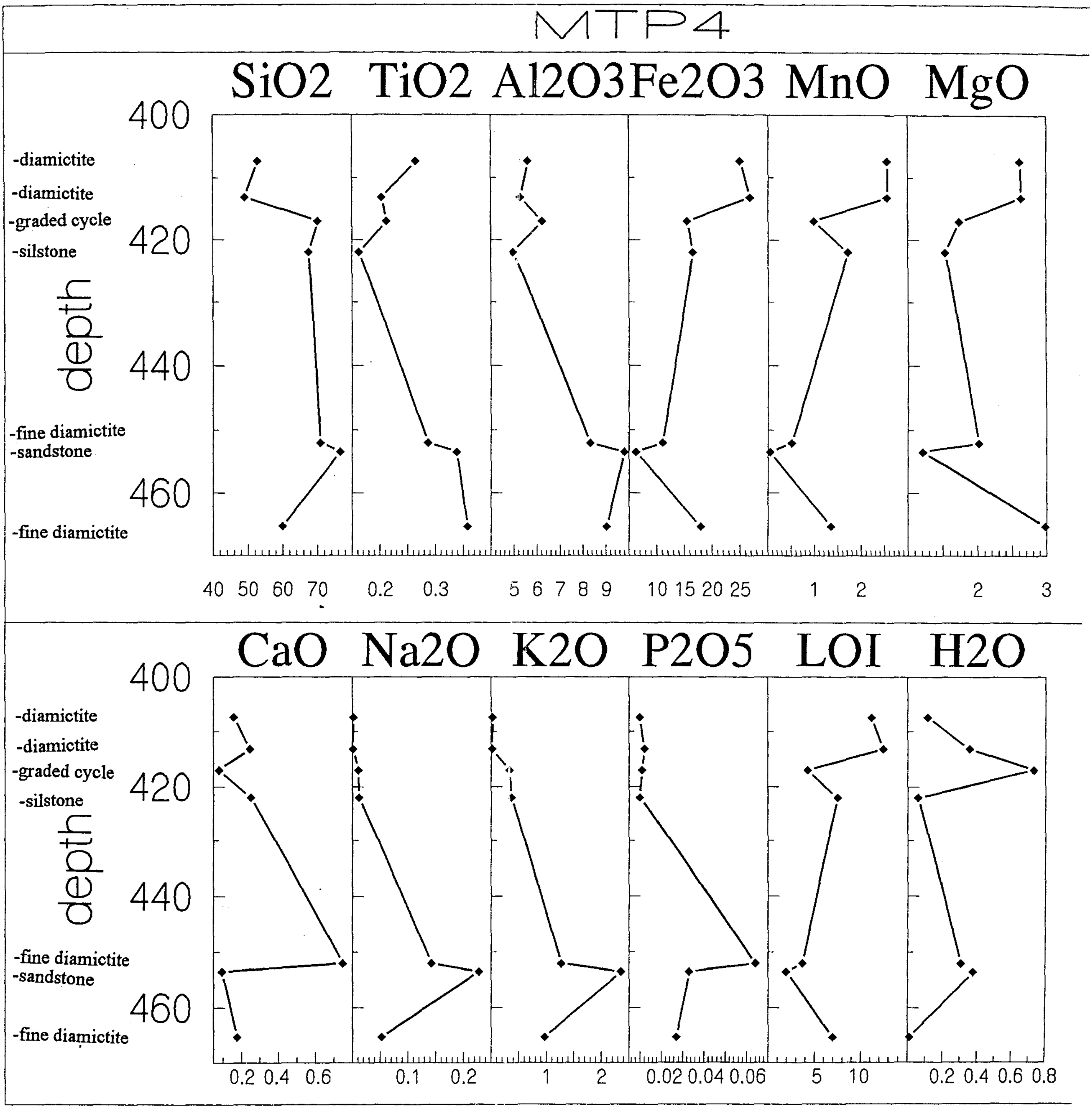

A7 GA129 vertical profile of major elements

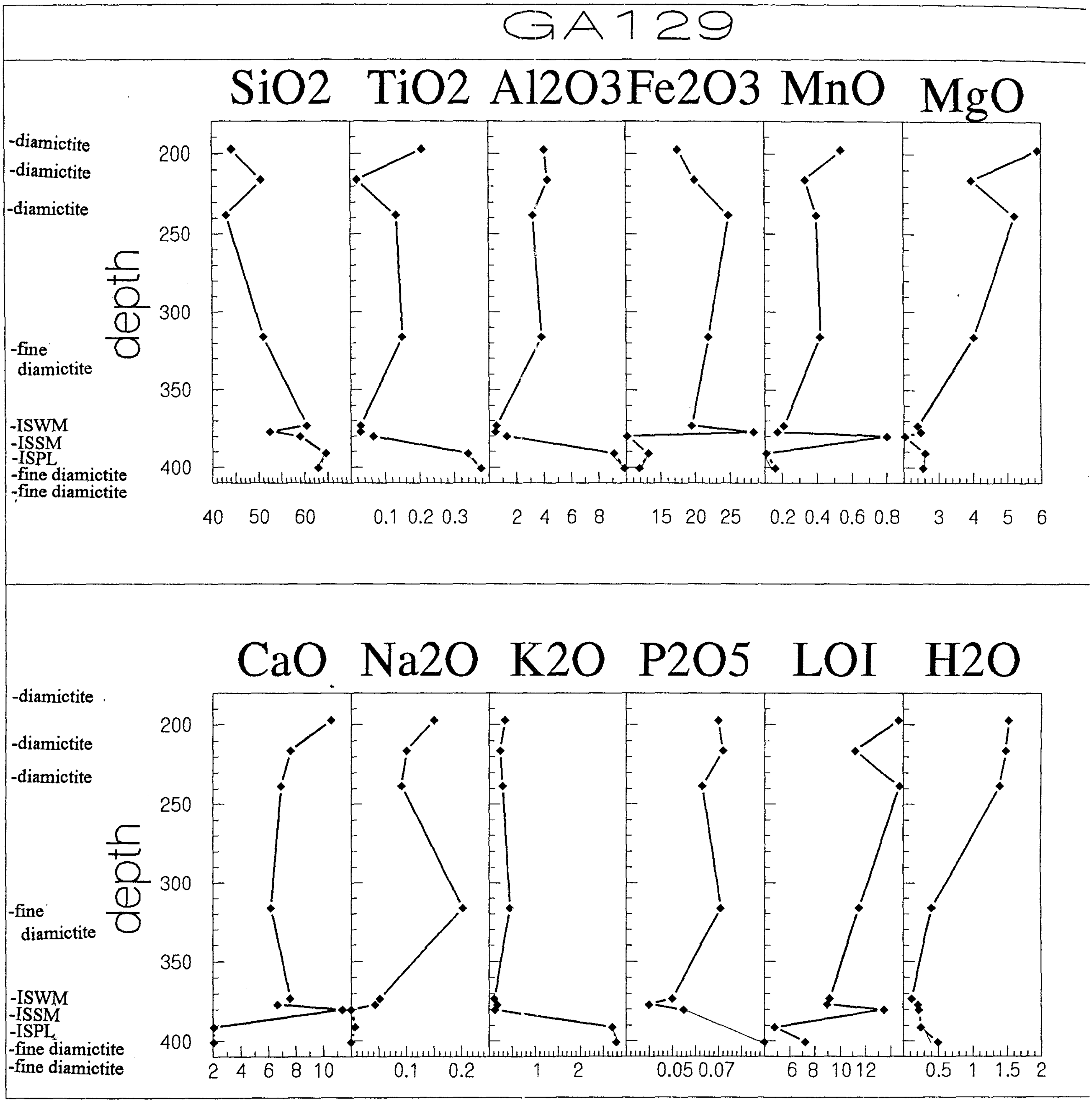


ISSM : banded iron-formation strongly magnetic

ISWM: banded iron-formation weakly magnetic

A8 GA171 vertical profile of major elements

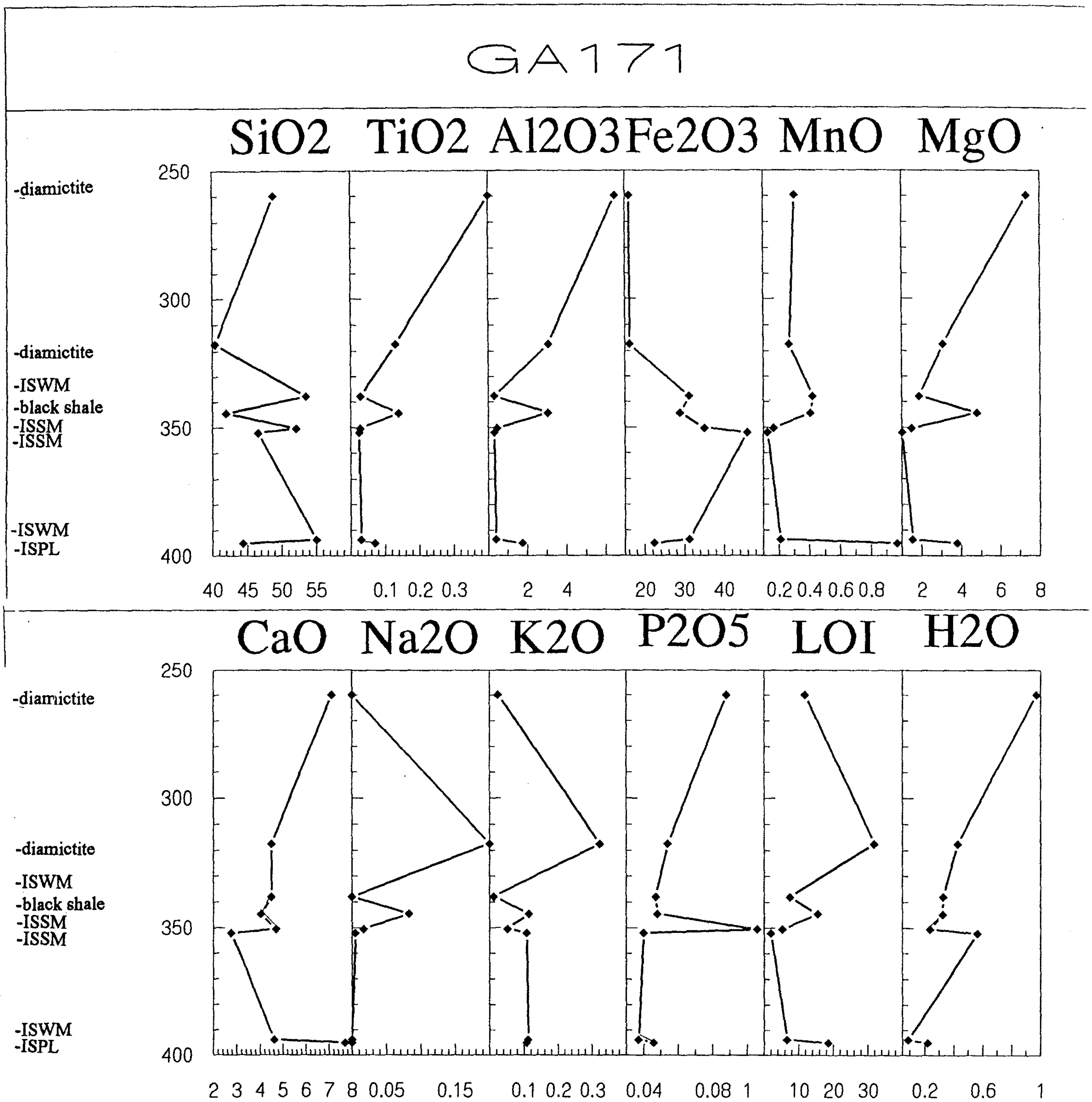


ISSM : banded iron-formation strongly magnetic

ISWM: banded iron-formation weakly magnetic

ISPL : banded iron-formation with pillow-lutite